

Deformations of Dimer Models

Akihiro HIGASHITANI ^a and Yusuke NAKAJIMA ^b

^{a)} *Department of Pure and Applied Mathematics, Graduate School of Information Science and Technology, Osaka University, Osaka 565-0871, Japan*
E-mail: higashitani@ist.osaka-u.ac.jp

^{b)} *Department of Mathematics, Kyoto Sangyo University, Motoyama, Kamigamo, Kita-Ku, Kyoto, 603-8555, Japan*
E-mail: ynakaji@cc.kyoto-su.ac.jp

Received August 06, 2021, in final form April 10, 2022; Published online April 16, 2022

<https://doi.org/10.3842/SIGMA.2022.030>

Abstract. The combinatorial mutation of polygons, which transforms a given lattice polygon into another one, is an important operation to understand mirror partners for two-dimensional Fano manifolds, and the mutation-equivalent polygons give \mathbb{Q} -Gorenstein deformation-equivalent toric varieties. On the other hand, for a dimer model, which is a bipartite graph described on the real two-torus, one can assign a lattice polygon called the perfect matching polygon. It is known that for each lattice polygon P there exists a dimer model having P as the perfect matching polygon and satisfying certain consistency conditions. Moreover, a dimer model has rich information regarding toric geometry associated with the perfect matching polygon. In this paper, we introduce a set of operations which we call deformations of consistent dimer models, and show that the deformations of consistent dimer models realize the combinatorial mutations of the associated perfect matching polygons.

Key words: dimer models; combinatorial mutation of polygons; mirror symmetry

2020 Mathematics Subject Classification: 52B20; 14M25; 14J33

Contents

1	Introduction	2
1.1	Background and motivations	2
1.2	Results	3
2	Dimer models and perfect matching polygons	4
2.1	What is a dimer model?	4
2.2	Perfect matchings and the perfect matching polygon	5
3	Zigzag paths and their properties	8
3.1	Consistency conditions	8
3.2	Relationships between perfect matchings and zigzag paths	10
4	Deformations of dimer models	14
4.1	Definition of deformations of dimer models	14
4.2	Examples of deformations of dimer models	18
5	Combinatorial mutations of perfect matching polygons	19
5.1	Preliminaries on combinatorial mutations of polytopes	19
5.2	The perfect matching polygons of deformed dimer models	23

6	Extended deformations of dimer models	25
7	Foundations of extended deformations of dimer models	30
7.1	The proof of the non-degeneracy	30
7.2	Behaviors of zigzag paths after extended deformations	33
7.3	Properties of zigzag paths on deformed dimer models	37
7.4	Remarks on the extended deformations of hexagonal and rectangular dimer models	40
8	Combinatorial mutations of the PM polygon are realized by extended deformations	42
A	Mutations of dimer models	46
B	Large examples	48
	References	51

1 Introduction

1.1 Background and motivations

Fano manifolds are one of the well studied classes in geometry, and the classification of Fano manifolds, which has been done in low dimensions, is a fundamental problem. Here, a *Fano manifold* X is a complex projective manifold such that the anticanonical line bundle $-K_X$ is ample. Recently, a new approach that uses mirror symmetry has been proposed for classifying Fano manifolds as follows. First, a Fano manifold is expected to correspond to a certain Laurent polynomial via mirror symmetry (see [8]). That is, a Laurent polynomial $f \in \mathbb{C}[x_1^\pm, \dots, x_n^\pm]$ is said to be a *mirror partner* for an n -dimensional Fano manifold X if the Taylor expansion of the *classical period* π_f of f coincides with a *generating function for Gromov–Witten invariants* of X (see the references quoted above for the details of these terminologies). Furthermore, if a Fano manifold X is a mirror partner of f , it is expected that X admits a toric degeneration X_P . Here, $P := \text{Newt}(f)$ is the Newton polytope of f , which is defined as the convex hull of exponents of monomials of f , and X_P is the toric variety defined by the *spanning fan* of P (i.e., the fan whose cones are spanned by the faces of P). Thus, Laurent polynomials having the same classical period are considered as mirror partners for the same Fano manifold X , and in general there are many Laurent polynomials that are mirror partners for X . In order to understand the relationship between such Laurent polynomials, an operation called the *mutation* of f , which is a birational transformation analogue to a cluster transformation, was introduced in [12]. In particular, it was shown that if $f, g \in \mathbb{C}[x_1^\pm, \dots, x_n^\pm]$ are transformed into each other by mutations, then their classical periods are the same, that is, $\pi_f = \pi_g$ [2, Lemma 1]. Moreover, this mutation of Laurent polynomials induces an operation, called the *combinatorial mutation*, which connects the associated Newton polytopes $P = \text{Newt}(f)$ and $Q = \text{Newt}(g)$ as defined in [2] (see also Section 5.1). Also, it was shown in [18] that if P and Q are Fano polytopes and are transformed into each other by combinatorial mutations, then the associated toric varieties X_P and X_Q are related by a \mathbb{Q} -Gorenstein (= qG) deformation; that is, there exists a flat family $\mathfrak{X} \rightarrow \mathbb{P}^1$ such that the relative canonical divisor is \mathbb{Q} -Cartier and $\mathfrak{X}_0 \cong X_P$, $\mathfrak{X}_\infty \cong X_Q$, where \mathfrak{X}_p is the fiber of $p \in \mathbb{P}^1$. Thus, it has been conjectured that there is a bijection between qG -deformation equivalence classes of “class TG” Fano manifolds and mutation equivalence classes of Fano polytopes. There have previously been several affirmative results (e.g., [1, 22]).

1.2 Results

As mentioned above, the combinatorial mutation of polytopes is quite important in mirror symmetry of Fano manifolds. In this paper, we focus on the two-dimensional case, and the polygons which we are interested in are not necessarily Fano. First, it is known that any lattice polygon in \mathbb{R}^2 can be realized as the *perfect matching polygon* Δ_Γ of a dimer model Γ satisfying the consistency condition (see Sections 2 and 3). A *dimer model* is a bipartite graph on the real two-torus (see Section 2 for more details), which was first introduced in the field of statistical mechanics. Since the 2000s, string theorists have been using dimer models to study quiver gauge theories (e.g., [11, 16, 23, 24] and references therein). As a result, relationships between dimer models and many branches of mathematics have been discovered, e.g., see [6] and references therein. (Note that a bipartite graph described on other surfaces, which is also called a dimer model, has also been studied actively. For example, dimer models on the disk are related to Grassmannians and their mirror symmetry, e.g., see [17, 29].) Based on this background, we expect that there is a certain operation on a consistent dimer model that realizes the combinatorial mutation of the associated perfect matching polygon. In this paper, we introduce a concept called the *deformations of consistent dimer models*. Note that there is another operation on dimer models, called *mutation of dimer models* (see Appendix A). Although a mutation changes the shape of a dimer model, it does not change the associated perfect matching polygon. Thus, we need a new operation different from the mutation to realize our expectation.

To explain our main theorem, we briefly recall the combinatorial mutations of polygons (see Section 5.1 for a more precise definition). Let $N \cong \mathbb{Z}^2$ be a rank two lattice and $M := \text{Hom}_{\mathbb{Z}}(N, \mathbb{Z}) \cong \mathbb{Z}^2$. First, we consider a lattice polygon P in $N_{\mathbb{R}} := N \otimes_{\mathbb{Z}} \mathbb{R}$ and choose an edge E of P . We then take a primitive inner normal vector $w \in M$ for E , and consider the linear map $\langle w, - \rangle: N_{\mathbb{R}} \rightarrow \mathbb{R}$. Using these notions, we determine the *height* $\langle w, u \rangle$ of each point $u \in P$. In particular, a primitive lattice element $u_E \in N$ satisfying $\langle w, u_E \rangle = 0$ plays an important role in defining the combinatorial mutation. Such an element u_E is determined uniquely up to sign; thus we fix one of them. Then, we define the line segment $F := \text{conv}\{\mathbf{0}, u_E\}$, which is called a *factor* of P with respect to w . Using these data, we have the lattice polygon $\text{mut}_w(P, F)$, which is called the *combinatorial mutation* of P given by the vector w and the factor F , as defined in Definition 5.2. In addition, we also define another combinatorial mutation $\text{mut}_w(P, -F)$ in a similar way. We note that although $\text{mut}_w(P, F)$ looks different from $\text{mut}_w(P, -F)$, they are transformed into each other by a $\text{GL}(2, \mathbb{Z})$ -transformation. On the other hand, for the given lattice polygon P there exists a consistent dimer model Γ such that $P = \Delta_\Gamma$.

Based on this background, the deformation of a consistent dimer model is compatible with the above combinatorial mutations in the following sense. Let Γ be the consistent dimer model. The deformations of Γ are defined for a certain set of “zigzag paths” $\{z_1, \dots, z_r\}$ on Γ corresponding to the vector $-w$ (see Section 3 concerning zigzag paths), and there are two kinds of deformations which we call the *zig-deformation* and the *zag-deformation*, which are respectively denoted by $\nu_{\mathbf{p}}^{\text{zig}}(\Gamma, \{z_1, \dots, z_r\})$ and $\nu_{\mathbf{p}}^{\text{zag}}(\Gamma, \{z_1, \dots, z_r\})$; see Definitions 4.3 and 4.4. For some cases, these deformations are compatible with the combinatorial mutations of the perfect matchings as follows.

Theorem 1.1 (see Proposition 4.5 and Theorem 5.10 for more details). *In addition to the above settings, we also assume that either one of the following conditions is satisfied:*

(i) $r = 1$ or

(ii) Γ is a hexagonal or rectangular dimer model (see Definition 2.1).

Then the deformations $\nu_{\mathbf{p}}^{\text{zig}}(\Gamma, \{z_1, \dots, z_r\})$ and $\nu_{\mathbf{p}}^{\text{zag}}(\Gamma, \{z_1, \dots, z_r\})$ are consistent dimer models, and we have

$$\text{mut}_w(\Delta_\Gamma, F) = \Delta_{\nu_{\mathbf{p}}^{\text{zig}}(\Gamma, \{z_1, \dots, z_r\})}, \quad \text{mut}_w(\Delta_\Gamma, -F) = \Delta_{\nu_{\mathbf{p}}^{\text{zag}}(\Gamma, \{z_1, \dots, z_r\})},$$

where $\Delta_{\nu_{\mathbf{p}}^{\text{zig}}(\Gamma, \{z_1, \dots, z_r\})}$ and $\Delta_{\nu_{\mathbf{p}}^{\text{zag}}(\Gamma, \{z_1, \dots, z_r\})}$ are the perfect matching polygons of $\nu_{\mathbf{p}}^{\text{zig}}(\Gamma, \{z_1, \dots, z_r\})$ and $\nu_{\mathbf{p}}^{\text{zag}}(\Gamma, \{z_1, \dots, z_r\})$, respectively.

Note that the combinatorial mutations $\text{mut}_w(\Delta_{\Gamma}, \pm F)$ are defined for the perfect matching polygon Δ_{Γ} , whereas the deformations $\nu_{\mathbf{p}}^{\text{zig/zag}}(\Gamma, \{z_1, \dots, z_r\})$ are defined independently of Δ_{Γ} . When we drop the both conditions (i) and (ii) in Theorem 1.1, the deformed dimer model does not necessarily realize the combinatorial mutation. In order to obtain the same results for a general situation, we have to add some algorithmic operations to the definitions of deformations. We formulate such operations as the *extended zig-deformation* $\nu_{\mathcal{X}}^{\text{zig}}(\Gamma, \{z_1, \dots, z_r\})$ and *extended zag-deformation* $\nu_{\mathcal{Y}}^{\text{zag}}(\Gamma, \{z_1, \dots, z_r\})$ as in Definitions 6.2 and 6.3. Then we can prove the statement in Theorem 1.1 for the extended deformations (see Proposition 6.7 and Theorem 8.3). By these results, the perfect matching polygons of the (extended) deformation of dimer models satisfy the properties which are exactly the same as the combinatorial mutation of a polygon (see Section 8).

Since dimer models are related with many branches of mathematics and physics, we considered that it would be of interest to compare certain objects (e.g., perfect matchings, the associated toric variety) related with a consistent dimer model Γ to those of $\nu_{\mathcal{X}}^{\text{zig}}(\Gamma, \{z_1, \dots, z_r\})$ (or $\nu_{\mathcal{Y}}^{\text{zag}}(\Gamma, \{z_1, \dots, z_r\})$).

The structure of this paper is as follows. In Section 2, we introduce dimer models and related concepts. In particular, the notion of the perfect matching polygon introduced in this section is one of main concepts in this paper. In Section 3, we introduce the notion of zigzag paths, which are special paths on a dimer model. We then define the consistency condition using zigzag paths, and discuss the relationships between perfect matchings and zigzag paths on a consistent dimer model. Next, we focus specifically on type I zigzag paths, which are zigzag paths having typical properties. Using these type I zigzag paths, we introduce the deformations of consistent dimer models in Section 4. In Section 5, we compare the perfect matching polygon of the deformed dimer model with the combinatorial mutation of the perfect matching polygon of the original dimer model. In particular, we see that these polygons coincide in some cases as in Theorem 1.1 (see Theorem 5.10). In Section 6, we consider some algorithmic operations and define the extended deformations of consistent dimer models. In Section 7, we show the fundamental properties of the extended deformation of consistent dimer models. In particular, we prove the compatibility of the extended deformations and the combinatorial mutations for general situations as in Theorem 8.3, and this induces Theorem 5.10. As we will mention in Remark 6.5, the extended deformation of a consistent dimer model depends on the choice of some of the data used in the processes (zig-5), (zag-5), as explained in Definitions 6.2 and 6.3 (see also Operation 6.6), whereas the perfect matching polygon of the extended deformation of a consistent dimer model is determined uniquely. This ambiguity is caused by the fact that there are several consistent dimer models giving the same perfect matching polygon. However, it has been conjectured that such consistent dimer models are transformed into each other by *mutations of dimer models*, and hence “conjecturally” our deformation of a consistent dimer model is determined uniquely up to the mutation. We include a survey of this mutation of dimer models in Appendix A. In Appendix B, we provide an additional example of the extended deformation, the explanation of which is too lengthy to include in the main body of this paper.

2 Dimer models and perfect matching polygons

2.1 What is a dimer model?

We first introduce dimer models. Some ideas and concepts contained in this subsection are originally derived from theoretical physics (e.g., [11, 16]).

A *dimer model* (or *brane tiling*) Γ is a finite bipartite graph on the real two-torus $\mathbb{T} := \mathbb{R}^2/\mathbb{Z}^2$; that is, the set Γ_0 of nodes is divided into two parts Γ_0^+, Γ_0^- , and the set Γ_1 of edges consists of the edges connecting nodes in Γ_0^+ with those in Γ_0^- . In order to make the situation clear, we color the nodes in Γ_0^+ white, and those in Γ_0^- black. A connected component of $\mathbb{T}\setminus\Gamma_1$ is called a *face* of Γ , and we denote by Γ_2 the set of faces. We also obtain the bipartite graph $\tilde{\Gamma}$ on \mathbb{R}^2 induced via the universal cover $\mathbb{R}^2 \rightarrow \mathbb{T}$. We call $\tilde{\Gamma}$ the universal cover of the dimer model Γ . For example, the bipartite graph shown on the left side of Figure 2.1 is a dimer model where the outer frame is the fundamental domain of \mathbb{T} .

As the dual of a dimer model Γ , we define the quiver Q_Γ associated with Γ . Namely, we assign a vertex dual to each face in Γ_2 , and an arrow dual to each edge in Γ_1 . The orientation of arrows is determined so that the white node is on the right of the arrow. For example, the right side of Figure 2.1 is the quiver associated with the dimer model on the left. Sometimes we simply denote the quiver Q_Γ by Q .

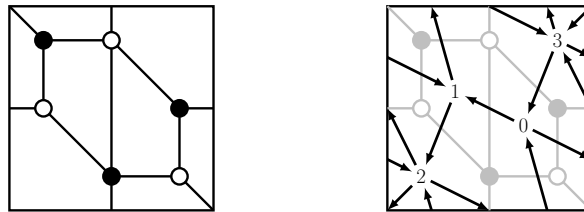


Figure 2.1. A dimer model and the associated quiver.

The *valency* of a node is the number of edges incident to that node. We say that a node on a dimer model is *n-valent* if its valency is n . We then define several operations on a dimer model. The *join move* is the operation removing a 2-valent node and joining the two distinct nodes connected to it as shown in Figure 2.2. Thus, using join moves we obtain a dimer model having no 2-valent nodes. We say that a dimer model is *reduced* if it has no 2-valent nodes. We can see that the quiver associated with a reduced dimer model contains no 2-cycles. On the other hand, there is the operation called the *split move*, which inserts a 2-valent node (see Figure 2.2).

We say that two reduced dimer models Γ, Γ' are *isomorphic*, which is denoted by $\Gamma \cong \Gamma'$, if their underlying cell decompositions of \mathbb{T} are homotopy-equivalent.

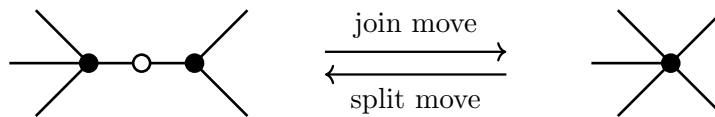


Figure 2.2. An example of the join and split move.

We sometimes focus on the following type of dimer models.

Definition 2.1. We say that a dimer model Γ is *hexagonal* (resp. *rectangular*) if any face of Γ is hexagon (resp. rectangle) and any node of Γ is 3-valent (resp. 4-valent). In particular, a hexagonal (resp. rectangular) dimer model is homotopy-equivalent to a dimer model whose faces are all regular hexagons (resp. squares).

2.2 Perfect matchings and the perfect matching polygon

Next, we assign a lattice polygon to each dimer model. For this purpose, we will introduce the notion of perfect matchings, and we construct a polygon called the *perfect matching polygon*.

Definition 2.2. A *perfect matching* (or *dimer configuration*) on a dimer model Γ is a subset P of Γ_1 such that each node is the end point of precisely one edge in P .

In general, not every dimer model necessarily has a perfect matching. In this paper, we will mainly discuss consistent dimer models, and such dimer models have perfect matchings. Moreover, we can extend a perfect matching P to one on $\tilde{\Gamma}$ via the universal cover $\mathbb{R}^2 \rightarrow \mathbb{T}$. We call this a *perfect matching* on $\tilde{\Gamma}$, and use the same notation P . For example, some perfect matchings on the dimer model given in Figure 2.1 are shown in Figure 2.3. (This dimer model has eight perfect matchings in total.)

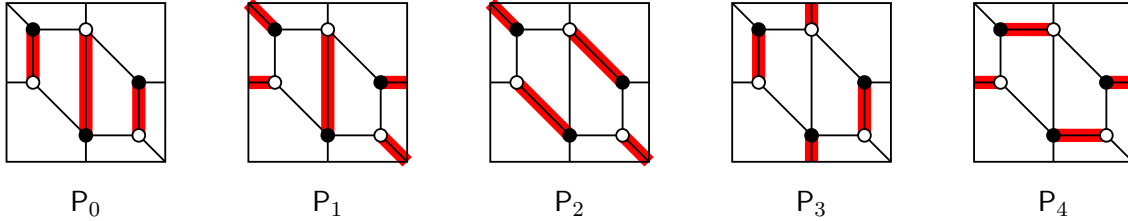


Figure 2.3. Some perfect matchings on the dimer model given in Figure 2.1.

We say that a dimer model is *non-degenerate* if every edge is contained in some perfect matchings. It is known that this non-degeneracy condition is equivalent to the *strong marriage condition*; that is, the dimer model has equal numbers of black and white nodes and every proper subset of the black nodes of size n is connected to at least $n + 1$ white nodes (e.g., [7, Remark 2.12]).

Following [20, Section 5], we next define the perfect matching polygon. We first fix a perfect matching P_0 , and call this the *reference perfect matching*. For any perfect matching P , we consider the connected components of the universal cover \mathbb{R}^2 divided by $P \cup P_0$. Then, we consider the *height function* h_{P,P_0} , which is a locally constant function on $\mathbb{R}^2 \setminus (P \cup P_0)$, defined as follows. First, we choose a connected component of $\mathbb{R}^2 \setminus (P \cup P_0)$, and define the value of h_{P,P_0} as 0. Then, this function increases by 1 when we cross

- an edge $e \in P$ with the black node on the right, or
- an edge $e \in P_0$ with the white node on the right,

and decreases by 1 when we cross

- an edge $e \in P$ with the white node on the right, or
- an edge $e \in P_0$ with the black node on the right.

This function is determined up to a choice of a connected component of value 0. For example, Figure 2.4 shows the height function h_{P_2,P_3} on the dimer model given in Figure 2.1, where the red square stands for a fundamental domain of \mathbb{T} , the edges in P_2 (resp. P_3) are colored blue (resp. green), and the number filled in each component is the value of h_{P_2,P_3} .

We then take a point $\mathbf{pt} \in \mathbb{R}^2 \setminus (P \cup P_0)$, and define the *height change*

$$h(P, P_0) = (h_x(P, P_0), h_y(P, P_0)) \in \mathbb{Z}^2$$

of P with respect to P_0 as the differences of the height function:

$$\begin{aligned} h_x(P, P_0) &= h_{P,P_0}(\mathbf{pt} + (1, 0)) - h_{P,P_0}(\mathbf{pt}), \\ h_y(P, P_0) &= h_{P,P_0}(\mathbf{pt} + (0, 1)) - h_{P,P_0}(\mathbf{pt}). \end{aligned}$$

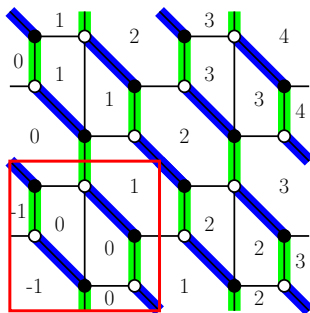


Figure 2.4. The height function h_{P_2, P_3} .

We remark that this does not depend on the choice of $\mathbf{pt} \in \mathbb{R}^2 \setminus (P \cup P_0)$. We then consider the height change $h(P, P')$ for any pair of perfect matchings P, P' , but since we have

$$h(P, P') = h(P, P_0) - h(P', P_0),$$

it is enough to consider height changes with respect to the reference perfect matching P_0 . Then, the *perfect matching (= PM) polygon* (or *characteristic polygon*) $\Delta_\Gamma \subset \mathbb{R}^2$ of a dimer model Γ is defined as the convex hull of $\{h(P, P_0) \in \mathbb{Z}^2 \mid P \in \text{PM}(\Gamma)\}$ where $\text{PM}(\Gamma)$ is the set of perfect matchings on Γ .

Remark 2.3. The description of height changes depends on the choice of the coordinate system fixed in \mathbb{T} (i.e., the choice of a fundamental domain). A change of a coordinate system induces a $GL(2, \mathbb{Z})$ -action on the PM polygon, and this action does not affect our problem. In the following, we say that two polygons P and Q are $GL(2, \mathbb{Z})$ -*equivalent* if they are transformed into each other by $GL(2, \mathbb{Z})$ -transformations, in which case we denote $P \cong Q$. Thus, we may fix some fundamental domain of \mathbb{T} . Also, we remark that the description of the polygon Δ_Γ depends on the choice of a reference perfect matching, but it is determined up to translations.

Definition 2.4. Fix a perfect matching P_0 and let Δ_Γ be the perfect matching polygon. We say that a perfect matching P is

- a *corner* (or *extremal*) *perfect matching* if $h(P, P_0)$ is a vertex of Δ_Γ ,
- a *boundary* (or *external*) *perfect matching* if $h(P, P_0)$ is a lattice point on an edge of Δ_Γ (in particular, corner perfect matchings are boundary perfect matchings),
- an *internal perfect matching* if $h(P, P_0)$ is an interior lattice point of Δ_Γ .

In the next subsection, we will introduce consistent dimer models (see Definition 3.2), which have several nice properties. If a dimer model is consistent, then there exists a unique corner perfect matching corresponding to each vertex of Δ_Γ (e.g., [7, Corollary 4.27], [20, Proposition 9.2]). Thus, we can give a cyclic order to corner perfect matchings along the corresponding vertices of Δ_Γ in the anti-clockwise direction. We say that two corner perfect matchings are *adjacent* if they are adjacent with respect to the given cyclic order.

Example 2.5. We consider the dimer model given in Figure 2.1, which is consistent as we will see in the next subsection. Fix the perfect matching P_0 shown in Figure 2.3 as the reference one. Then, we see that the perfect matchings P_1, \dots, P_4 correspond to lattice points $(1, 0), (1, 1), (-1, 0), (0, -1)$, respectively. Since P_0 is the reference perfect matching, it corresponds to $(0, 0)$. In addition, this dimer model has three perfect matchings that are not listed in Figure 2.3, and such perfect matchings also correspond to $(0, 0)$. Thus, the PM polygon takes the form shown in Figure 2.5, and hence P_1, \dots, P_4 are corner perfect matchings.

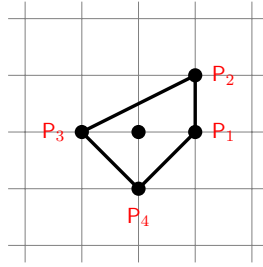


Figure 2.5. The PM polygon of the dimer model given in Figure 2.1.

In this way, we can obtain the PM polygon from a dimer model. On the other hand, it is known that any lattice polygon can be obtained as the PM polygon of a certain dimer model.

Theorem 2.6 ([14, 20]). *For any lattice polygon Δ in \mathbb{R}^2 , there exists a dimer model Γ giving Δ as the PM polygon Δ_Γ . Furthermore, we can take this Γ as it satisfies the consistency condition (see Definition 3.2).*

Thus, for a given lattice polygon Δ , we say that Γ is a *dimer model associated with Δ* if the PM polygon of Γ coincides with Δ . We remark that for a given polygon Δ , the associated consistent dimer model is not unique in general.

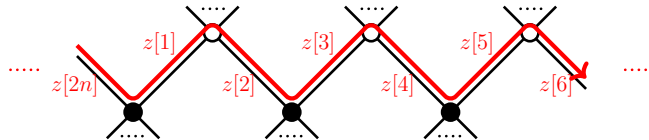
3 Zigzag paths and their properties

3.1 Consistency conditions

In this subsection, we introduce the consistency condition. In order to define this condition, we first introduce the notion of zigzag paths. These paths are also the main ingredients for introducing deformations of dimer models.

Definition 3.1. We say that a path on a dimer model is a *zigzag path* if it makes a maximum turn to the right on a white node and a maximum turn to the left on a black node. Also, we say that a zigzag path is *reduced* if it does not pass through 2-valent nodes. (We remark that we can make a zigzag path reduced using the join moves. In particular, any zigzag path on a reduced dimer model is reduced.)

Since a dimer model has only finitely many edges, we see that all zigzag paths are periodic. For a zigzag path z on Γ , we define the length of z , which is denoted by $\ell(z)$, as the number of edges of Γ constituting z . In particular, we see that $\ell(z)$ is an even integer. Thus, edges on a zigzag path are indexed by elements in $\mathbb{Z}/(2n)\mathbb{Z}$ for some integer $\ell(z)/2 = n \geq 1$. Fix a black node on a zigzag path z as the starting point of z , and denote z as a sequence of edges starting from the fixed black node: $z = z[1]z[2] \cdots z[2n-1]z[2n]$.



An edge in a zigzag path z is called a *zig* (resp. *zag*) of z if it is indexed by an odd (resp. even) integer. We denote by $\text{Zig}(z)$ (resp. $\text{Zag}(z)$) the set of zigs (resp. zags) appearing in a zigzag path z , which is a finite set. Two zigzag paths are said to *intersect* if they share an edge (not a node). We note that if z does not have a self-intersection, $\text{Zig}(z)$ and $\text{Zag}(z)$ are disjoint sets. For any edge e of a dimer model, we can consider the zigzag path containing e as a zig and the

zigzag path containing e as a zag. Thus, any edge e is contained in at most two zigzag paths. If such zigzag paths do not have a self-intersection, e is contained in exactly two zigzag paths. For example, zigzag paths on the dimer model given in the left of Figure 2.1 are shown in Figure 3.1.

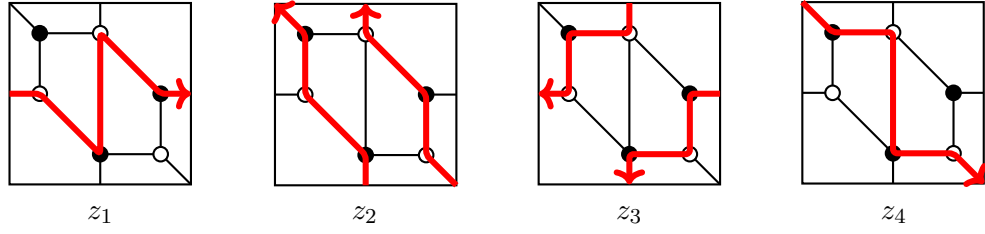


Figure 3.1. All zigzag paths on the dimer model given in Figure 2.1.

For a zigzag path z on a dimer model Γ , we also consider the lift of z to the universal cover $\tilde{\Gamma}$. Let $\tilde{z}(\alpha)$ denote a zigzag path on $\tilde{\Gamma}$ whose projection on Γ is z where $\alpha \in \mathbb{Z}$. When we do not need to specify these, we simply denote each of them by \tilde{z} . Then, we see that a zigzag path on $\tilde{\Gamma}$ is either periodic or infinite in both directions. Using these notions, we introduce the consistency condition.

Definition 3.2 (see [19, Definition 3.5]). We say that a dimer model is (*zigzag*) *consistent* if it satisfies the following conditions:

- (1) there is no homologically trivial zigzag path,
- (2) no zigzag path on the universal cover has a self-intersection,
- (3) no pair of zigzag paths on the universal cover intersect each other in the same direction more than once. That is, if a pair of zigzag paths (\tilde{z}, \tilde{w}) on the universal cover has two intersected edges a_1, a_2 and \tilde{z} points from a_1 to a_2 , then \tilde{w} points from a_2 to a_1 .

In the literature, there are several conditions that are equivalent to Definition 3.2 (for more details, see [4, 19]), and it is known that a consistent dimer model is non-degenerate (e.g., [20, Proposition 8.1]). For example, we see that the dimer model given in Figure 2.1 is consistent by checking all zigzag paths, which are shown in Figure 3.1. We also remark that this dimer model satisfies the stronger condition called *isoradial* (see Definition 3.4).

In this paper, we also use another condition called *properly ordered*. To explain the proper ordering, we prepare several notation. First, considering a zigzag path z as a 1-cycle on \mathbb{T} , we have the homology class $[z] \in H_1(\mathbb{T}) \cong \mathbb{Z}^2$. We call this element $[z] \in \mathbb{Z}^2$ the *slope* of z . We remark that even if we apply the join and split moves to nodes contained in a zigzag path, such operations do not change the slope. If a zigzag path does not have any self-intersection, the slope of each zigzag path is primitive. Now, we consider slopes $(a, b) \in \mathbb{Z}^2$ of zigzag paths that are not homologically trivial. The set of such slopes has a natural cyclic order by considering (a, b) as an element of the unit circle:

$$\frac{(a, b)}{\sqrt{a^2 + b^2}} \in S^1.$$

We say that two zigzag paths are *adjacent* if their slopes are adjacent with respect to the above cyclic order. Using this cyclic order, we define a properly ordered dimer model below. In particular, it is known that a dimer model is consistent in the sense of Definition 3.2 if and only if it is properly ordered (see [19, Proposition 4.4]).

Definition 3.3 (see [14, Section 3.1]). A dimer model is said to be *properly ordered* if

- (1) there is no homologically trivial zigzag path,
- (2) no zigzag path on the universal cover has a self-intersection,
- (3) no pair of zigzag paths with the same slope have a common node,
- (4) for any node on the dimer model, the natural cyclic order on the set of zigzag paths incident to that node coincides with the cyclic order determined by their slopes.

We also introduce isoradial dimer models which are stronger than consistent ones. The dimer model given in Figure 2.1 is isoradial in particular.

Definition 3.4 ([25, Theorem 5.1]; see also [10, 26]). We say that a dimer model Γ is *isoradial* (or *geometrically consistent*) if

- (1) every zigzag path is a simple closed curve,
- (2) any pair of zigzag paths on the universal cover share at most one edge.

3.2 Relationships between perfect matchings and zigzag paths

We can now discuss the relationship between perfect matchings and zigzag paths. The following proposition is essential throughout this paper.

Proposition 3.5 (see [14, Theorem 3.3 and Corollary 3.8], [20, Proposition 9.2 and Corollary 9.3]). *There exists a one-to-one correspondence between the set of slopes of zigzag paths on a consistent dimer model Γ and the set of primitive side segments of the PM polygon Δ_Γ . More precisely, each slope of a zigzag path is the primitive outer normal vector for a primitive side segment of Δ_Γ .*

Moreover, zigzag paths having the same slope arise as the difference of two adjacent corner perfect matchings P, P' (i.e., the edges in $P \cup P' \setminus P \cap P'$ form zigzag paths). Thus, any corner perfect matching intersects with half of the edges constituting a certain zigzag path.

For example, the zigzag path z_1 shown in Figure 3.1 is obtained from the pair of adjacent corner perfect matchings (P_1, P_2) given in Figure 2.3. Also, the zigzag paths z_2, z_3, z_4 are obtained by pairs $(P_2, P_3), (P_3, P_4), (P_4, P_1)$, respectively.

By Proposition 3.5, we can assign each edge of the PM polygon to a zigzag path z ; thus we will call this the edge corresponding to z . In particular, the edges corresponding to zigzag paths having the same slope are all the same.

Let P, P' be adjacent corner perfect matchings on a consistent dimer model, and z_1, \dots, z_r be the zigzag paths arising from P and P' as in Proposition 3.5. In particular, these zigzag paths have the same slope. We see that $P \cap z_i = \text{Zig}(z_i)$ and $P' \cap z_i = \text{Zag}(z_i)$ (or $P \cap z_i = \text{Zag}(z_i)$ and $P' \cap z_i = \text{Zig}(z_i)$) for any $i = 1, \dots, r$. Here, $P \cap z_i$ denotes the subset of edges in P contained in z_i . Then, we have the description of boundary perfect matchings using the corner ones.

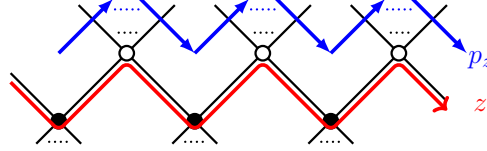
Proposition 3.6 (e.g., [7, Proposition 4.35], [14, Corollary 3.8]). *Let P, P' and z_1, \dots, z_r be as above. Let E be the edge of the PM polygon of Γ corresponding to z_1, \dots, z_r . We assume that $P \cap z_i = \text{Zig}(z_i)$ and $P' \cap z_i = \text{Zag}(z_i)$. Then, any boundary perfect matching corresponding to a lattice point on E can be described as*

$$\left(P \setminus \bigcup_{i \in I} \text{Zig}(z_i) \right) \cup \bigcup_{i \in I} \text{Zag}(z_i) \quad \text{or} \quad \left(P' \setminus \bigcup_{i \in I} \text{Zag}(z_i) \right) \cup \bigcup_{i \in I} \text{Zig}(z_i),$$

where I is a subset of $\{1, \dots, r\}$. In particular, the number of perfect matchings corresponding to a lattice point \mathbf{q} on E is $\binom{r}{m}$, where m is the number of primitive side segments of E between \mathbf{q} and one of the endpoints of E .

We then observe the relationships between zigzag paths and height changes of perfect matchings. Some of these relationships are well-known to experts, but we will consider them in detail because these statements are quite important when we define the deformation of consistent dimer models in Section 4, and also for the self-containedness.

Observation 3.7 (cf. [20, Section 5.3]). Let Γ be a consistent dimer model. For any zigzag path z , the slope $[z]$ is an element in $H_1(\mathbb{T})$. On the other hand, we can consider height changes as elements in the cohomology group $H^1(\mathbb{T}) \cong \mathbb{Z}^2$. We consider a pairing $\langle -, - \rangle : H^1(\mathbb{T}) \times H_1(\mathbb{T}) \rightarrow \mathbb{Z}$. By Propositions 3.5 and 3.6, there is a perfect matching P' that intersects half of the edges constituting z . Then, for any perfect matching P , we have $\langle h(P, P'), [z] \rangle \leq 0$. In fact, we first replace z by the path p_z on the quiver Q_Γ going along the left side of z (see the figure below).



Then, considering this path p_z as the element $[p_z] \in H_1(\mathbb{T})$, we have $[z] = [p_z]$. By a choice of P' , this p_z does not cross any edge in P' , and if p_z crosses an edge in P , we can see the white node on the right by the definition of Q_Γ . Thus, we have the desired inequality.

For a perfect matching P and a zigzag path z on a dimer model Γ , we denote by $|P \cap z|$ the number of edges in $P \cap z$. Since the number of perfect matchings is finite, the maximum (resp. minimum) number $\omega_{\max}(z)$ (resp. $\omega_{\min}(z)$) of $|P \cap z|$ exists for each zigzag path z . For a consistent dimer model, z can be obtained as the difference of adjacent perfect matchings (see Proposition 3.6); thus we clearly have $\ell(z)/2 = \omega_{\max}(z)$. We set

$$\begin{aligned} \text{PM}_{\max}(z) &= \{P \in \text{PM}(\Gamma) \mid |P \cap z| = \omega_{\max}(z)\}, \\ \text{PM}_{\min}(z) &= \{P \in \text{PM}(\Gamma) \mid |P \cap z| = \omega_{\min}(z)\}. \end{aligned}$$

In particular, if P, P' are adjacent corner perfect matchings on a consistent dimer model Γ , and z is one of the zigzag paths obtained by P, P' , then we have $P \cap z = \text{Zig}(z)$ and $P' \cap z = \text{Zag}(z)$ (or $P \cap z = \text{Zag}(z)$ and $P' \cap z = \text{Zig}(z)$), and hence the next lemma easily follows from Propositions 3.5 and 3.6.

Lemma 3.8. *Let z be a zigzag path on a consistent dimer model Γ , and E be the edge of the PM polygon of Γ corresponding to z . If P_1, \dots, P_s are boundary perfect matchings corresponding to lattice points on E , then we have $\{P_1, \dots, P_s\} = \text{PM}_{\max}(z)$, and $\omega_{\max}(z) = |P_i \cap z| = \ell(z)/2$ for any $i = 1, \dots, s$.*

Next, we prepare several lemmas, which play crucial roles to define deformations of consistent dimer models.

Lemma 3.9. *Let the notation be the same as Lemma 3.8. For any perfect matching P , we have*

$$|P \cap z| = \ell(z)/2 - \langle h(P, P_i), -[z] \rangle.$$

In particular, we have

$$\langle h(P, P_i), -[z] \rangle \leq \omega_{\max}(z) - \omega_{\min}(z),$$

and the equality holds for $P \in \text{PM}_{\min}(z)$.

Proof. First, the maximum number of $|\mathbf{P} \cap z|$ is $\ell(z)/2$, in which case $\mathbf{P} = \mathbf{P}_i$ by Lemma 3.8. If the path p_z as in Observation 3.7 crosses an edge e in \mathbf{P} , it means that e is not an edge constituting z , and thus any edge sharing the same white node as e is not contained in \mathbf{P} . By Observation 3.7, we see that for any perfect matching \mathbf{P} the number of edges in \mathbf{P} intersecting with p_z coincides with $-\langle h(\mathbf{P}, \mathbf{P}_i), [z] \rangle$, and thus we have the first equation.

The second assertion follows from the first equation and Lemma 3.8. \blacksquare

By this lemma, we see that $\mathbf{P} \in \text{PM}_{\min}(z)$ if and only if $\langle h(\mathbf{P}, \mathbf{P}_i), [z] \rangle \leq \langle h(\mathbf{P}', \mathbf{P}_i), [z] \rangle$ for any $\mathbf{P}' \in \text{PM}(\Gamma)$. Thus, we see that $\mathbf{P} \in \text{PM}_{\min}(z)$ lies either on a vertex of the PM polygon Δ_Γ or an edge of Δ_Γ . Also, even if two zigzag paths z_j and z_k have the same slope, $\ell(z_j) \neq \ell(z_k)$ and $|\mathbf{P} \cap z_j| \neq |\mathbf{P} \cap z_k|$ in general, but the difference of these values is the same in the following sense:

Lemma 3.10. *Let Γ be a consistent dimer model, and z, z' be zigzag paths on Γ having the same slope. Then, for any perfect matching \mathbf{P} , we have*

$$\ell(z)/2 - |\mathbf{P} \cap z| = \ell(z')/2 - |\mathbf{P} \cap z'|.$$

In particular, we have

$$\ell(z)/2 - \omega_{\min}(z) = \ell(z')/2 - \omega_{\min}(z').$$

Proof. Since $[z] = [z']$, the first equation follows from Lemma 3.9. Considering a perfect matching \mathbf{P} such that the value of $\langle h(\mathbf{P}, \mathbf{P}_i), -[z] \rangle = \langle h(\mathbf{P}, \mathbf{P}_i), -[z'] \rangle$ is maximal, we have the second equation. \blacksquare

We then divide zigzag paths on a consistent dimer model into the following two types. Note that type I zigzag paths are used to define the deformation of consistent dimer models.

Definition 3.11. Let Γ be a dimer model, and z be a zigzag path on Γ .

- (1) We say that z is *type I* if z is reduced and \tilde{z} intersects with any other zigzag path on the universal cover $\tilde{\Gamma}$ at most once.
- (2) We say that z is *type II* if z is reduced and there exists a zigzag path \tilde{w} on the universal cover $\tilde{\Gamma}$ such that \tilde{w} intersects with \tilde{z} in the opposite direction more than once.

We note that any zigzag path on a reduced consistent dimer model is either type I or type II. In particular, if Γ is isoradial, then all zigzag paths are type I (see Definition 3.4).

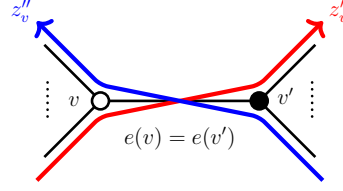
As the following lemmas show, the properties of type I zigzag paths are particularly nice.

Lemma 3.12. *Let z be a type I zigzag path on a consistent dimer model Γ . Then, there exists a perfect matching \mathbf{P} on Γ satisfying $|\mathbf{P} \cap z| = 0$, which means that \mathbf{P} is in $\text{PM}_{\min}(z)$.*

Proof. In order to find a perfect matching \mathbf{P} , we will use the method discussed in [14, Section 3], [7, Section 4]. For this, we first prepare some notation.

We consider the sequence $[z_1], \dots, [z_n]$ of slopes of zigzag paths on Γ . Since Γ is consistent, it is properly ordered, and thus we can assume that the slopes are ordered cyclically with this order. We note that some of the slopes may coincide. Then, we define the normal fan in $H_1(\mathbb{T}) \otimes_{\mathbb{Z}} \mathbb{R}$ whose rays are slopes $[z_1], \dots, [z_n]$. In particular, each two-dimensional cone σ is generated by different adjacent slopes. We denote by θ_i the angle formed by $[z_i]$. Here, we suppose that $z = z_k$. Let \mathcal{R} be a ray whose angle is $\theta_k + \pi + \epsilon$ where $\epsilon > 0$ is a sufficiently small angle satisfying the condition that $\theta_k + \pi + \epsilon$ does not coincide with any θ_i .

Then, for each node $v \in \Gamma_0$, we define the fan $\xi(v)$ generated by the slopes of zigzag paths factoring through v . In this fan $\xi(v)$, we can find the zigzag path z'_v whose slope makes the smallest clockwise angle with \mathcal{R} , and the zigzag path z''_v whose slope makes the smallest anti-clockwise angle with \mathcal{R} . Since Γ is properly ordered, these zigzag paths are consecutive around v . The intersection of z'_v and z''_v is the edge $e(v)$ which has v as an endpoint.



We then apply the same argument to the node v' which is the other endpoint of $e(v)$. The proper ordering on Γ leads to the conclusion that $e(v) = e(v')$ (see the above figure). We repeat these arguments for any node, but it is enough to consider $e(v)$'s for any $v \in \Gamma_0^+$ (or $v \in \Gamma_0^-$). By [14, Section 3.2] or [7, Lemma 4.19], we see that the subset of edges $e(v)$ for all $v \in \Gamma_0^+$ forms a perfect matching. Furthermore, since $z = z_k$ is type I, there exists a zigzag path whose slope is located at an angle less than π in an anti-clockwise (resp. clockwise) direction from $[z]$ in $\xi(v)$ by [7, Lemma 4.11 and its proof], in which case such a slope is located between $[z]$ and $[z'_v]$ (resp. $[z''_v]$) or coincides with $[z'_v]$ (resp. $[z''_v]$). Thus, we have $z \neq z'_v$ and $z \neq z''_v$ by the definition of the ray \mathcal{R} . Therefore, in this case $e(v)$ is not contained in z by the above construction. Also, we see that if a node v does not lie on z , $e(v)$ is not contained in z . Thus, the perfect matching constructed in the above fashion satisfies the desired condition. ■

Lemma 3.13. *Let z be a type I zigzag path on a consistent dimer model. Then, we have $\omega_{\min}(z) = 0$, and hence $\ell(z)$ is the same for all type I zigzag paths having the same slope.*

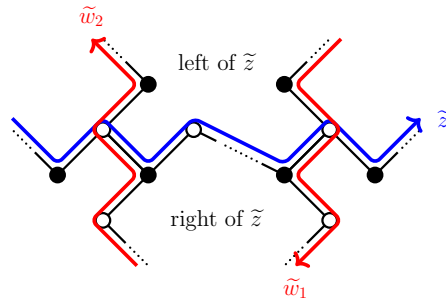
Proof. This follows from Lemmas 3.10 and 3.12. ■

For zigzag paths z, w on a dimer model Γ , we denote by $z \cap w$ the subset of edges that are intersections of z and w on Γ . We remark that if z is type I then the number of intersections of \tilde{z} and \tilde{w} on $\tilde{\Gamma}$ is less than or equal to one, but there are possibly more intersections of z and w if we consider them on Γ .

Lemma 3.14. *Let z be a type I zigzag path on a reduced consistent dimer model Γ . We suppose that a zigzag path w has intersections with z on Γ . Then, we see that $z \cap w \subset \text{Zig}(z)$ or $z \cap w \subset \text{Zag}(z)$.*

Proof. Let e_1, e_2 be edges of Γ , and we assume that w intersects with z at e_1 and e_2 . If e_i is a zig of z , then it is a zag of w , and vice versa. We assume that e_1 is a zig of z and e_2 is a zag of z .

We then lift these edges on the universal cover $\tilde{\Gamma}$. Let \tilde{e}_1, \tilde{e}_2 be edges of $\tilde{\Gamma}$ whose restrictions on Γ are e_1, e_2 , respectively. In particular, \tilde{e}_1 is a zig of \tilde{z} and \tilde{e}_2 is a zag of \tilde{z} . Then, there exist zigzag paths \tilde{w}_1, \tilde{w}_2 on $\tilde{\Gamma}$ whose restriction on Γ is just w , and \tilde{w}_1 (resp. \tilde{w}_2) intersects with \tilde{z} at \tilde{e}_1 (resp. \tilde{e}_2). The zigzag path \tilde{z} splits \mathbb{R}^2 into two pieces, and \tilde{w}_1 (resp. \tilde{w}_2) intersects with \tilde{z} from left to right (resp. right to left) by the definition of zigzag paths (see the figure below).



Since z is type I, there is no intersections of \tilde{z} and \tilde{w}_i except \tilde{e}_i where $i = 1, 2$. Thus, we can not superimpose \tilde{w}_1 and \tilde{w}_2 using translations. This contradicts a choice of \tilde{w}_1, \tilde{w}_2 . ■

The following lemma follows from the argument in the proof of [7, Proposition 3.12].

Lemma 3.15. *Let z, w be zigzag paths on a consistent dimer model Γ . We assume that \tilde{z} intersects with \tilde{w} on the universal cover $\tilde{\Gamma}$ at most once. Then, the slopes $[z], [w]$ are linearly independent if and only if \tilde{z} and \tilde{w} intersect on precisely one edge.*

Lemma 3.16. *Let z_1, \dots, z_r be type I zigzag paths on a reduced consistent dimer model Γ having the same slope. We suppose that a zigzag path w has intersections with z_j for some j . Then, w intersects with every z_i ($i = 1, \dots, r$), and the intersections $w \cap z_1, \dots, w \cap z_r$ are all in $\text{Zig}(w)$ or all in $\text{Zag}(w)$. Moreover, we have $|w \cap z_1| = \dots = |w \cap z_r|$.*

Proof. Since z_1, \dots, z_r are type I, \tilde{w} intersects with each \tilde{z}_i at most once. Thus, each pair of zigzag paths (\tilde{w}, \tilde{z}_i) for $i = 1, \dots, r$ satisfies the assumption in Lemma 3.15. Since w has intersections with z_j , \tilde{w} intersects with \tilde{z}_j precisely once on the universal cover. By Lemma 3.15, we see that $[w]$ and $[z_j]$ are linearly independent, and hence $[w]$ and $[z_i]$ are linearly independent for any i . Thus, \tilde{w} intersects with \tilde{z}_i precisely once for any $i = 1, \dots, r$.

The latter assertion follows from a similar argument as in the proof of Lemma 3.14. More precisely, since \tilde{w} intersects with \tilde{z}_i precisely once for any $i = 1, \dots, r$, if \tilde{w} intersects with \tilde{z}_i from right to left (resp. left to right), then so do zigzag paths having the same slope. This means that intersections are all in $\text{Zig}(w)$ (resp. all in $\text{Zag}(w)$).

Also, let \tilde{z}_1 and \tilde{z}'_1 be zigzag paths on $\tilde{\Gamma}$ that are projected onto the zigzag path z_1 on Γ . We assume that there is no zigzag path projected onto z_1 between \tilde{z}_1 and \tilde{z}'_1 . Also, we assume that \tilde{w} first intersects with \tilde{z}_1 , then intersects with \tilde{z}'_1 . Then, for all $i = 2, \dots, r$ we can find a unique zigzag path \tilde{z}_i on $\tilde{\Gamma}$ such that it is projected onto z_i and is located between \tilde{z}_1 and \tilde{z}'_1 . Thus, after \tilde{w} intersects with \tilde{z}_1 , it intersects with $\tilde{z}_2, \dots, \tilde{z}_r$ precisely once and then arrives at \tilde{z}'_1 . We can apply the same arguments for any pair $(\tilde{z}_1, \tilde{z}'_1)$ of zigzag paths on $\tilde{\Gamma}$ satisfying the above properties. Thus, projecting onto Γ we have $|w \cap z_1| = \dots = |w \cap z_r|$. ■

4 Deformations of dimer models

In this section, we will introduce the concept of a deformation of consistent dimer models. This operation is defined for type I zigzag paths on a consistent dimer model, and there are two kinds of deformations, which we call the zig-deformation (see Definition 4.3) and the zag-deformation (see Definition 4.4). For some special cases, these deformations preserve the consistency condition (see Proposition 4.5), but they change the associated PM polygon, whereas we will see that the PM polygon of the deformed dimer model is exactly the combinatorial mutation of a polygon (see Theorem 5.10).

4.1 Definition of deformations of dimer models

Let Γ be a reduced consistent dimer model. In particular, any slope of a zigzag path on Γ is primitive. Let $\mathcal{Z}_v(\Gamma)$ be the subset of zigzag paths on Γ whose slopes are the primitive vector $v \in \mathbb{Z}^2$, and $\mathcal{Z}_v^I(\Gamma)$ be the subset of $\mathcal{Z}_v(\Gamma)$ consisting of type I zigzag paths. We first prepare the *deformation data*.

Definition 4.1 (deformation data). Let Γ be a reduced consistent dimer model. In order to define the deformation of Γ , we fix the following data.

- (1) We choose a type I zigzag path z , and let $2n := \ell(z)$ and $v := [z]$.
- (2) We then fix a positive integer r such that $r \leq |\mathcal{Z}_v^I(\Gamma)|$, and let $h = n - r$.

- (3) We take a subset $\{z_1, \dots, z_r\} \subset \mathcal{Z}_v^I(\Gamma)$ of type I zigzag paths, in which case we have $2n = \ell(z_1) = \dots = \ell(z_r)$ by Lemma 3.13. Therefore, each z_i can be described as

$$z_i = z_i[1]z_i[2] \cdots z_i[2n-1]z_i[2n].$$

- (4) We consider non-negative integers $p_1, \dots, p_r \in \mathbb{Z}_{\geq 0}$ such that $p_1 + \dots + p_r = n - r = h$. We call $\mathbf{p} := (p_1, \dots, p_r)$ a *deformation weight* of $\{z_1, \dots, z_r\}$.

Remark 4.2. To define the deformation data, we need a type I zigzag path. If a dimer model is isoradial, then any zigzag path is type I (see Definition 3.4), and hence $|\mathcal{Z}_v^I(\Gamma)| = |\mathcal{Z}_v(\Gamma)|$. Also, even if Γ contains no type I zigzag paths, we sometimes change a type II zigzag path into type I by using the *mutations of dimer models* (see Appendix A, especially Example A.4).

Definition 4.3 (zig-deformation). Let the notation be the same as in Definition 4.1. For a deformation weight $\mathbf{p} = (p_1, \dots, p_r)$ of $\{z_1, \dots, z_r\}$, we consider the following procedures:

- (zig-1) Using split moves, we insert p_i white nodes and p_i black nodes in each zig of z_i .

[Notation]

- For any zig $z_i[2m-1]$ of z_i where $m = 1, \dots, n$ and $i = 1, \dots, r$, we denote by $b_i[2m-1]$ (resp. $w_i[2m-1]$) the black (resp. white) node that is the endpoint of $z_i[2m-1]$.
- We denote the white nodes added in the zig $z_i[2m-1]$ by $w_{i,1}[2m-1], \dots, w_{i,p_i}[2m-1]$, and the black ones by $b_{i,1}[2m-1], \dots, b_{i,p_i}[2m-1]$. Here, the subscripts increase in the direction from $b_i[2m-1]$ to $w_i[2m-1]$.

- (zig-2) We remove all zags of z_i for every $i = 1, \dots, r$.

- (zig-3) If $p_i \neq 0$, then we connect the white node $w_{i,j}[2m-1]$ to the black node $b_{i,j}[2m+1]$ where $j = 1, \dots, p_i$ and $m = 1, \dots, n$. (Note that $w_{i,j}[2n-1]$ is connected to $b_{i,j}[2n+1] := b_{i,j}[1]$.) We denote by $z_{i,j}$ the new 1-cycle, which will be a zigzag path on the deformed dimer model, obtained by connecting

$$w_{i,j}[2n-1], b_{i,j}[2n-1], w_{i,j}[2n-3], b_{i,j}[2n_i-3], \dots, w_{i,j}[1], b_{i,j}[1]$$

cyclically ($i = 1, \dots, r$ and $j = 1, \dots, p_i$).

- (join) If there exist 2-valent nodes, then we apply the join moves to the dimer model obtained by the above procedures and make it reduced.

We denote the resulting dimer model by $\nu_{\mathbf{p}}^{\text{zig}}(\Gamma, \{z_1, \dots, z_r\})$, and call it the *zig-deformation of Γ at $\{z_1, \dots, z_r\}$ with respect to the weight \mathbf{p}* . If a situation is clear, we simply denote this by $\nu_{\mathbf{p}}^{\text{zig}}(\Gamma)$.

Similarly, we can define the “zag version” of this deformation as follows.

Definition 4.4 (zag-deformation). Let the notation be the same as Definition 4.1. For a deformation weight $\mathbf{p} = (p_1, \dots, p_r)$ of $\{z_1, \dots, z_r\}$, we consider the following procedures:

- (zag-1) Using split moves, we insert p_i white nodes and p_i black nodes in each zag of z_i .

[Notation]

- For any zag $z_i[2m]$ of z_i where $m = 1, \dots, n$ and $i = 1, \dots, r$, we denote by $w_i[2m]$ (resp. $b_i[2m]$) the white (resp. black) node that is the endpoint of $z_i[2m]$.
- We denote the white nodes added in the zag $z_i[2m]$ by $w_{i,1}[2m], \dots, w_{i,p_i}[2m]$, and the black ones by $b_{i,1}[2m], \dots, b_{i,p_i}[2m]$. Here, the subscripts increase in the direction from $w_i[2m]$ to $b_i[2m]$.

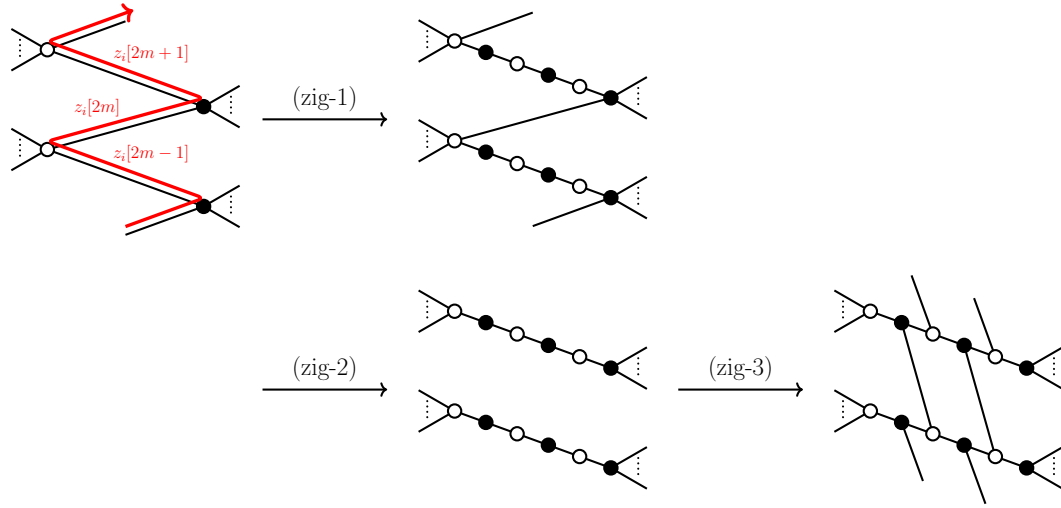


Figure 4.1. The zig-deformation at z_i with $p_i = 2$.

(zag-2) We remove all zigs of z_i for every $i = 1, \dots, r$.

(zag-3) If $p_i \neq 0$, then we connect the black node $b_{i,j}[2m]$ to the white node $w_{i,j}[2m+2]$ where $j = 1, \dots, p_i$ and $m = 1, \dots, n$. (Note that $b_{i,j}[2n]$ is connected to $w_{i,j}[2n+2] := w_{i,j}[2]$.) We denote by $z_{i,j}$ the new 1-cycle, which will be a zigzag path on the deformed dimer model, obtained by connecting

$$b_{i,j}[2n], w_{i,j}[2n], b_{i,j}[2n-2], w_{i,j}[2n-2], \dots, b_{i,j}[2], w_{i,j}[2]$$

cyclically ($i = 1, \dots, r$ and $j = 1, \dots, p_i$).

(join) If there exist 2-valent nodes, then we apply the join moves to the dimer model obtained by the above procedures and make it reduced.

We denote the resulting dimer model by $\nu_{\mathbf{p}}^{\text{zag}}(\Gamma, \{z_1, \dots, z_r\})$, and call it the *zag-deformation* of Γ at $\{z_1, \dots, z_r\}$ with respect to the weight \mathbf{p} . If a situation is clear, we simply denote this by $\nu_{\mathbf{p}}^{\text{zag}}(\Gamma)$.

For some special cases, these deformations preserve the consistency condition as in Proposition 4.5 below. Note that in Section 6 we will introduce extended deformations of dimer models which always preserve the consistency condition (see Proposition 6.7).

Proposition 4.5. *Let the notation be the same as Definitions 4.1, 4.3 and 4.4. We assume that either one of the following conditions is satisfied:*

(i) $r = 1$ or

(ii) Γ is a hexagonal or rectangular dimer model (see Definition 2.1).

Then, the dimer models $\nu_{\mathbf{p}}^{\text{zig}}(\Gamma, \{z_1, \dots, z_r\})$ and $\nu_{\mathbf{p}}^{\text{zag}}(\Gamma, \{z_1, \dots, z_r\})$ are consistent.

Proof. This follows from Proposition 6.7 (see also Remark 6.4 and Proposition 7.12). ■

We note that for some cases the zig-deformation and zag-deformation are mutually inverse operations on the level of dimer models as in Proposition 4.6 below. To observe this, let $\nu_{\mathbf{p}}^{\text{zig}}(\Gamma, \{z_1, \dots, z_r\})$ be the zig-deformed dimer model as in Definition 4.3. We assume that $p_i = 1$ for some i and consider the zigzag path $z_{i,p_i} = z_{i,1}$ on $\nu_{\mathbf{p}}^{\text{zig}}(\Gamma)$ created in place of z_i on Γ

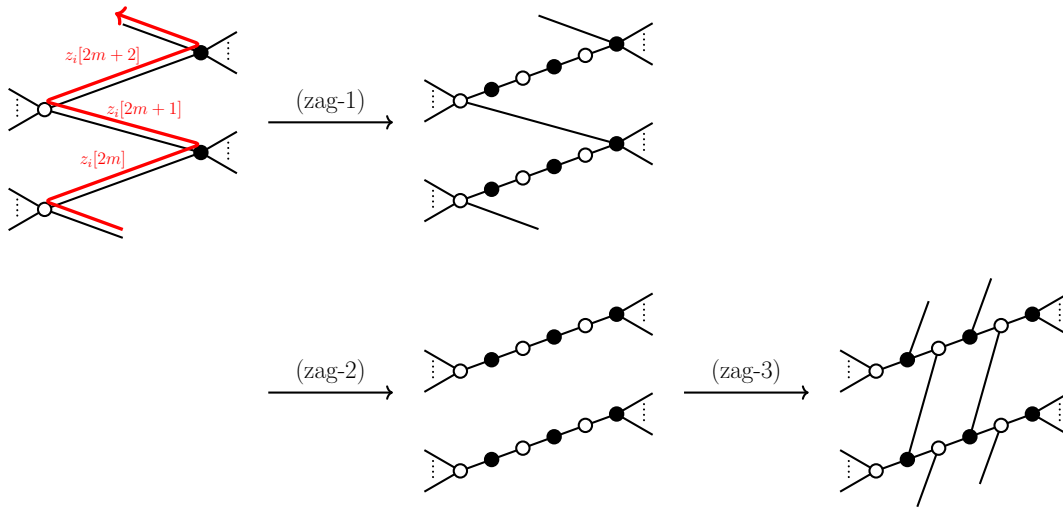


Figure 4.2. The zag-deformation at z_i with $p_i = 2$.

via the zig-deformation. Note that $z_{i,1}$ is type I (see Proposition 7.5). Then, we take a new deformation data \mathbf{q} so that $z_{i,1}$ is chosen in the data with the weight 1, and consider the zag-deformation of $\nu_{\mathbf{p}}^{\text{zig}}(\Gamma)$ at some set of zigzag paths with respected to \mathbf{q} . Through this operation, $z_{i,1}$ changes into the original zigzag path z_i as in Figure 4.3.

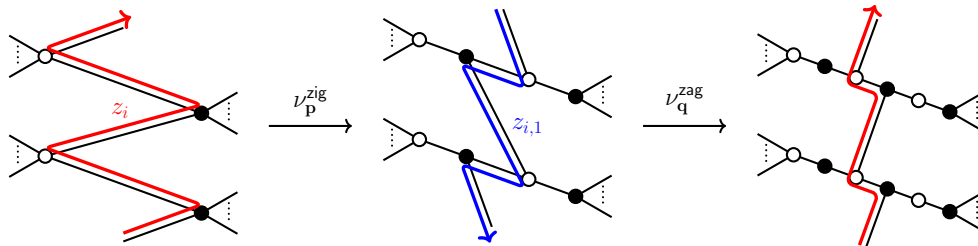


Figure 4.3. Transitions of z_i via the composition of the zig-deformation and zag-deformation. (In the rightmost figure, we still do not apply (join). The zigzag path in this figure coincides with z_i after applying (join).)

The next proposition follows from these observations.

Proposition 4.6. *We consider the situation as in Definition 4.1, and assume that $p_1 = \dots = p_r = 1$, in which case $r = h$. Let $z_{i,p_i} = z_{i,1}$ ($i = 1, \dots, r$) be the zigzag path of $\nu_{\mathbf{p}}^{\text{zig}}(\Gamma, \{z_1, \dots, z_r\})$ (resp. $\nu_{\mathbf{p}}^{\text{zag}}(\Gamma, \{z_1, \dots, z_r\})$) created by modifying z_i as in Definition 4.3 (resp. Definition 4.4). We take $\mathbf{q} = (1, \dots, 1)$ as a deformation weight of $\{z_{1,1}, \dots, z_{r,1}\}$. Then, we respectively have*

$$\begin{aligned} \nu_{\mathbf{q}}^{\text{zag}}(\nu_{\mathbf{p}}^{\text{zig}}(\Gamma, \{z_1, \dots, z_r\}), \{z_{1,1}, \dots, z_{r,1}\}) &= \Gamma, \\ \nu_{\mathbf{q}}^{\text{zig}}(\nu_{\mathbf{p}}^{\text{zag}}(\Gamma, \{z_1, \dots, z_r\}), \{z_{1,1}, \dots, z_{r,1}\}) &= \Gamma. \end{aligned}$$

This property depends on a choice of a deformation data, thus in general these deformations are not mutually inverse as in Example 4.9 given in the next subsection. Whereas, on the level of the PM polygons, they are mutually inverse as we will see in Corollary 8.6.

4.2 Examples of deformations of dimer models

In this subsection we give several examples for the case of $r = 1$, in which the deformed dimer model is consistent (see Proposition 4.5).

Example 4.7. Let Γ be the dimer model given in Figure 2.1. We consider zigzag paths on Γ given in Figure 3.1. We first collect the deformation data (see Definition 4.1). Let us choose the zigzag path z_3 , and denote it by z . We see that $\ell(z) = 6$, $v := [z] = (-1, -1)$, and $|\mathcal{Z}_v^I(\Gamma)| = 1$. Since $|\mathcal{Z}_v^I(\Gamma)| = 1$, we can take only $r = 1$, in which case $h = \ell(z)/2 - r = 2$. Thus, we consider the deformation weight $p = h = 2$. The zig-deformation $\nu_p^{\text{zig}}(\Gamma, z)$ of Γ at z with $p = 2$ is shown in Figure 4.4.

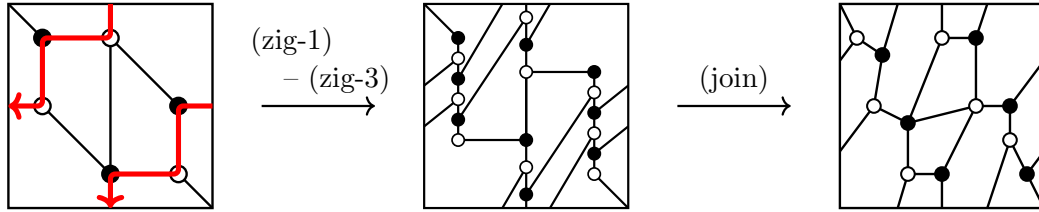


Figure 4.4. The zig-deformation $\nu_p^{\text{zig}}(\Gamma, z)$ of Γ at z .

We give the zag-deformation $\nu_p^{\text{zag}}(\Gamma, z)$ of Γ at z with $p = 2$ as in Figure 4.5.

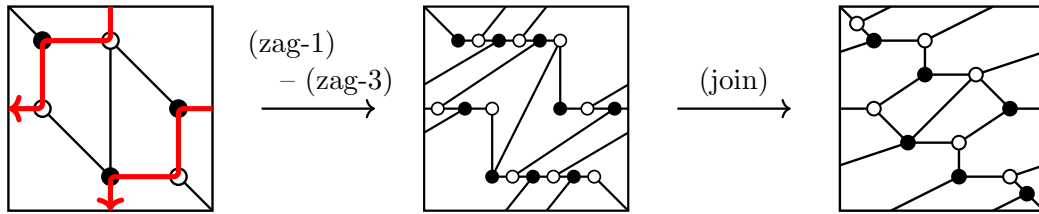


Figure 4.5. The zag-deformation $\nu_p^{\text{zag}}(\Gamma, z)$ of Γ at z .

Example 4.8. We remark that even if Γ is an isoradial dimer model, the deformed ones are not necessarily isoradial. For example, the leftmost dimer model Γ in Figure 4.6 is isoradial. We choose a type I zigzag path z whose slope is $v = (-1, 0)$, in which case $|\mathcal{Z}_v^I(\Gamma)| = 2$ and $\ell(z) = 4$. We fix $r = 1$, and hence $h = \ell(z)/2 - r = 1$. Applying the zig-deformation at z with $p = 1$ to Γ , we have the rightmost one in Figure 4.6. One can check that the deformed dimer model is consistent but not isoradial.

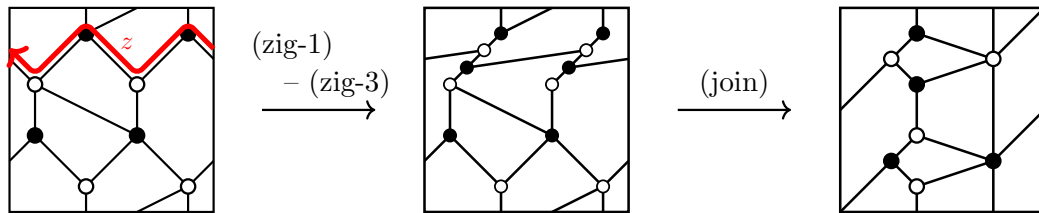


Figure 4.6. An example of the deformed dimer model that is not isoradial.

Example 4.9. We here give an example showing that the zig-deformation and zag-deformation are not mutually inverse operations on the level of dimer models in general.

We consider the consistent dimer model Γ that takes the form as in the top-left of Figure 4.7, and the type I zigzag path z on Γ . We see that $[z] = (-1, 0)$ and $\ell(z) = 4$. Let $r = 1$, and hence $h = \ell(z)/2 - r = 1$. Then, the zig-deformation $\nu_p^{\text{zig}}(\Gamma, z)$ of Γ at z with the deformation weight $p = h = 1$ is the top-right of Figure 4.7. Through this process, the new zigzag path on $\nu_p^{\text{zig}}(\Gamma, z)$ whose slope is $(1, 0)$ has been created. If we apply the zag-deformation with the deformation weight $q = 1$ to this new zigzag path, then we recover the original dimer model Γ as we saw in Proposition 4.6. On the other hand, there is another type I zigzag path on $\nu_p^{\text{zig}}(\Gamma, z)$ whose slope is $(1, 0)$, which is denoted by z' . We see that $\ell(z') = 4$, and consider $r = 1$, and hence $h = \ell(z')/2 - r = 1$. Applying the zag deformation at z' with the deformation weight $q = h = 1$ to $\nu_p^{\text{zig}}(\Gamma, z)$, we have the dimer model $\nu_q^{\text{zag}}(\nu_p^{\text{zig}}(\Gamma, z), z')$ shown in the bottom-right of Figure 4.7, which is not isomorphic to Γ . Nevertheless, Γ and $\nu_q^{\text{zag}}(\nu_p^{\text{zig}}(\Gamma, z), z')$ are “mutation-equivalent” (see, e.g., [27, Section 5.11]) and hence their PM polygons are the same, see Appendix A for more details of the mutation.

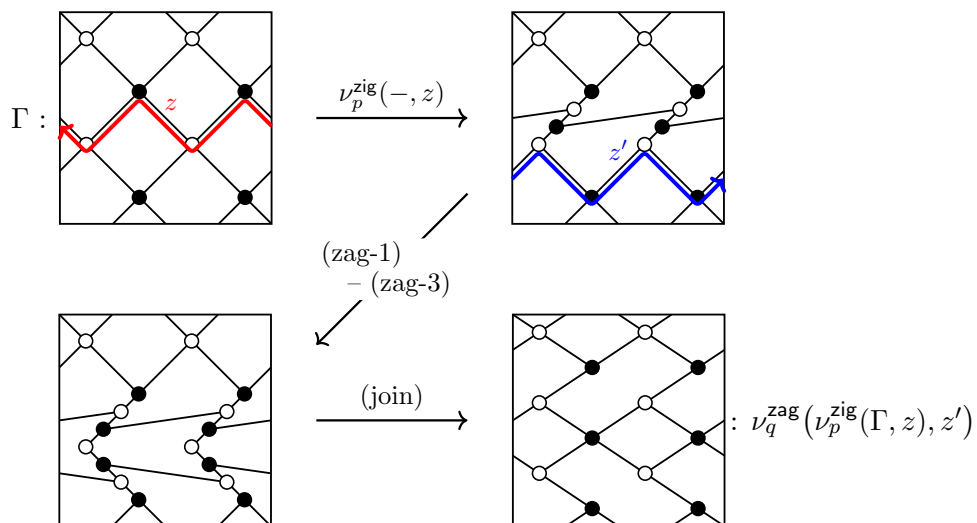


Figure 4.7. An example showing that the zig-deformation and zag-deformation are not mutually inverse operations.

5 Combinatorial mutations of perfect matching polygons

In this section, we discuss a relationship between deformations of consistent dimer models and combinatorial mutations of polygons. We first define combinatorial mutations for lattice polytopes of any dimension, and then we mainly discuss the case of polygons.

5.1 Preliminaries on combinatorial mutations of polytopes

Following [2], we introduce combinatorial mutations of polytopes. Let $N \cong \mathbb{Z}^d$ be a lattice of rank d , and $P \subset N_{\mathbb{R}} := N \otimes_{\mathbb{Z}} \mathbb{R}$ be a convex lattice polytope. We assume that P contains the origin $\mathbf{0}$. We denote by $\mathcal{V}(P)$ the set of vertices of P . We say that two polytopes $P, Q \subset N_{\mathbb{R}}$ are *isomorphic* if they are transformed into each other by $\text{GL}(d, \mathbb{Z})$ -transformations, in which case we denote $P \cong Q$.

We first prepare some notions used in the definition of combinatorial mutations of polytopes.

Definition 5.1 (mutation data). Let P be a convex lattice polytope as above. In order to define a combinatorial mutation of P , we fix the data consisting of a vector w and the associated integers $h_{\max}(P, w)$, $h_{\min}(P, w)$ and $\text{width}(P, w)$ defined as follows.

Let $w \in M := \text{Hom}_{\mathbb{Z}}(N, \mathbb{Z}) \cong \mathbb{Z}^d$ be a primitive lattice vector. The element $w \in M$ determines the linear map $\langle w, - \rangle : N_{\mathbb{R}} \rightarrow \mathbb{R}$, where $\langle -, - \rangle$ is the natural inner product. We set

$$h_{\max}(P, w) := \max\{\langle w, u \rangle \mid u \in P\} \quad \text{and} \quad h_{\min}(P, w) := \min\{\langle w, u \rangle \mid u \in P\},$$

which are integers since P is a lattice polytope. When the situation is clear, we simply denote these by h_{\max} and h_{\min} , respectively. We define the *width* of P with respect to w as

$$\text{width}(P, w) := h_{\max}(P, w) - h_{\min}(P, w).$$

We note that if the origin $\mathbf{0}$ is contained in the strict interior P° of P , then $h_{\min} < 0$ and $h_{\max} > 0$, in which case we have $\text{width}(P, w) \geq 2$. We say that a lattice point $u \in N$ (resp. a subset $F \in N_{\mathbb{R}}$) is at *height* m with respect to w if $\langle w, u \rangle = m$ (resp. $\langle w, u \rangle = m$ for any $u \in F$).

For each height $h \in \mathbb{Z}$, we let

$$w_h(P) := \text{conv}\{u \in P \cap N \mid \langle w, u \rangle = h\},$$

which is the (possibly empty) convex hull of all lattice points in P at height h . By definition, $w_{h_{\min}}(P)$ and $w_{h_{\max}}(P)$ are faces of P . Using these notions, a combinatorial mutation of P is defined as follows.

Definition 5.2. Let the notation be the same as above. We assume that there exists a lattice polytope $F \subset N_{\mathbb{R}}$ such that $\langle w, u \rangle = 0$ for any $u \in F$, and for each negative height $h_{\min} \leq h < 0$ there exists a possibly empty lattice polytope $G_h \subset N_{\mathbb{R}}$ satisfying

$$\{u \in \mathcal{V}(P) \mid \langle w, u \rangle = h\} \subseteq G_h + (-h)F \subseteq w_h(P), \quad (5.1)$$

where $+$ means the Minkowski sum, and we especially define $Q + \emptyset = \emptyset$ for any polytope Q . We call F a *factor* of P with respect to w . Then, we define the *combinatorial mutation* of P given by the vector w , factor F and polytopes $\{G_h\}$ as

$$\text{mut}_w(P, F) := \text{conv} \left(\bigcup_{h=h_{\min}}^{-1} G_h \cup \bigcup_{h=0}^{h_{\max}} (w_h(P) + hF) \right).$$

We note that the combinatorial mutation is independent of the choice of the polytopes $\{G_h\}$ (see [2, Proposition 1]). Also, a translation of the factor F does not affect the combinatorial mutation; that is, for any $u \in N$ with $\langle w, u \rangle = 0$ we have $\text{mut}_w(P, F) \cong \text{mut}_w(P, u + F)$; see [2] for more details.

Remark 5.3 (the combinatorial mutation for the case of $d = 2$). When $d = 2$, we choose an edge E of a lattice polygon P , and take $w \in M \cong \mathbb{Z}^2$ as a primitive inner normal vector for E . By the choice of w , we see that $w_{h_{\min}}(P) = E$ and $w_{h_{\max}}(P)$ is either a vertex or an edge of P . Then, we take a primitive lattice element $u_E \in N$ satisfying $\langle w, u_E \rangle = 0$, and define the line segment $F := \text{conv}\{\mathbf{0}, u_E\}$, which is parallel to E at height 0 and has unit lattice length. Since u_E is uniquely determined up to sign, so is F . In this case, P admits a combinatorial mutation with respect to w (equivalently, there exist polytopes $\{G_h\}$ satisfying (5.1)) if and only if $|E \cap N| - 1 \geq -h_{\min}$, see [22, Lemma 1]. We note that the combinatorial mutation does not depend on the choice of u_E (and hence F). That is, $\text{mut}_w(P, F) \cong \text{mut}_w(P, -F)$, which means they are $\text{GL}(2, \mathbb{Z})$ -equivalent.

Example 5.4. We consider the polygon P given in the left of Figure 5.1 below, which coincides with the PM polygon of the dimer model given in Figure 2.1 (see also Figure 2.5). Here, the double circle stands for the origin $\mathbf{0}$. We consider the edge E whose primitive inner normal vector is $w = (1, 1)$, in which case $h_{\min} = -1$ and $h_{\max} = 2$. We take $u_E = (1, -1) \in N$, which satisfies $\langle w, u_E \rangle = 0$, and consider the line segment $F = \text{conv}\{\mathbf{0}, u_E\}$. The combinatorial mutation $\text{mut}_w(P, F)$ of the polygon P is shown in the upper part of Figure 5.1. On the other hand, if we consider the line segment $-F = \text{conv}\{\mathbf{0}, -u_E\}$, the combinatorial mutation $\text{mut}_w(P, -F)$ is as shown in the lower part of Figure 5.1.

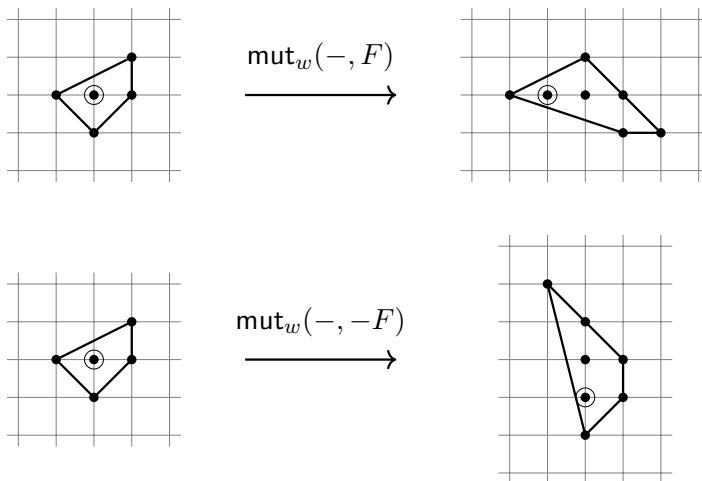


Figure 5.1. Examples of the combinatorial mutations of P .

Now, we collect fundamental properties of this combinatorial mutation.

Proposition 5.5 (see [2, Lemma 2 and Proposition 2]). *Let the notation be the same as above.*

- (1) If $Q := \text{mut}_w(P, F)$, then we have $P = \text{mut}_{(-w)}(Q, F)$.
- (2) P is a Fano polytope if and only if $\text{mut}_w(P, F)$ is a Fano polytope.

Here, we recall that a convex lattice polytope $P \subset N_{\mathbb{R}}$ with $\dim P = d$ is called *Fano* if the origin is contained in the strict interior of P , and the vertices $\mathcal{V}(P)$ of P are primitive lattice points of N .

Then, we consider the combinatorial mutation of a lattice polytope P in terms of the polar dual P^* of P in M . To do this, we must first discuss the polar dual P^* for a polyhedron P . We consider the family of polyhedra (not necessarily convex polytopes) which are of the following form:

$$\mathcal{P}^d := \left\{ \bigcap_{v \in S} H_{v, \geq -k_v} \cap \bigcap_{v' \in T} H_{v', \geq 0} \subset N_{\mathbb{R}} \mid S, T \subset M, |S|, |T| < \infty, k_v \in \mathbb{Z}_{>0} \right\},$$

where $H_{v, \geq k} = \{u \in N_{\mathbb{R}} \mid \langle v, u \rangle \geq k\}$ for $v \in M$ and $k \in \mathbb{R}$. We note that any lattice polytope containing the origin of $N_{\mathbb{R}}$ belongs to \mathcal{P}^d but the ones not containing the origin do not belong to \mathcal{P}^d since one of the supporting hyperplanes of such a polytope is of the form $H_{v, \geq k}$ for some $v \in M$ and some positive integer k . Similarly, we define \mathcal{Q}^d by swapping the roles of $N_{\mathbb{R}}$ and $M_{\mathbb{R}}$.

For a given $P \in \mathcal{P}^d$, we consider the *polar dual* $P^* \subset M_{\mathbb{R}}$ of P defined as

$$P^* := \{v \in M_{\mathbb{R}} \mid \langle v, u \rangle \geq -1 \text{ for all } u \in P\} \subset M_{\mathbb{R}}.$$

Then, we have the following statements.

Proposition 5.6. *Let the notation be the same as above. Then, for any $P \in \mathcal{P}^d$ we have*

- (i) $P^* \in \mathcal{Q}^d$,
- (ii) $(P^*)^* = P$.

Proof. (i) Let $P \in \mathcal{P}^d$. Since P is a polyhedron, there exist a polytope Q and a polyhedral cone C such that $P = Q + C$, where $+$ denotes the Minkowski sum (see [30, Corollary 7.1b]). Let $Q = \text{conv}\left(\left\{\frac{1}{k_1}u_1, \dots, \frac{1}{k_p}u_p\right\}\right)$ and let $C = \text{cone}(\{u'_1, \dots, u'_q\})$. Note that we can choose u_i, u'_j from N and $k_i \in \mathbb{Z}_{>0}$ because of the form of P . In what follows, we will show that

$$P^* = \bigcap_{i=1}^p H_{u_i, \geq -k_i} \cap \bigcap_{j=1}^q H_{u'_j, \geq 0}.$$

First, we take $v \in P^*$. Then, we have $\langle v, u \rangle \geq -1$ for any $u \in P$. Since $\frac{1}{k_i}u_i \in Q + \mathbf{0} \subset P$, where $\mathbf{0} \in C$ denotes the origin, we see that $\langle v, \frac{1}{k_i}u_i \rangle \geq -1$, i.e., $\langle v, u_i \rangle \geq -k_i$ for each i . If there is j with $\langle v, u'_j \rangle < 0$, then $\langle v, u' + ru'_j \rangle < -1$ for some $u' \in Q$ and some sufficiently large r . Moreover, we have $u' + ru'_j \in Q + C = P$. This contradicts $v \in P^*$; thus $\langle v, u'_j \rangle \geq 0$ for each j . Therefore, $v \in \bigcap_{i=1}^p H_{u_i, \geq -k_i} \cap \bigcap_{j=1}^q H_{u'_j, \geq 0}$.

On the other hand, we take $v \in \bigcap_{i=1}^p H_{u_i, \geq -k_i} \cap \bigcap_{j=1}^q H_{u'_j, \geq 0}$. For any $u \in P$, as mentioned above, there exist $u' \in Q$ and $u'' \in C$ such that $u = u' + u''$. Let $u' = \sum_{i=1}^p \frac{r_i}{k_i}u_i$, where $r_i \geq 0$ with $\sum_{i=1}^p r_i = 1$, and let $u'' = \sum_{j=1}^q s_j u'_j$, where $s_j \geq 0$. By using these expressions together with the inequalities $\langle v, u_i \rangle \geq -k_i$ for each i and $\langle v, u'_j \rangle \geq 0$ for each j , we see that

$$\langle v, u \rangle = \langle v, u' \rangle + \langle v, u'' \rangle = \sum_{i=1}^p \frac{r_i}{k_i} \langle v, u_i \rangle + \sum_{j=1}^q s_j \langle v, u'_j \rangle \geq -\sum_{i=1}^p r_i = -1,$$

and thus we have $v \in P^*$.

(ii) For any $u \in P$, we have $\langle v, u \rangle \geq -1$ for any $v \in P^*$, which means that $P \subset (P^*)^*$. For the other inclusion, we take $u \in N_{\mathbb{R}} \setminus P$. Let $P = \bigcap_{v \in S} H_{v, \geq -k_v} \cap \bigcap_{v' \in T} H_{v', \geq 0}$. Then either $\langle v, u \rangle < -k_v$ for some $v \in S$ or $\langle v', u \rangle < 0$ for some $v' \in T$ holds. In the former case, since $\langle v, u' \rangle \geq -k_v$ for any $u' \in P$, we have $\frac{1}{k_v}v \in P^*$. This means that there is $v'' := \frac{1}{k_v}v \in P^*$ such that $\langle v'', u \rangle < -1$, and hence $u \notin (P^*)^*$. Similarly, in the latter case, since $\langle rv', u' \rangle \geq 0 \geq -1$ for any $u' \in P$ and $r \geq 0$, we have $rv' \in P^*$. This implies that $u \notin (P^*)^*$ for sufficiently large r , and hence $u \notin (P^*)^*$. Therefore, we obtain $(P^*)^* \subset P$, as required. \blacksquare

We next define a map

$$\varphi_{w,F}: M_{\mathbb{R}} \rightarrow M_{\mathbb{R}} \quad \text{as} \quad \varphi_{w,F}(v) := v - v_{\min}w,$$

where $v_{\min} := \min\{\langle v, u \rangle \mid u \in F\}$. In particular, when $d = 2$ (see Remark 5.3), this map can be described as

$$\varphi_{w,F}(v) = \begin{cases} v & \text{if } \langle v, u_E \rangle \geq 0, \\ v - \langle v, u_E \rangle w & \text{if } \langle v, u_E \rangle < 0, \end{cases} \quad (5.2)$$

with $F = \text{conv}\{\mathbf{0}, u_E\}$. The next proposition is crucial to prove our main result Theorem 8.3.

Proposition 5.7. *For any $P \in \mathcal{P}^d$, we have*

$$\varphi_{w,F}(P^*) = \text{mut}_w(P, F)^*.$$

Proof. Although this equality essentially follows from [2, Proposition 4] and the discussions in [2, p. 12], we give a precise proof for completeness.

Let $\varphi = \varphi_{w,F}$ and $Q = \text{mut}_w(P, F)$. To show $\varphi(P^*) \subset Q^*$, we take $v \in P^*$ arbitrarily and consider $\varphi(v) = v - v_{\min}w \in \varphi(P^*)$. We will show that $\langle v - v_{\min}w, u \rangle \geq -1$ for any $u \in Q$. It suffices to show this for each vertex $u \in \mathcal{V}(Q)$.

- Let $u \in \mathcal{V}(Q)$ with $\langle w, u \rangle \geq 0$. Then we can write $u = u_P + \langle w, u_P \rangle u_F$ for some $u_P \in \mathcal{V}(P)$ and $u_F \in \mathcal{V}(F)$. In particular, we have

$$\langle v - v_{\min}w, u \rangle = \langle v, u_P \rangle + \langle w, u_P \rangle (\langle v, u_F \rangle - v_{\min}) \geq \langle v, u_P \rangle \geq -1.$$

- Let $u \in \mathcal{V}(Q)$ with $\langle w, u \rangle < 0$. For any $u_F \in \mathcal{V}(F)$, we have $u - \langle w, u \rangle u_F \in P$. Hence, $\langle v, u - \langle w, u \rangle u_F \rangle \geq -1$. In particular, $\langle v, u \rangle \geq -1 + v_{\min} \langle w, u \rangle$. Thus, we see that

$$\langle v - v_{\min}w, u \rangle = \langle v, u \rangle - v_{\min} \langle w, u \rangle \geq -1.$$

To show $Q^* \subset \varphi(P^*)$, we will show that for any $v \in Q^*$ there is $v' \in P^*$ such that $v = \varphi(v')$. Let Δ_F be the normal fan of F in $M_{\mathbb{R}}$ and let $\sigma \in \Delta_F$ be a maximal cone in Δ_F . The discussions in [2, p. 12] say that there exists $M_{\sigma} \in \text{GL}_d(\mathbb{Z})$ such that the map φ is equal to M_{σ} , i.e., $\varphi(v) = vM_{\sigma}$. Thus, we conclude that $\varphi(v') = v$ for $v' = vM_{\sigma}^{-1}$. ■

Example 5.8. Let P be the polygon used in Example 5.4. The polar dual P^* takes the form as in the left of Figure 5.2 below. We take $w = (1, 1)$, $u_E = (1, -1)$ and consider the line segment $F = \text{conv}\{\mathbf{0}, u_E\}$ just like Example 5.4. Then, applying the piecewise-linear map (5.2) with u_E (resp. $-u_E$) to the polar dual P^* , we have the new polygon shown in the upper (resp. lower) part of Figure 5.2. In this figure, the red line imply the points $v \in \mathbb{R}^2$ satisfying $\langle v, u_E \rangle = 0$. We see that the resulting polygons are the polar dual of $\text{mut}_w(P, F)$ and $\text{mut}_w(P, -F)$ given in Example 5.4 as shown in Proposition 5.7.

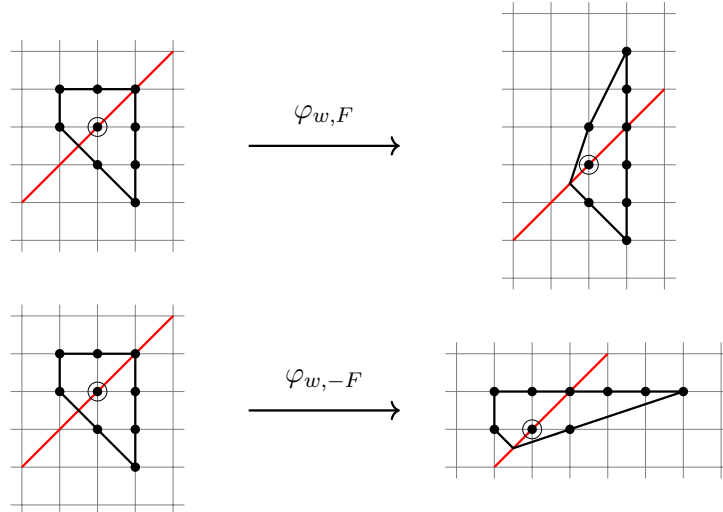
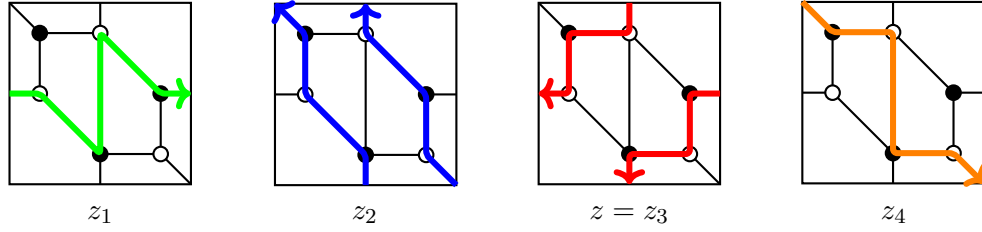


Figure 5.2. Examples of the image of P^* under the piecewise-linear map (5.2).

5.2 The perfect matching polygons of deformed dimer models

We here consider the PM polygons of deformed dimer models.

Example 5.9. Let Γ be the consistent dimer model given in Figure 2.1, and let $\nu_p^{\text{zig}}(\Gamma, z)$ (resp. $\nu_p^{\text{zag}}(\Gamma, z)$) be the zig-deformed (resp. zag-deformed) dimer model at z as shown in Figure 4.4 (resp. Figure 4.5) in Example 4.7. Here, we note the changes of zigzag paths on Γ under these deformations. First, we recall the zigzag paths on Γ given in Figure 3.1.



Then, we observe zigzag paths on $\nu_p^{\text{zig}}(\Gamma, z)$ and $\nu_p^{\text{zag}}(\Gamma, z)$, but it would be more convenient to see the zigzag paths on the dimer model shown in the middle of Figures 4.4 and 4.5 for observing the changes of zigzag paths as in Figures 5.3 and 5.4. In both cases, the zigzag path $z = z_3$ on Γ is removed and the new zigzag paths, which are colored by red, are created. The slopes of these new zigzag paths are $-[z]$. On the other hand, some slopes of zigzag paths on Γ are preserved even if we apply the deformations. For example, we have the zigzag path whose slope is $[z_2]$ on $\nu_p^{\text{zig}}(\Gamma, z)$ which is colored by blue in Figure 5.3. Also, we have the zigzag paths whose slopes are $[z_1]$, $[z_4]$ on $\nu_p^{\text{zag}}(\Gamma, z)$ which are respectively colored by green and orange in Figure 5.4. We will see these phenomena for more general situations in Propositions 7.5 and 7.6.

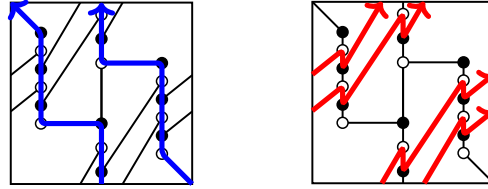


Figure 5.3. Some zigzag paths on the dimer model shown in the middle of Figure 4.4 which can be reduced to $\nu_p^{\text{zig}}(\Gamma, z)$.

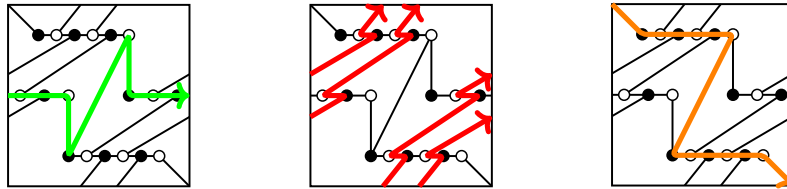


Figure 5.4. Some zigzag paths on the dimer model shown in the middle of Figure 4.5 which can be reduced to $\nu_p^{\text{zag}}(\Gamma, z)$.

Then, we respectively have the PM polygons as in Figure 5.5. We see that the shape of the PM polygon $\Delta_{\nu_p^{\text{zig}}(\Gamma, z)}$ (resp. $\Delta_{\nu_p^{\text{zag}}(\Gamma, z)}$) coincides with the combinatorial mutation $\text{mut}_w(P, F)$ (resp. $\text{mut}_w(P, -F)$) given in Example 5.4.

Example 5.9 indicates a close connection between the PM polygon of a deformed dimer model and the combinatorial mutation of the PM polygon of the original dimer model. In Section 8, we will show this phenomenon for a general situation by considering the *extended deformations* introduced in Section 6. In particular, as a special case of Theorem 8.3, we have Theorem 5.10

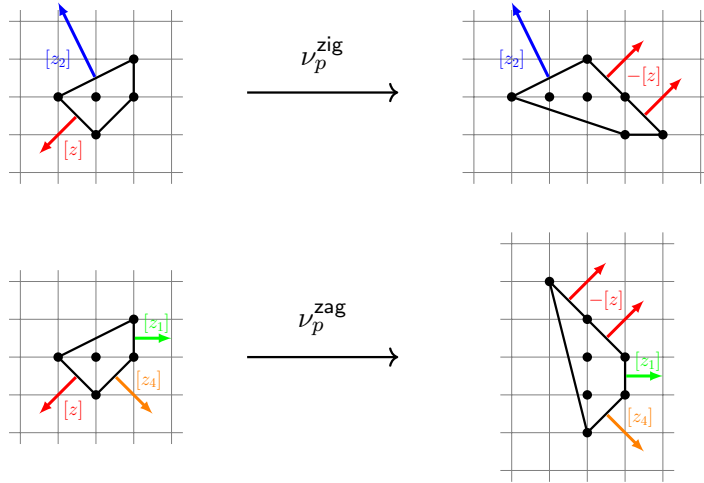


Figure 5.5. The changes of the associated PM polygon via the zig-deformation (upper) and the zag-deformation (lower).

below (see also Remark 6.4 and Proposition 7.12), and this explains the phenomenon observed in Example 5.9.

Theorem 5.10. *Let the notation be the same as in Definitions 4.1, 4.3 and 4.4. We assume that either one of the following conditions is satisfied:*

- (i) $r = 1$ or
- (ii) Γ is a hexagonal or rectangular dimer model (see Definition 2.1).

Then we have

$$\begin{aligned} \text{mut}_w(\Delta_\Gamma, F) &= \Delta_{\nu_{\mathbf{p}}^{\text{zig}}(\Gamma, \{z_1, \dots, z_r\})}, \\ \text{mut}_w(\Delta_\Gamma, -F) &= \Delta_{\nu_{\mathbf{p}}^{\text{zag}}(\Gamma, \{z_1, \dots, z_r\})} \end{aligned}$$

for certain choices of the deformation data and the mutation data (see Setting 8.1).

Combining this result with some properties of the combinatorial mutation given in Section 5.1, we have the following corollary, which will be generalized in Section 8 (see Corollaries 8.4 and 8.7).

Corollary 5.11. *Using the same setting as in Theorem 5.10, we see that*

- $\Delta_{\nu_{\mathbf{p}}^{\text{zig}}(\Gamma, \{z_1, \dots, z_r\})} \cong \Delta_{\nu_{\mathbf{p}}^{\text{zag}}(\Gamma, \{z_1, \dots, z_r\})}$
- Δ_Γ is Fano if and only if $\Delta_{\nu_{\mathbf{p}}^{\text{zig}}(\Gamma, \{z_1, \dots, z_r\})}$ (resp. $\Delta_{\nu_{\mathbf{p}}^{\text{zag}}(\Gamma, \{z_1, \dots, z_r\})}$) is Fano.

6 Extended deformations of dimer models

In this section, we add some procedures to the deformations given in Definitions 4.3 and 4.4 to construct a consistent dimer model having the same properties as Theorem 5.10 in a more general situation. The operations which will be introduced in this section might be complicated, thus we refer the reader to Figures 7.4–7.9 in the next section and Appendix B for recognizing their points.

Setting 6.1. Let Γ be a reduced consistent dimer model. As in Definition 4.1, we choose a type I zigzag path z , and we let $2n := \ell(z)$ and $v := [z]$. We fix positive integers r, h such that $r \leq |\mathcal{Z}_v^1(\Gamma)|$ and $n = r + h$, and take a subset $\{z_1, \dots, z_r\} \subset \mathcal{Z}_v^1(\Gamma)$ of type I zigzag paths. We recall that we have $2n = \ell(z_1) = \dots = \ell(z_r)$ by Lemma 3.13, and hence we write z_i as

$$z_i = z_i[1]z_i[2] \cdots z_i[2n-1]z_i[2n].$$

Then we prepare the additional data as follows.

- (1) We consider all zigzag paths x_1, \dots, x_s (resp. y_1, \dots, y_t) intersecting with z at some zags (resp. zigs) of z . In this case, each of x_1, \dots, x_s (resp. y_1, \dots, y_t) intersects with any z_i at some zags (resp. zigs) of z_i for all $i = 1, \dots, r$ by Lemma 3.16. We may assume that z_1, \dots, z_r are ordered cyclically in the sense that if x_j (resp. y_k) intersects with z_i , then it also intersects with z_{i-1} (resp. z_{i+1}).
- (2) We recall that $|x_j \cap z_i|$ (resp. $|y_k \cap z_i|$) is the same number for any $i = 1, \dots, r$ by Lemma 3.16. Thus, for $j \in \{1, \dots, s\}$ let $m_j := |x_j \cap z_i|$ be this constant, and for $k \in \{1, \dots, t\}$ let $m'_k := |y_k \cap z_i|$. We note that $n = m_1 + \dots + m_s = m'_1 + \dots + m'_t$.
- (3) Then, we divide each zigzag path x_j into m_j parts $x_j^{(1)}, \dots, x_j^{(m_j)}$ as follows. We first fix one of the intersections of z_r and x_j as the starting edge of $x_j^{(1)}$, and tracing along x_j we will arrive at another intersection of z_r and x_j . We consider the edge of x_j just before this intersection as the ending edge of $x_j^{(1)}$, and consider the second intersection as the starting edge of $x_j^{(2)}$. Repeating this procedure, we obtain $x_j^{(1)}, \dots, x_j^{(m_j)}$ and the set of sub-zigzag paths:

$$\{x_1^{(1)}, \dots, x_1^{(m_1)}, x_2^{(1)}, \dots, x_2^{(m_2)}, \dots, x_s^{(1)}, \dots, x_s^{(m_s)}\}. \quad (6.1)$$

Similarly, we also divide each zigzag path y_k into m'_k parts $y_k^{(1)}, \dots, y_k^{(m'_k)}$ by considering one of the intersections of z_1 and y_k as the starting edge of $y_k^{(1)}$, and obtain the set of sub-zigzag paths:

$$\{y_1^{(1)}, \dots, y_1^{(m'_1)}, y_2^{(1)}, \dots, y_2^{(m'_2)}, \dots, y_t^{(1)}, \dots, y_t^{(m'_t)}\}. \quad (6.2)$$

- (4) We then assign one of $\{z_1, \dots, z_r\}$ to $x_j^{(a_j)}$ for $j = 1, \dots, s$ and $a_j = 1, \dots, m_j$. Then, we define X_i as the set of edges consisting of the intersections between z_i and the sub-zigzag paths in (6.1) that are assigned with z_i . We can make this assignment so that $|X_i| \geq 1$, and then set $p_i := |X_i| - 1$ for $i = 1, \dots, r$. We call $\mathcal{X} := \{X_1, \dots, X_r\}$ a *zig-deformation parameter* with respect to z_1, \dots, z_r and call the tuple $\mathbf{p} = (p_1, \dots, p_r) \in \mathbb{Z}_{\geq 0}^r$ the *weight* of \mathcal{X} . Similarly, we assign one of $\{z_1, \dots, z_r\}$ to $y_k^{(b_k)}$ for $k = 1, \dots, t$ and $b_k = 1, \dots, m'_k$. Then, we define Y_i as the set of edges consisting of the intersections between z_i and the sub-zigzag paths in (6.2) that are assigned with z_i . We can make this assignment so that $|Y_i| \geq 1$, and then set $q_i := |Y_i| - 1$ for $i = 1, \dots, r$. We call $\mathcal{Y} := \{Y_1, \dots, Y_r\}$ a *zag-deformation parameter* with respect to z_1, \dots, z_r and call the tuple $\mathbf{q} = (q_1, \dots, q_r) \in \mathbb{Z}_{\geq 0}^r$ the *weight* of \mathcal{Y} . We remark that $p_1 + \dots + p_r = m_1 + \dots + m_s - r = n - r = h$, and also that $q_1 + \dots + q_r = h$.

Definition 6.2 (extended zig-deformation). Let the notation be the same as in Setting 6.1. For a zig-deformation parameter $\mathcal{X} = \{X_1, \dots, X_r\}$ of weight $\mathbf{p} = (p_1, \dots, p_r)$, we consider the operations (zig-1), (zig-2), (zig-3) defined in Definition 4.3 and use the same notation. Then we conduct the following procedures:

(zig-4) For $m = 1, \dots, n$ and $i = 1, \dots, r$, if the zag $z_i[2m]$ of the original zigzag path z_i on Γ is not contained in X_i , then we add edges, which we call *bypasses* (since these edges provide a new route that connect edges of the zigzag path x_j contained in non-deformed parts, see Figure 7.9), connecting the following pairs of black and white nodes:

$$(w_{i,1}[2m-1], b_{i,1}[2m+1]), (w_{i,2}[2m-1], b_{i,1}[2m+1]), \\ \dots, (w_{i,p_i}[2m-1], b_{i,p_i-1}[2m+1]), (w_i[2m-1], b_{i,p_i}[2m+1]).$$

We denote the resulting dimer mode by $\bar{\nu}_{\mathcal{X}}^{\text{zig}}(\Gamma, \{z_1, \dots, z_r\})$.

We note that $\bar{\nu}_{\mathcal{X}}^{\text{zig}}(\Gamma, \{z_1, \dots, z_r\})$ is non-degenerate by Proposition 7.1.

(zig-5) Then, we make the dimer model $\bar{\nu}_{\mathcal{X}}^{\text{zig}}(\Gamma, \{z_1, \dots, z_r\})$ consistent using the method given in the proof of [3, Theorem 1.1] (see Operation 6.6 and Proposition 6.7).

At the end, we perform the operation (join) if the resulting dimer model contains 2-valent nodes. We denote the resulting dimer model by $\nu_{\mathcal{X}}^{\text{zig}}(\Gamma, \{z_1, \dots, z_r\})$, and call it the *extended zig-deformation of Γ at $\{z_1, \dots, z_r\}$ with respect to the zig-deformation parameter \mathcal{X}* . If the situation is clear, we simply denote this by $\nu_{\mathcal{X}}^{\text{zig}}(\Gamma)$.

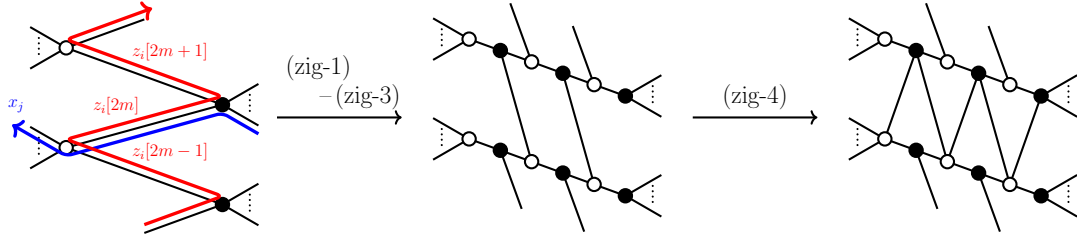


Figure 6.1. The operations (zig-1)–(zig-4) at z_i for the case $p_i = |X_i| - 1 = 2$ and $z_i[m] \notin X_i$.

Similarly, we can define the “zag version” of this extended deformation as follows.

Definition 6.3 (extended zag-deformation). Let the notation be the same as in Setting 6.1. For a zag-deformation parameter $\mathcal{Y} = \{Y_1, \dots, Y_r\}$ of weight $\mathbf{q} = (q_1, \dots, q_r)$, we consider the operations (zag-1), (zag-2), (zag-3) defined in Definition 4.4 and use the same notation. Then we conduct the following procedures:

(zag-4) For $m = 1, \dots, n$ and $i = 1, \dots, r$, if the zig $z_i[2m-1]$ of the original zigzag path z_i on Γ is not contained in Y_i , then we add edges, which we call *bypasses*, connecting the following pairs of black and white nodes:

$$(b_{i,1}[2m], w_i[2m+2]), (b_{i,2}[2m], w_{i,1}[2m+2]), \\ \dots, (b_{i,q_i}[2m], w_{i,q_i-1}[2m+2]), (b_i[2m], w_{i,q_i}[2m+2]).$$

We denote the resulting dimer mode by $\bar{\nu}_{\mathcal{Y}}^{\text{zag}}(\Gamma, \{z_1, \dots, z_r\})$.

We note that $\bar{\nu}_{\mathcal{Y}}^{\text{zag}}(\Gamma, \{z_1, \dots, z_r\})$ is non-degenerate by Proposition 7.1.

(zag-5) Then, we make the dimer model $\bar{\nu}_{\mathcal{Y}}^{\text{zag}}(\Gamma, \{z_1, \dots, z_r\})$ consistent using the method given in the proof of [3, Theorem 1.1] (see Operation 6.6 and Proposition 6.7).

At the end, we perform the operation (join) if the resulting dimer model contains 2-valent nodes. We denote the resulting dimer model by $\nu_{\mathcal{Y}}^{\text{zag}}(\Gamma, \{z_1, \dots, z_r\})$, and call it the *extended zag-deformation of Γ at $\{z_1, \dots, z_r\}$ with respect to the zag-deformation parameter \mathcal{Y}* . If the situation is clear, we simply denote this by $\nu_{\mathcal{Y}}^{\text{zag}}(\Gamma)$.

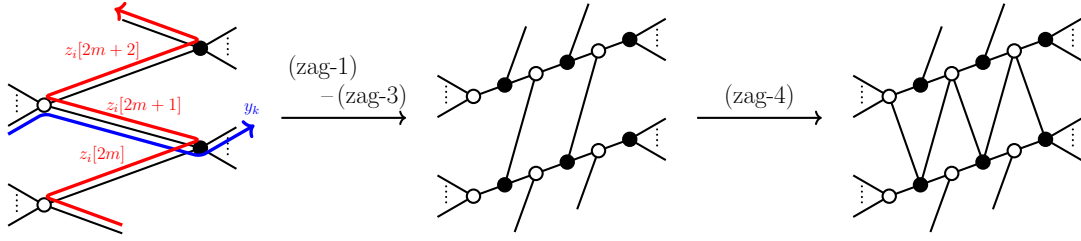


Figure 6.2. The operations (zag-1)–(zag-4) at z_i for the case $q_i = |Y_i| - 1 = 2$ and $z_i[2m+1] \notin Y_i$.

Remark 6.4. If $r = 1$, then we consider deformation parameters $\mathcal{X} = \{X_1\}$ and $\mathcal{Y} = \{Y_1\}$ in Setting 6.1, where X_1 (resp. Y_1) is the set of intersections between a chosen type I zigzag path z and x_1, \dots, x_s (resp. y_1, \dots, y_t). In particular, X_1 (resp. Y_1) coincides with the set of zags (resp. zigs) of z , and hence they are determined uniquely. Thus, in this case we may skip the operations (zig-4) (resp. (zag-4)), in which case we may also skip (zig-5) (resp. (zag-5)), since there are no bypasses (see also Observations 7.3, 7.4 and Lemma 7.7). Thus, in this case, the extended deformations coincide with the usual deformations:

$$\nu_{\mathcal{X}}^{\text{zig}}(\Gamma, \{z\}) = \nu_p^{\text{zig}}(\Gamma, \{z\}) \quad \text{and} \quad \nu_{\mathcal{Y}}^{\text{zag}}(\Gamma, \{z\}) = \nu_q^{\text{zag}}(\Gamma, \{z\}),$$

where $p := |X_1| - 1 = \ell(z)/2 - 1$ and $q := |Y_1| - 1 = \ell(z)/2 - 1$.

Remark 6.5. The non-degenerate dimer model $\bar{\nu}_{\mathcal{X}}^{\text{zig}}(\Gamma, \{z_1, \dots, z_r\})$ is determined uniquely for given deformation data, but in the operation (zig-5), the procedure for removing edges is not unique. Therefore, the resulting consistent dimer model is not unique, whereas, since the set of slopes of zigzag paths is the same for all possible consistent dimer models (see Proposition 6.7(2)), the associated PM polygon is the same by Proposition 3.6. In addition, it is generally believed that all consistent dimer models associated with the same lattice polygon are transformed into each other by the *mutations of dimer models* (see Appendix A). Thus, we expect that the extended deformation of a consistent dimer model is determined uniquely up to “*mutation equivalence*”. (We encounter the same situation for the extended zag-deformation.)

We observe that under the operations (zig-1)–(zig-4) (resp. (zag-1)–(zag-4)), (self-)intersections of zigzag paths may appear in the universal cover. We follow the strategy [3] to deal with this as we explain now.

Operation 6.6. We note the operation given in the proof of [3, Theorem 1.1], which we use in (zig-5) and (zag-5).

- (a) The dimer model $\bar{\nu}_{\mathcal{X}}^{\text{zig}}(\Gamma, \{z_1, \dots, z_r\})$ (resp. $\bar{\nu}_{\mathcal{Y}}^{\text{zag}}(\Gamma, \{z_1, \dots, z_r\})$), which is obtained by applying the operations (zig-1)–(zig-4) (resp. (zag-1)–(zag-4)) to the reduced consistent dimer model Γ , sometimes contains zigzag paths having self-intersections in the universal cover. In this case, we use the operation given in the proof of [3, Theorem 1.1]; that is, we remove all edges at self-intersections (see Figure 6.3). We note that this operation does not change the slope of the argued zigzag path.

After this process, there might be a connected component of the resulting bipartite graph that is contained in a simply-connected domain in \mathbb{T} . In that case, we remove such a connected component. We note that this removal does not affect our purpose, because our main concern is the PM polygon which is recovered from the slopes of zigzag paths, and the slope of the zigzag path corresponding to the argued connected component is trivial.

- (b) On the other hand, the dimer model $\bar{\nu}_{\mathcal{X}}^{\text{zig}}(\Gamma, \{z_1, \dots, z_r\})$ (resp. $\bar{\nu}_{\mathcal{Y}}^{\text{zag}}(\Gamma, \{z_1, \dots, z_r\})$) might have a pair of zigzag paths on the universal cover that intersect with each other in the

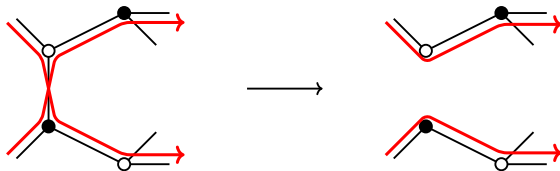


Figure 6.3. An example of removing a self-intersection of a zigzag path.

same direction more than once. In this case, we use another operation given in the proof of [3, Theorem 1.1], that is, we choose any such pair of zigzag paths and remove pairs of consecutive intersections of this pair of zigzag paths (see Figure 6.4). We note that this operation does not change the slopes of zigzag paths and the resulting bipartite graph is also a dimer model because $\bar{\nu}_\chi^{\text{zig}}(\Gamma, \{z_1, \dots, z_r\})$ (resp. $\bar{\nu}_\chi^{\text{zag}}(\Gamma, \{z_1, \dots, z_r\})$) satisfies the strong marriage condition, as we will see in Proposition 7.1.

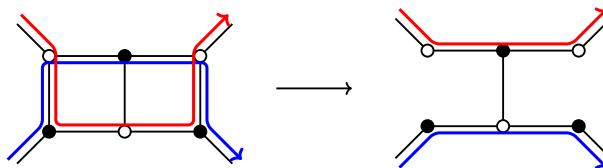


Figure 6.4. An example of removing a pair of consecutive intersections of zigzag paths.

Since the dimer model $\bar{\nu}_\chi^{\text{zig}}(\Gamma, \{z_1, \dots, z_r\})$ (resp. $\bar{\nu}_\chi^{\text{zag}}(\Gamma, \{z_1, \dots, z_r\})$) is non-degenerate by Proposition 7.1 and since it does not contain a homologically trivial zigzag path (see the proofs of Propositions 7.5, 7.6 and 7.9), we can produce a dimer model satisfying the conditions in Definition 3.2 from $\bar{\nu}_\chi^{\text{zig}}(\Gamma, \{z_1, \dots, z_r\})$ (resp. $\bar{\nu}_\chi^{\text{zag}}(\Gamma, \{z_1, \dots, z_r\})$) by iterated application of Operation 6.6. Thus, $\nu_\chi^{\text{zig}}(\Gamma, \{z_1, \dots, z_r\})$ and $\nu_\chi^{\text{zag}}(\Gamma, \{z_1, \dots, z_r\})$ are consistent dimer models, but those are not necessarily isoradial even if Γ is isoradial (see Example 4.8). Furthermore, since the operation (join) does not change the slopes of zigzag paths, this proves the following proposition.

Proposition 6.7. *Let the notation be the same as Definitions 6.2 and 6.3. Then, we have the following.*

- (1) *The dimer models $\nu_\chi^{\text{zig}}(\Gamma, \{z_1, \dots, z_r\})$ and $\nu_\chi^{\text{zag}}(\Gamma, \{z_1, \dots, z_r\})$ are consistent.*
- (2) *The set of slopes of zigzag paths on $\nu_\chi^{\text{zig}}(\Gamma, \{z_1, \dots, z_r\})$ (resp. $\nu_\chi^{\text{zag}}(\Gamma, \{z_1, \dots, z_r\})$) is the same as that of $\bar{\nu}_\chi^{\text{zig}}(\Gamma, \{z_1, \dots, z_r\})$ (resp. $\bar{\nu}_\chi^{\text{zag}}(\Gamma, \{z_1, \dots, z_r\})$).*

Remark 6.8. We note several additional points concerning the definition of the extended deformations.

- (1) The join move does not change the slopes of zigzag paths, and hence it does not affect the associated PM polygon. Thus, when we are interested in only the PM polygon, we may skip (join).
- (2) Even if we choose different sets of intersections X'_1, \dots, X'_r (resp. Y'_1, \dots, Y'_r) in Definition 4.1(7), the PM polygon of the deformed dimer model is the same as that of $\nu_\chi^{\text{zig}}(\Gamma)$ (resp. $\nu_\chi^{\text{zag}}(\Gamma)$), as we will show in Proposition 7.10.

- (3) If a dimer model Γ is hexagonal or rectangular (see Definition 2.1), we may skip the operations (zig-4), (zig-5), (zag-4) and (zag-5) when we define $\nu_{\mathcal{X}}^{\text{zig}}(\Gamma, \{z_1, \dots, z_r\})$ and $\nu_{\mathcal{Y}}^{\text{zag}}(\Gamma, \{z_1, \dots, z_r\})$, as we will show in Proposition 7.12.

7 Foundations of extended deformations of dimer models

In this section, we observe the fundamental properties of extended zig-deformations and zag-deformations. In particular, we will pursue the change of zigzag paths under these deformations in Sections 7.2 and 7.3. We refer the reader to Appendix B for understanding those observation in a concrete example.

Throughout this section, we keep the notation of Sections 4 and 6 unless otherwise stated.

7.1 The proof of the non-degeneracy

In this subsection, we prove the non-degeneracy of the dimer models $\bar{\nu}_{\mathcal{X}}^{\text{zig}}(\Gamma, \{z_1, \dots, z_r\})$ and $\bar{\nu}_{\mathcal{Y}}^{\text{zag}}(\Gamma, \{z_1, \dots, z_r\})$.

Proposition 7.1. *The dimer models $\bar{\nu}_{\mathcal{X}}^{\text{zig}}(\Gamma, \{z_1, \dots, z_r\})$, and $\bar{\nu}_{\mathcal{Y}}^{\text{zag}}(\Gamma, \{z_1, \dots, z_r\})$ are non-degenerate.*

Proof. We prove this for $\bar{\nu}_{\mathcal{X}}^{\text{zig}}(\Gamma) = \bar{\nu}_{\mathcal{X}}^{\text{zig}}(\Gamma, \{z_1, \dots, z_r\})$, the other case is similar. Let Γ' be the dimer model obtained by applying the operations (zig-1)–(zig-3) to Γ .

The first step. We recall that the non-degeneracy condition is equivalent to the strong marriage condition; that is, a dimer model has equal numbers of black and white nodes and every proper subset S of the black nodes satisfies the condition that S is connected to at least $|S| + 1$ white nodes.

Suppose that Γ' is non-degenerate. Then Γ' satisfies the strong marriage condition. By applying the operation (zig-4), we obtain the dimer model $\bar{\nu}_{\mathcal{X}}^{\text{zig}}(\Gamma, \{z_1, \dots, z_r\})$. Since (zig-4) is the operation that adds new edges, it also satisfies the strong marriage condition, and hence it is non-degenerate. Therefore, it is enough to show that Γ' is non-degenerate.

The second step. We next consider a sub-dimer model Γ'' of Γ satisfying the condition (*) below. Note that Γ'' is said to be a *sub-dimer model* of Γ if the set of the nodes coincide and the set of edges in Γ'' is a subset of edges in Γ .

Condition (*): For any given edge e in Γ'' , let z' and z'' be the two different zigzag paths on Γ'' containing e . Then either (*1) or (*2) holds:

- (*1) Either $[z'] \in \{[z_i], -[z_i]\}$ or $[z''] \in \{[z_i], -[z_i]\}$ holds;
- (*2) For any i , if z' intersects with z_i in $\text{Zig}(z_i)$ (resp. $\text{Zag}(z_i)$), then z'' intersects with z_i in $\text{Zag}(z_i)$ (resp. $\text{Zig}(z_i)$).

A sub-dimer model Γ'' of Γ satisfying (*) can be constructed using the algorithm developed in [14, 20] for proving Theorem 2.6. We adapt it to our situation.

First, let us consider the original dimer model Γ and let E_1, E_2, \dots, E_m be all edges of Δ_{Γ} , where the primitive outer normal vector for E_1 is the slope $[z_1] = \dots = [z_r]$. We assume that these edges are ordered cyclically in the anti-clockwise direction (see Figure 8.1 as a reference). Also, let v_j be the primitive outer normal vector corresponding to E_j , for $1 \leq j \leq m$. Let a be the index such that $v_a = -v_1$ if there exists such an edge among E_2, \dots, E_m ; that is, E_a is parallel to E_1 . If there is no such edge, then let $E_a = \emptyset$ for simplicity of notation. We recall that by Proposition 3.5, for each $E_j \neq \emptyset$ there exist zigzag paths on Γ such that the associated slopes coincide with v_j , and the set of such zigzag paths is denoted by $\mathcal{Z}_{v_j} = \mathcal{Z}_{v_j}(\Gamma)$. By our assumption, each slope of the zigzag paths in $\mathcal{Z}_1 := \mathcal{Z}_{v_2} \cup \dots \cup \mathcal{Z}_{v_{a-1}}$ and v_1 are linearly

independent. Thus, the zigzag paths in \mathcal{Z}_1 intersect with a type I zigzag path z_i precisely once in the universal cover (see Lemma 3.15). By definition of E_2, \dots, E_{a-1} , such an intersection is given from the right of z_i to the left of z_i , and hence zigzag paths in \mathcal{Z}_1 intersect with z_i in $\mathbf{Zag}(z_i)$. Similarly, we find that the zigzag paths in $\mathcal{Z}_2 := \mathcal{Z}_{v_{a+1}} \cup \dots \cup \mathcal{Z}_{v_m}$ intersect with z_i precisely once in the universal cover, and specifically, they intersect with z_i in $\mathbf{Zig}(z_i)$.

If there are at least two edges between E_2 and E_{a-1} (i.e., $a \geq 4$), then we take two adjacent edges, say, E_2 and E_3 . Since v_2 and v_3 are linearly independent, the zigzag paths $z'_2 \in \mathcal{Z}_{v_2}$ and $z'_3 \in \mathcal{Z}_{v_3}$ intersect at some edge of Γ . Clearly, such an intersection $z'_2 \cap z'_3$ is neither any edge constituting any zigzag path whose slope is $[z_i]$ nor $-[z_i]$. Now, remove an edge in $z'_2 \cap z'_3$. This operation merges z'_2 and z'_3 , in which case the resulting dimer model stays consistent and the associated PM polygon changes into the polygon obtained by cutting the corner of the original PM polygon consisting of edges whose outer normal vectors are $[z'_2]$ and $[z'_3]$ (see [14, Sections 5 and 6] for more details). Furthermore, since $z'_2 \cap z_i \subset \mathbf{Zag}(z_i)$ and $z'_3 \cap z_i \subset \mathbf{Zag}(z_i)$ for each i , edges in $z'_2 \cap z'_3$ do not share a node with z_i for any i . Thus, z_i is still type I even if we apply this operation and the merged zigzag path intersects with z_i in $\mathbf{Zag}(z_i)$. We repeat this procedure until there are no two edges between E_2 and E_{a-1} .

Similarly, if there are at least two edges between E_{a+1} and E_m (i.e., $m-a \geq 2$), then we do the same procedures as above until there are no two edges between E_{a+1} and E_m . After removing all suitable edges from Γ , we get a consistent dimer model, which is clearly a sub-dimer model of Γ , and we denote this by Γ_{sub} . Since we do not remove edges contained in a zigzag path whose slope is $\pm[z_i]$ in the above arguments, the edges E_1 and E_a (if this is not empty) of Δ_Γ are preserved on $\Delta_{\Gamma_{\text{sub}}}$ (and hence we will use the same notation). Also, the edges E_2, \dots, E_{a-1} (resp. E_{a+1}, \dots, E_m) of Δ_Γ are substituted by a single edge in $\Delta_{\Gamma_{\text{sub}}}$. We denote such an edge by E'_2 (resp. E'_m). We note that zigzag paths corresponding to E'_2 (resp. E'_m) are obtained by merging the ones corresponding to E_2, \dots, E_{a-1} (resp. E_{a+1}, \dots, E_m). In particular, the PM polygon $\Delta_{\Gamma_{\text{sub}}}$ is formed by E_1, E'_2, E_a, E'_m , in which case $\Delta_{\Gamma_{\text{sub}}}$ is a triangle or a trapezoid. Then, it follows from the construction of Γ_{sub} that

- the zigzag paths z_1, \dots, z_r on Γ are preserved on Γ_{sub} and they are type I;
- the zigzag paths on Γ corresponding to E_a (if this is not empty) are preserved on Γ_{sub} ;
- the zigzag paths corresponding to E'_2 (resp. E'_m) are intersected with z_i in $\mathbf{Zag}(z_i)$ (resp. $\mathbf{Zig}(z_i)$) (see also the argument in the proof of Lemma 3.14).

From these facts, it is easy to verify that Γ_{sub} is a sub-dimer model Γ'' of Γ satisfying the condition (*).

The third step. Now, we apply the operations (zig-1)–(zig-3) in Definition 4.3 to Γ_{sub} , which is possible since z_1, \dots, z_r are preserved on Γ_{sub} . We denote the resulting dimer model by Γ'_{sub} . By construction, Γ' can be obtained by adding some edges to Γ'_{sub} . Thus, similar to the discussion in the first step, it is enough to show that Γ'_{sub} is non-degenerate to prove the non-degeneracy of Γ' .

Thus, we now show that Γ'_{sub} is non-degenerate. To do this, we prove the existence of a perfect matching that contains a given edge e of Γ'_{sub} . We divide the set of edges into four cases (i)–(iv):

- (i) e is of the form $(b_{i,j-1}[2m-1], w_{i,j}[2m-1])$ for some $1 \leq i \leq r, 1 \leq j \leq p_i + 1$ and $1 \leq m \leq n$, where we let $b_{i,0}[2m-1] = b_i[2m-1]$ and $w_{i,p_i+1}[2m-1] = w_i[2m-1]$;
- (ii) e is of the form $(w_{i,j}[2m-1], b_{i,j}[2m-1])$ for some $1 \leq i \leq r, 1 \leq j \leq p_i$ and $1 \leq m \leq n$;
- (iii) e is of the form $(b_{i,j}[2m-1], w_{i,j}[2m-3])$ for some $1 \leq i \leq r, 1 \leq j \leq p_i$ and $1 \leq m \leq n$;
- (iv) e is of a form other than those in (i)–(iii).

Namely, (i) and (ii) are the edges emanating from the process (zig-1), (iii) is an edge added in the process (zig-3), and (iv) is an edge that is invariant between Γ'_{sub} and Γ_{sub} .

Since Γ_{sub} is consistent and contains the type I zigzag paths z_1, \dots, z_r , there exist corner perfect matchings P and P' on Γ_{sub} that are adjacent and satisfy $P \cap z_i = \text{Zig}(z_i)$ and $P' \cap z_i = \text{Zag}(z_i)$ for $1 \leq i \leq r$ (see Section 3.2). Similarly, let Q be a corner perfect matching on Γ_{sub} with $Q \cap z_i = \emptyset$ for $1 \leq i \leq r$. The existence of such Q is guaranteed by Lemma 3.12. We will use these P , P' and Q in order to find a suitable perfect matching on Γ'_{sub} containing a given edge e . We divide our discussions into the following cases (i)–(iv) that correspond to the above division of edges.

Case (i): Let

$$P'' = \left(P \setminus \bigcup_{i=1}^r \text{Zig}(z_i) \right) \cup \left(\bigcup_{i=1}^r \bigcup_{j=1}^{p_i+1} \bigcup_{m=1}^n (b_{i,j-1}[2m-1], w_{i,j}[2m-1]) \right); \quad (7.1)$$

see Figure 7.1. It is easy to see that P'' is a perfect matching on Γ'_{sub} containing e in the case (i).

Case (ii): Let

$$P'' = Q \cup \left(\bigcup_{i=1}^r \bigcup_{j=1}^{p_i} \bigcup_{m=1}^n (w_{i,j}[2m-1], b_{i,j}[2m-1]) \right);$$

see Figure 7.2. Then, we see that P'' is a perfect matching on Γ'_{sub} containing e in the case (ii).

Case (iii): Let

$$P'' = Q \cup \left(\bigcup_{i=1}^r \bigcup_{j=1}^{p_i} \bigcup_{m=1}^n (b_{i,j}[2m-1], w_{i,j}[2m-3]) \right);$$

see Figure 7.3. Then, we see that P'' is a perfect matching on Γ'_{sub} containing e in the case (iii).

Case (iv): We note that an edge e in the case (iv) also appears in Γ_{sub} , since e is unchanged even if we apply (zig-1)–(zig-3). Thus, we can regard e as an edge of Γ_{sub} . Since Γ_{sub} satisfies the condition (*), the zigzag paths z' , z'' on Γ_{sub} that contain e satisfy either (*1) or (*2).

- We assume that z' and z'' satisfy (*1).
 - Let, say, $[z'] = [z_i]$. Since zigzag paths having the same slopes are obtained as the difference of adjacent corner perfect matchings, either P or P' contains e . If $e \in P$, then we let P'' be as in (7.1). Then, P'' is a perfect matching on Γ'_{sub} containing e . Even if $e \in P'$, we have the same conclusion by letting

$$P'' = \left(P' \setminus \bigcup_{i=1}^r \text{Zag}(z_i) \right) \cup \left(\bigcup_{i=1}^r \bigcup_{j=1}^{p_i+1} \bigcup_{m=1}^n (b_{i,j-1}[2m-1], w_{i,j}[2m-1]) \right).$$

- Let, say, $[z'] = -[z_i]$, in which case $E_a \neq \emptyset$ and z' corresponds to E_a . Let Q' and Q'' be the corner perfect matchings on Γ_{sub} whose difference forms z' . Let $e \in Q'$. Since $h(Q', P_0)$ lies on E_a , where P_0 is the reference perfect matching, we have $Q' \cap z_i = \emptyset$ for any i by Lemma 3.9. Thus, we let

$$P'' = Q' \cup \left(\bigcup_{i=1}^r \bigcup_{j=1}^{p_i} \bigcup_{m=1}^n (w_{i,j}[2m-1], b_{i,j}[2m-1]) \right),$$

and see that P'' is a perfect matching on Γ'_{sub} containing e .

- We assume that z' and z'' satisfy (*2).

Let, say, z' intersect with each z_i in $\text{Zig}(z_i)$. Let Q' and Q'' be the corner perfect matchings on Γ_{sub} whose difference forms z' . Let $e \in Q'$. As noted above, we see that all zigzag paths in Γ_{sub} intersecting with z_i at some zig of z_i have the same slopes. This implies that Q' contains all zigs of z_i , i.e., $Q' \cap z_i = \text{Zig}(z_i)$. This also means that $Q' = P$. Hence, we let P'' be the same as (7.1) and see that P'' is a perfect matching containing e . ■

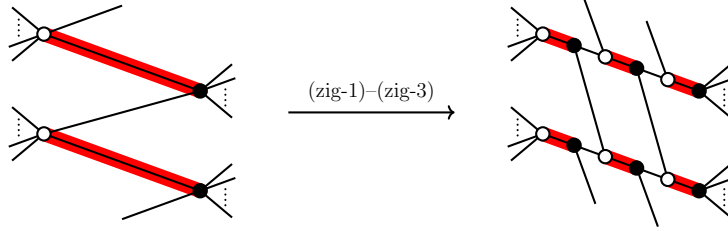


Figure 7.1. The perfect matchings P on Γ_{sub} (left) and P'' on Γ'_{sub} (right) for the case (i).

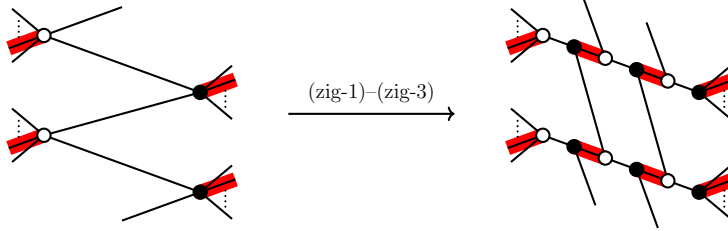


Figure 7.2. The perfect matchings Q on Γ_{sub} (left) and P'' on Γ'_{sub} (right) for the case (ii).

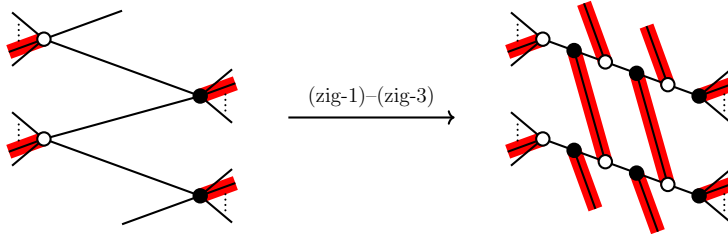


Figure 7.3. The perfect matchings Q on Γ_{sub} (left) and P'' on Γ'_{sub} (right) for the case (iii).

7.2 Behaviors of zigzag paths after extended deformations

In this subsection, we study zigzag paths of the deformed dimer models and their slopes. We mainly discuss the extended zig-deformation, but the same assertions hold for the extended zag-deformation by a similar argument. We will work with the notation in Definition 4.1 and Setting 6.1. We consider the extended deformation $\nu_{\mathcal{X}}^{\text{zig}}(\Gamma, \{z_1, \dots, z_r\})$ of Γ (see Definitions 4.3 and 6.2).

First, we observe zigzag paths of Γ and fix the notation which we will use throughout this section.

Observation 7.2. Let z_1, \dots, z_r be type I zigzag paths of Γ with $[z_1] = \dots = [z_r]$. These zigzag paths are ordered cyclically along the subscript $i = 1, \dots, r$. For any $\alpha \in \mathbb{Z}$ and $i = 1, \dots, r$,

let $\tilde{z}_i(\alpha)$ be a zigzag path on the universal cover $\tilde{\Gamma}$ whose projection on Γ is z_i . Each $\tilde{z}_i(\alpha)$ divides \mathbb{R}^2 into two parts, and thus it makes sense to consider the left of $\tilde{z}_i(\alpha)$ and the right of $\tilde{z}_i(\alpha)$. Then, we can write a straight line $\ell_{i,\alpha}^L$ (resp. $\ell_{i,\alpha}^R$) on the left (resp. right) of $\tilde{z}_i(\alpha)$ such that the gradient of $\ell_{i,\alpha}^L$ (resp. $\ell_{i,\alpha}^R$) is $v = [z_i]$ and the nodes contained in the region obtained as the intersection of the right of $\ell_{i,\alpha}^L$ and the left of $\ell_{i,\alpha}^R$ are precisely the nodes located on $\tilde{z}_i(\alpha)$. We will call such a region the (i, α) -th deformed part (see Figure 7.4).

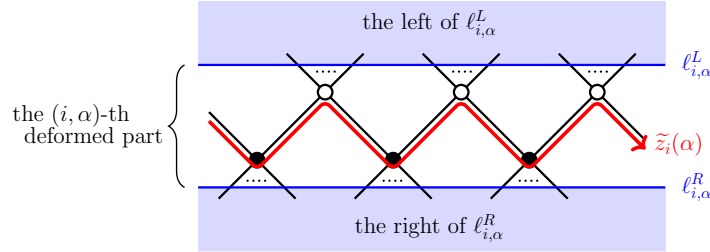


Figure 7.4.

Also, we call the region obtained as the intersection of the right of $\ell_{i-1,\alpha}^R$ and the left of $\ell_{i,\alpha}^L$ the (i, α) -th irrelevant part. Here, we say that the intersection of the right of $\ell_{r,\alpha}^R$ and the left of $\ell_{1,\alpha+1}^L$ is the $(1, \alpha + 1)$ -th irrelevant part. We remark that sometimes there are no nodes in an irrelevant part. We sometimes omit $\alpha \in \mathbb{Z}$ from the notation unless it causes confusion. We also use these terminologies for Γ . That is, a part of Γ obtained by projecting a deformed (resp. irrelevant) part of $\tilde{\Gamma}$ onto Γ is said to be a deformed (resp. irrelevant) part of Γ .

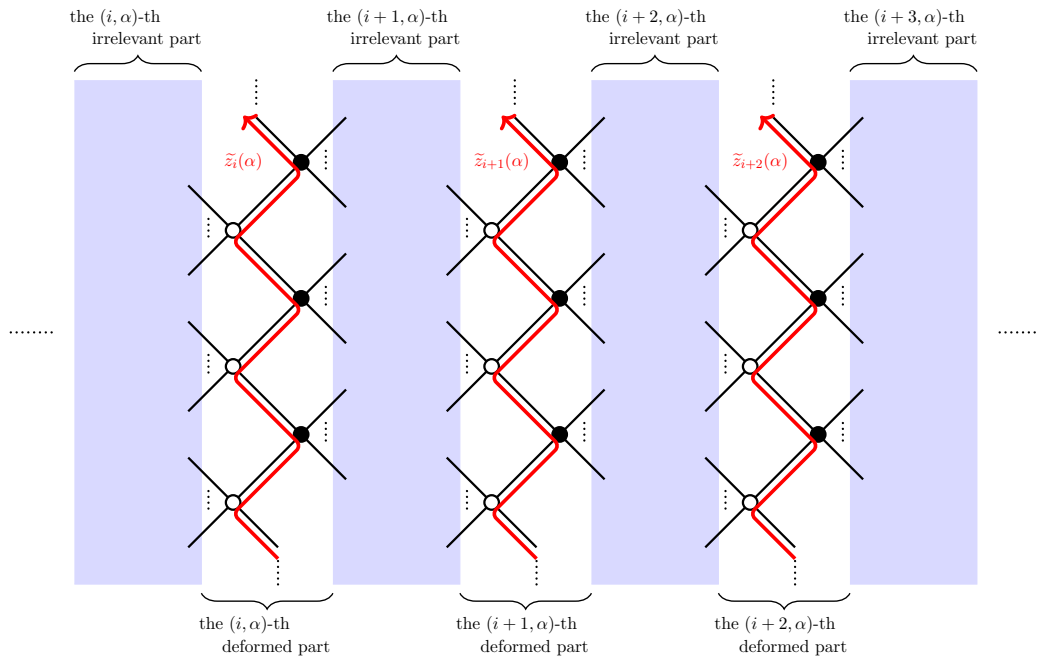


Figure 7.5.

By the condition of Definition 3.3(3), z_1, \dots, z_r do not have a common node, and therefore the irrelevant parts do not overlap each other. Since the operations (zig-1)–(zig-4) (or (zag-1)–(zag-4)) are local operations on each deformed part, any irrelevant part will be unchanged even if we apply these operations. Thus, we continue to use these terminologies “deformed parts” and “irrelevant parts”. We then consider a zigzag path w satisfying the following properties:

- (a) If $[z_i]$ and $[w]$ are linearly independent, then by Lemma 3.15, \tilde{w} intersects with $\tilde{z}_i(\alpha)$ precisely once, and so does any $\tilde{z}_i(\alpha)$ with $i = 1, \dots, r$ and $\alpha \in \mathbb{Z}$. In particular, all intersections are zigs of w or zags of w by Lemma 3.16. If \tilde{w} intersects with $\tilde{z}_i(\alpha)$ at a zig (resp. zag) of $\tilde{z}_i(\alpha)$, then we easily see that \tilde{w} crosses the (i, α) -th deformed part in the direction from the (i, α) -th (resp. $(i + 1, \alpha)$ -th) irrelevant part to the $(i + 1, \alpha)$ -th (resp. (i, α) -th) irrelevant part.
- (b) If $[z_i]$ and $[w]$ are linearly dependent, then by Lemma 3.15, \tilde{w} and $\tilde{z}_i(\alpha)$ do not intersect for any $i = 1, \dots, r$ and $\alpha \in \mathbb{Z}$. This is equivalent to the condition that \tilde{w} is contained in some irrelevant part. In this case, w is unchanged even if we apply the extended deformations because (zig-1)–(zig-4) (or (zag-1)–(zag-4)) are operations on the deformed parts, and (zig-5) (or (zag-5)) does not affect w by Lemma 7.7 below.

In the remainder of this subsection, we discuss the behavior of zigzag paths after applying the operations (zig-1)–(zig-4). (We can apply the same arguments for the case of (zag-1)–(zag-4).)

Observation 7.3. We consider a zigzag path y_k on a consistent dimer model Γ intersecting with z_i at a zig of z_i . Let \tilde{z}_i and \tilde{y}_k be zigzag paths on $\tilde{\Gamma}$ projecting onto z_i and y_k , respectively. By Observation 7.2(a), \tilde{y}_k crosses the i -th deformed part in the direction from the i -th irrelevant part to the $(i + 1)$ -th irrelevant part, and \tilde{y}_k intersects with \tilde{z}_i precisely once. We suppose that the zig $\tilde{z}_i[2m - 1]$ of \tilde{z}_i is such an intersection. In this case, $\tilde{z}_i[2m - 1]$ is also a zag of \tilde{y}_k ; thus we may write it as $\tilde{y}_k[2m]$.

Now, we apply the operations (zig-1)–(zig-3) to Γ , and we denote the resulting dimer model by Γ' and its universal cover by $\tilde{\Gamma}'$. Then, some new nodes are inserted in $\tilde{z}_i[2m - 1] = \tilde{y}_k[2m]$, and zigzag paths $\tilde{z}_{i,1}, \dots, \tilde{z}_{i,p_i}$ on $\tilde{\Gamma}'$, which project onto zigzag paths $z_{i,1}, \dots, z_{i,p_i}$ on Γ' , respectively, appear in the i -th deformed part.

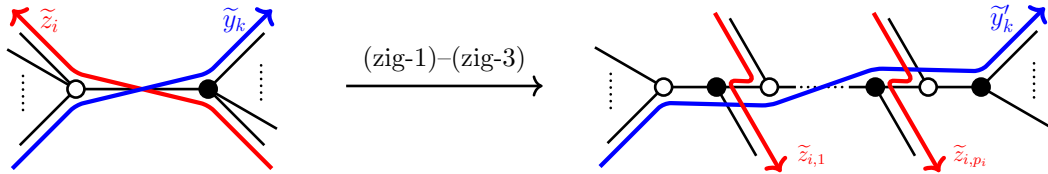


Figure 7.6.

We consider the zigzag path \tilde{y}'_k on $\tilde{\Gamma}'$ passing through $\tilde{y}_k[2m - 1]$ as a zig. That is, \tilde{y}'_k starts from $\tilde{y}_k[2m - 1]$, crosses through zigzag paths $\tilde{z}_{i,1}, \dots, \tilde{z}_{i,p_i}$ in the i -th deformed part, and arrives at $\tilde{y}_k[2m + 1]$ (see the right of Figure 7.6). In particular, it crosses the i -th deformed part in the direction from the i -th irrelevant part to the $(i + 1)$ -th irrelevant part. Although \tilde{y}'_k looks different from \tilde{y}_k in the deformed parts, it connects the zigs $\tilde{y}_k[2m - 1]$ and $\tilde{y}_k[2m + 1]$ of \tilde{y}_k in the i -th deformed part for all i , and thus \tilde{y}'_k shares the same nodes and edges as \tilde{y}_k in any irrelevant part. We conclude that \tilde{y}'_k coincides with \tilde{y}_k in all irrelevant parts, and behaves as depicted on the right-hand side of Figure 7.6 in each deformed part. Also, we see that bypasses inserted in the operation (zig-4) do not affect the behavior of \tilde{y}'_k , because \tilde{y}'_k never passes through bypasses.

Observation 7.4. We consider a zigzag path x_j on Γ intersecting with z_i at a zag of z_i . Let \tilde{x}_j be a zigzag path on $\tilde{\Gamma}$ projecting onto x_j . By Observation 7.2(a), \tilde{x}_j crosses the i -th deformed part in the direction from the $(i + 1)$ -th irrelevant part to the i -th irrelevant part, and \tilde{x}_j intersects with \tilde{z}_i precisely once. We suppose that the zag $\tilde{z}_i[2m]$ of \tilde{z}_i is such an intersection. In this case, $\tilde{z}_i[2m]$ is also a zig of \tilde{x}_j , and thus we may write it as $\tilde{x}_j[2m + 1]$. We then apply the operations (zig-1)–(zig-4) to Γ , and we have the dimer model $\tilde{\nu}_\chi^{\text{zig}}(\Gamma) = \tilde{\nu}_\chi^{\text{zig}}(\Gamma, \{z_1, \dots, z_r\})$.

If $z_i[2m]$, which is the projection of $\tilde{z}_i[2m] = \tilde{x}_j[2m+1]$ on Γ , is not contained in X_i , then bypasses are inserted. We consider the zigzag path \tilde{x}'_j on the universal cover of $\bar{\nu}_{\mathcal{X}}^{\text{zig}}(\Gamma)$ passing through $\tilde{x}_j[2m]$ as a zag of \tilde{x}'_j . That is, \tilde{x}'_j starts from $\tilde{x}_j[2m]$, behaves as depicted on the right-hand side of Figure 7.7, and arrives at $\tilde{x}_j[2m+2]$. In particular, \tilde{x}'_j crosses the i -th deformed part in the direction from the $(i+1)$ -th irrelevant part to the i -th irrelevant part, and behaves in the same manner as \tilde{x}_j in each irrelevant part.

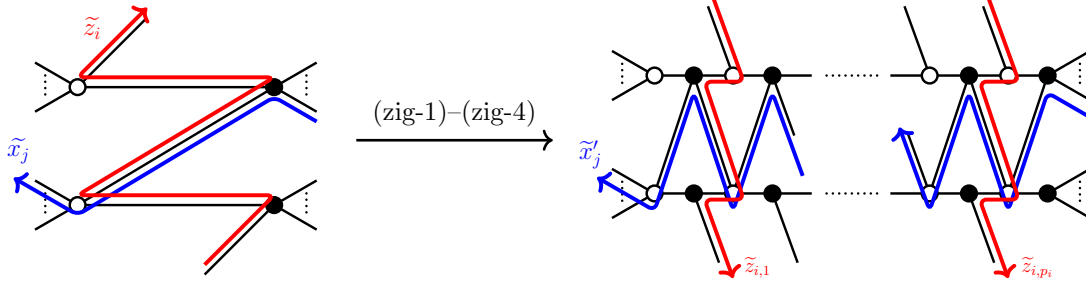


Figure 7.7. The case where the projection of $\tilde{z}_i[2m] = \tilde{x}_j[2m+1]$ on Γ is not contained in X_i .

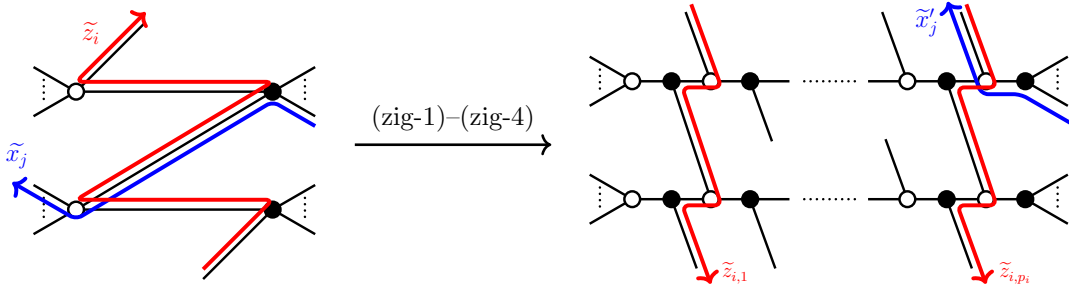


Figure 7.8. The case where the projection of $\tilde{z}_i[2m] = \tilde{x}_j[2m+1]$ on Γ is contained in X_i .

If $z_i[2m]$ is contained in X_i , then no bypasses are inserted. We again consider the zigzag path \tilde{x}'_j on the universal cover of $\bar{\nu}_{\mathcal{X}}^{\text{zig}}(\Gamma)$ passing through $\tilde{x}_j[2m]$ as a zag of \tilde{x}'_j (e.g., see Figure 7.8). Unlike in the previous case, after passing through $\tilde{x}_j[2m]$, \tilde{x}'_j goes to the edge $\{\tilde{b}_i[2m+1], \tilde{w}_{i,1}[2m+1]\}$. (Here, we denote the edge whose endpoints are a black node b and a white node w by $\{b, w\}$.)

If $z_i[2m+2] \in X_i$, in which case bypasses are not inserted, then \tilde{x}'_j goes to the edge $\{\tilde{w}_{i,1}[2m+1], \tilde{b}_{i,1}[2m+3]\}$.

On the other hand, if $z_i[2m+2] \notin X_i$, in which case we insert bypasses, then \tilde{x}'_j goes to the edge $\{\tilde{w}_{i,1}[2m+1], \tilde{b}_i[2m+3]\}$. In such a way, \tilde{x}'_j crosses the i -th deformed part in the direction from the $(i+1)$ -th irrelevant part to the i -th irrelevant part. More precisely, if we assume that \tilde{x}'_j goes through the edge $\{\tilde{b}_{i,s}[2m-1], \tilde{w}_{i,s+1}[2m-1]\}$ in the i -th deformed part, then \tilde{x}'_j behaves as follows:

- (1) if $z_i[2m] \in X_i$, in which case bypasses are not inserted, then \tilde{x}'_j goes through the edge $\{\tilde{w}_{i,s+1}[2m-1], \tilde{b}_{i,s+1}[2m+1]\}$ and then $\{\tilde{b}_{i,s+1}[2m+1], \tilde{w}_{i,s+2}[2m+1]\}$,
- (2) if $z_i[2m] \notin X_i$, in which case we insert bypasses, then \tilde{x}'_j goes through the edge $\{\tilde{w}_{i,s+1}[2m-1], \tilde{b}_{i,s}[2m+1]\}$ and then $\{\tilde{b}_{i,s}[2m+1], \tilde{w}_{i,s+1}[2m+1]\}$,

where $m = 1, \dots, n$ and $s = 0, \dots, p_i - 1$ with $\tilde{b}_{i,0}[-] = \tilde{b}_i[-]$ and $\tilde{w}_{i,p_i+1}[-] = \tilde{w}_i[-]$. When we consider \tilde{x}'_j in the i -th deformed part, we encounter case (1) $|X_i|$ times and case (2) $\ell(z_i)/2 - |X_i|$

times. Since $p_i = |X_i| - 1$, we see that \tilde{x}'_j goes out the i -th deformed part from $\tilde{w}_i[2m - 1 + 2n] = \tilde{w}_i[2m - 1 + \ell(z_i)]$, and then it goes into the i -th irrelevant part. Thus, \tilde{x}'_j behaves in the same manner as the shift of \tilde{x}_j in the i -th irrelevant part. For example, if we consider the type I zigzag path z_i with $\ell(z_i) = 8$, and the zig-deformation parameter X_i with $|X_i| = 3$ and $z_i[2m + 4] \notin X_i$, then the i -th deformed part will change as shown in Figure 7.9.

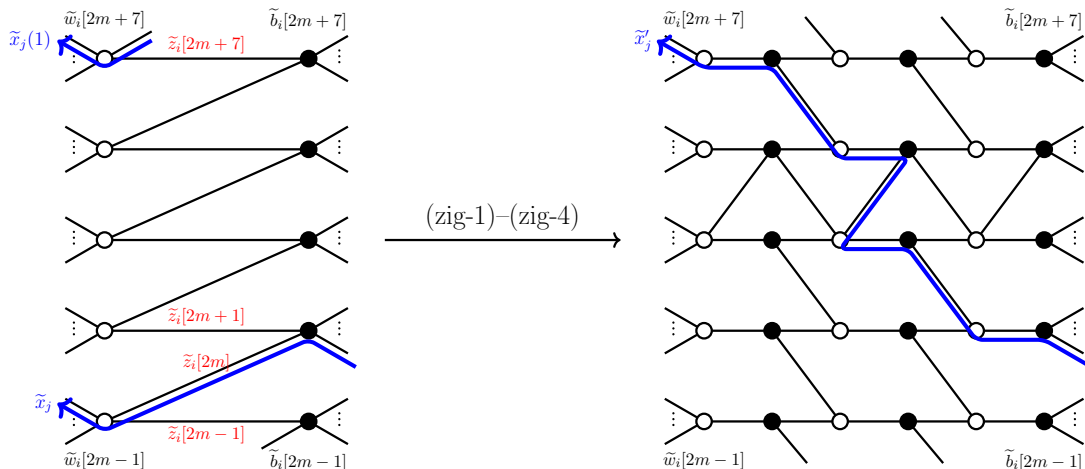


Figure 7.9. An example of the behavior of \tilde{x}'_j in the i -th deformed part.

7.3 Properties of zigzag paths on deformed dimer models

In this subsection, we study the slopes of zigzag paths on deformed dimer models. In particular, we can describe them in terms of zigzag paths of the original dimer model, and this description plays a crucial role when discussing the relationship with the combinatorial mutations of the associated polygons.

Proposition 7.5. *The path $z_{i,j}$ given in (zig-3) of Definition 4.3 (resp. (zag-3) of Definition 4.4) is a type I zigzag path $z_{i,j}$ of $\nu_{\mathcal{X}}^{\text{zig}}(\Gamma)$ (resp. $\nu_{\mathcal{Y}}^{\text{zag}}(\Gamma)$) with $\ell(z_{i,j}) = \ell(z_i)$. Moreover, $z_{i,j}$ does not have any self-intersections on the universal cover, and satisfies $[z_{i,j}] = -[z_i] = -v$, and hence it is not homologically trivial.*

Proof. We consider the case of $\nu_{\mathcal{X}}^{\text{zig}}(\Gamma)$. The case of $\nu_{\mathcal{Y}}^{\text{zag}}(\Gamma)$ is similar.

First, $z_{i,j}$ is a zigzag path of $\bar{\nu}_{\mathcal{X}}^{\text{zig}}(\Gamma)$ by definition. We see that zigzag paths of $\bar{\nu}_{\mathcal{X}}^{\text{zig}}(\Gamma)$ intersecting with $\tilde{z}_{i,j}$ take either the form of \tilde{y}'_k given in Observation 7.3 or \tilde{x}'_j given in Observation 7.4. In particular, these intersect with $\tilde{z}_{i,j}$ precisely once in each deformed part, and \tilde{y}'_k crosses the i -th deformed part in the direction from the i -th irrelevant part to the $(i+1)$ -th irrelevant part, and \tilde{x}'_j crosses the i -th deformed part in the direction from the $(i+1)$ -th irrelevant part to the i -th irrelevant part for all i . Since other zigzag paths do not intersect with $\tilde{z}_{i,j}$, we see that $z_{i,j}$ is a type I zigzag path of $\bar{\nu}_{\mathcal{X}}^{\text{zig}}(\Gamma)$. Also, $\tilde{z}_{i,j}$ does not have any self-intersections by definition. By these properties, the edges constituting $z_{i,j}$ are not removed by the operation (zig-5). In addition, since $z_{i,j}$ contains no 2-valent nodes, the operation (join) does not affect $z_{i,j}$. Therefore, we see that $z_{i,j}$ is a type I zigzag path of $\nu_{\mathcal{X}}^{\text{zig}}(\Gamma)$, and the remaining assertions follow from the definition of $z_{i,j}$. \blacksquare

Proposition 7.6. *The paths y_1, \dots, y_t (resp. the paths x_1, \dots, x_s) are zigzag paths of Γ intersecting with a chosen type I zigzag path z at some zigs (resp. zags) of z . We have the following.*

- (1) For any zigzag path y_k of Γ , there exists a unique zigzag path y'_k of $\nu_{\mathcal{X}}^{\text{zig}}(\Gamma)$ without self-intersections on the universal cover and satisfying $[y_k] = [y'_k]$ where $k = 1, \dots, t$.
- (2) For any zigzag path x_j of Γ , there exists a unique zigzag path x'_j of $\nu_{\mathcal{Y}}^{\text{zag}}(\Gamma)$ without self-intersections on the universal cover and satisfying $[x_j] = [x'_j]$ where $j = 1, \dots, s$.

Proof. We consider the case of $\nu_{\mathcal{X}}^{\text{zig}}(\Gamma)$. The case of $\nu_{\mathcal{Y}}^{\text{zag}}(\Gamma)$ is similar.

We use the same notation used in Observation 7.3. In particular, we consider the zigzag path \tilde{y}'_k of $\tilde{\Gamma}'$ which coincides with \tilde{y}_k in all irrelevant parts, and behaves as depicted on the right-hand side of Figure 7.6 in each deformed part, and therefore does not have any self-intersections. Since bypasses inserted in the operation (zig-4) do not affect the behavior of \tilde{y}'_k , we can extend \tilde{y}'_k to a zigzag path of the universal cover of $\nu_{\mathcal{X}}^{\text{zig}}(\Gamma)$. By projecting \tilde{y}'_k onto $\nu_{\mathcal{X}}^{\text{zig}}(\Gamma)$, we have the zigzag path y'_k of $\nu_{\mathcal{X}}^{\text{zig}}(\Gamma)$. By the construction given in Observation 7.3, we see that $[y_k] = [y'_k]$. Since \tilde{y}'_k coincides with \tilde{y}_k in all irrelevant parts and Γ is consistent, it does not behave pathologically in irrelevant parts as it infringes on the consistency condition. Furthermore, \tilde{y}'_k intersects with zigzag paths of the forms $\tilde{z}_{i,j}$ and \tilde{x}'_j (see Observation 7.4) in some deformed parts, but they do not intersect with each other in the same direction more than once. Therefore, the edges constituting y'_k are not removed by the operation (zig-5), and hence y'_k is not changed by (zig-5). In addition, the operation (join) does not change the slopes. Thus, we naturally extend this zigzag path y'_k as the path of $\nu_{\mathcal{X}}^{\text{zig}}(\Gamma)$, which is determined uniquely and satisfies $[y_k] = [y'_k]$ by construction. \blacksquare

By the proof of Propositions 7.5 and 7.6, the zigzag paths $\tilde{z}_{i,j}$ and \tilde{y}'_k do not have any self-intersections, and do not intersect with other zigzag paths in the same direction more than once. Furthermore, the intersections between \tilde{x}'_j and $\tilde{z}_{i,j}$ or \tilde{y}'_k are not bypasses (see Observations 7.3 and 7.4). This proves the following lemma.

Lemma 7.7. *We have the following.*

- (1) The edges removed by the operation (zig-5) are a part of the bypasses added in (zig-4) or edges appearing in some irrelevant parts that are intersections between pairs of zigzag paths x_1, \dots, x_s .
- (2) The edges removed by the operation (zag-5) are a part of the bypasses added in (zag-4) or edges appearing in some irrelevant parts that are intersections between pairs of zigzag paths y_1, \dots, y_t .

Before showing the next proposition, we introduce some notation.

Setting 7.8. Let z be a zigzag path on a consistent dimer model Γ . We recall that corner perfect matchings are ordered in the anti-clockwise direction along the vertices of Δ_{Γ} (see Section 2.2). Let P, P' be adjacent corner perfect matchings on Γ such that the difference of P and P' contains z (see Proposition 3.5). We assume that P, P' are ordered with this order, in which case $P \cap z = \text{Zig}(z)$ and $P' \cap z = \text{Zag}(z)$. Then, we set $P_z := P$ and $P'_z := (P \setminus \text{Zig}(z)) \cup \text{Zag}(z)$. By Proposition 3.6, P_z, P'_z are boundary perfect matchings corresponding to certain lattice points on the edge of Δ_{Γ} whose outer normal vector is $[z]$, and we see that the difference of P_z and P'_z , namely $P_z \cup P'_z \setminus P_z \cap P'_z$, forms z . Thus, by this construction, $h(P'_z, P_z) \in \mathbb{Z}^2$ is a primitive lattice element with $\langle [z], h(P'_z, P_z) \rangle = 0$.

Proposition 7.9. *Let $h(P'_z, P_z)$ be a primitive lattice element as above. We have the following.*

- (1) For any zigzag path x_j of Γ , there exists a unique zigzag path x'_j of $\nu_{\mathcal{X}}^{\text{zig}}(\Gamma)$ such that for every $j = 1, \dots, s$

$$[x'_j] = [x_j] + \langle [x_j], h(P'_z, P_z) \rangle [z].$$

- (2) For any zigzag path y_k of Γ , there exists a unique zigzag path y'_k of $\nu_y^{\text{zag}}(\Gamma)$ such that for every $k = 1, \dots, t$

$$[y'_k] = [y_k] + \langle [y_k], h(\mathbf{P}'_z, \mathbf{P}_z) \rangle [z].$$

Proof. We consider the case of $\nu_{\mathcal{X}}^{\text{zig}}(\Gamma)$. The case of $\nu_y^{\text{zag}}(\Gamma)$ is similar.

We recall that $|x_j \cap z| = |x_j \cap z_i|$ for all $i = 1, \dots, r$, and that this number is denoted by m_j (see Definition 4.1). We first show that

$$m_j = \langle [x_j], h(\mathbf{P}'_z, \mathbf{P}_z) \rangle \quad (7.2)$$

for $j = 1, \dots, s$. Let p_{x_j} be the path of the quiver Q_Γ going along the left side of x_j (see Observation 3.7). In particular, considering p_{x_j} as an element in $H_1(\mathbb{T})$, we have $[p_{x_j}] = [x_j]$. By our assumption, the intersections $x_j \cap z$ are contained in $\text{Zag}(z) = \mathbf{P}' \cap z$. Thus, p_{x_j} crosses z at a zig of z . Since $\mathbf{P} \cap z = \text{Zig}(z)$, every time p_{x_j} crosses z , the height function $h_{\mathbf{P}', \mathbf{P}}$ increases by 1. Since $m_j = |x_j \cap z|$, we have the equation (7.2).

Then, we show that for each x_j where $j = 1, \dots, s$, there exists a zigzag path x'_j on $\bar{\nu}_{\mathcal{X}}^{\text{zig}}(\Gamma) = \bar{\nu}_{\mathcal{X}}^{\text{zig}}(\Gamma, \{z_1, \dots, z_r\})$ such that

$$[x'_j] = [x_j] + m_j [z]. \quad (7.3)$$

We divide x_j into sub-zigzag paths $x_j^{(1)}, \dots, x_j^{(m_j)}$. By definition, $x_j^{(1)}$ intersects with z_r at a zag of z_r . We denote this zag by $z_r[2m] := x_j^{(1)} \cap z_r$, in which case the white (resp. black) node that is the end point of $z_r[2m]$ is denoted by $w_r[2m-1]$ (resp. $b_r[2m+1]$). By considering the universal cover $\tilde{\Gamma}$, we naturally define $\tilde{x}_j, \tilde{x}_j^{(1)}, \tilde{z}_r, \tilde{z}_r[2m], \tilde{w}_r[2m-1], \tilde{b}_r[2m+1]$, etc. Also, we assume that \tilde{z}_r is contained in the $(r, 0)$ -th deformed part. Then, \tilde{x}_j crosses the $(r, 0)$ -th deformed part in the direction from the $(r+1, 0)$ -th irrelevant part to the $(r, 0)$ -th irrelevant part, in which case the entrance of the $(r, 0)$ -th deformed part is $\tilde{b}_r[2m+1]$ and the exit is $\tilde{w}_r[2m-1]$.

In what follows, we use the same notation used in Observation 7.4. In particular, we pay attention to the zigzag path \tilde{x}'_j of the universal cover $\bar{\nu}_{\mathcal{X}}^{\text{zig}}(\Gamma)^\sim$ of $\bar{\nu}_{\mathcal{X}}^{\text{zig}}(\Gamma)$, which behaves as follows:

- (A_r) If $z_r[2m] \notin X_r$, then \tilde{x}'_j goes into the $(r, 0)$ -th deformed part of $\bar{\nu}_{\mathcal{X}}^{\text{zig}}(\Gamma)^\sim$ from $\tilde{b}_r[2m+1]$ and goes out from $\tilde{w}_r[2m-1]$ (see also Figure 7.7). After crossing the $(r, 0)$ -th deformed part, it goes into the $(r, 0)$ -th irrelevant part, and it behaves in the same manner as \tilde{x}_j in that part.
- (B_r) If $z_r[2m] \in X_r$, then \tilde{x}'_j goes into the $(r, 0)$ -th deformed part of $\bar{\nu}_{\mathcal{X}}^{\text{zig}}(\Gamma)^\sim$ from $\tilde{b}_r[2m+1]$ and goes out from $\tilde{w}_r[2m-1+2n] = \tilde{w}_r[2m-1+\ell(z)]$ (see also Figures 7.8 and 7.9). After crossing the $(r, 0)$ -th deformed part, it goes into the $(r, 0)$ -th irrelevant part, and it behaves in the same manner as the shift of \tilde{x}_j , which we denote as $\tilde{x}_j(1)$, in that part.

Then, \tilde{x}'_j goes into the $(r-1, 0)$ -th deformed part of $\bar{\nu}_{\mathcal{X}}^{\text{zig}}(\Gamma)^\sim$. We let $\tilde{z}_{r-1}[2m'] := \tilde{x}_j \cap \tilde{z}_{r-1}$ and $\tilde{z}_{r-1}[2m''] := \tilde{x}_j(1) \cap \tilde{z}_{r-1}$. We note that on the dimer model Γ we have $z_{r-1}[2m'] = z_{r-1}[2m''] = x_j^{(1)} \cap z_{r-1}$ by definition.

- If $z_r[2m] \in X_r$ in the above argument, then $z_{r-1}[2m'] \notin X_{r-1}$ by the definition of X_r and X_{r-1} . (Furthermore, $x_j^{(1)} \cap z_i \notin X_i$ for any $i \neq r$.) In this case, \tilde{x}'_j crosses the $(r-1, 0)$ -th deformed part of $\bar{\nu}_{\mathcal{X}}^{\text{zig}}(\Gamma)^\sim$ in the same manner as (A_r) above. Then, it behaves in the same manner as $\tilde{x}_j(1)$ in the $(r-1, 0)$ -th irrelevant part.
- Let $z_r[2m] \notin X_r$ in the above argument.

- If $z_{r-1}[2m'] \notin X_{r-1}$, then \tilde{x}'_j crosses the $(r-1, 0)$ -th deformed part of $\bar{\nu}_{\mathcal{X}}^{\text{zig}}(\Gamma)^\sim$ in the same way as (A_r) . Then, it behaves in the same manner as \tilde{x}_j in the $(r-1, 0)$ -th irrelevant part.
- If $z_{r-1}[2m'] \in X_{r-1}$, then \tilde{x}'_j crosses the $(r-1, 0)$ -th deformed part of $\bar{\nu}_{\mathcal{X}}^{\text{zig}}(\Gamma)^\sim$ in the same way as (B_r) . Then, it behaves in the same manner as $\tilde{x}_j(1)$ in the $(r-1, 0)$ -th irrelevant part.

Repeating these inductive arguments, we see that \tilde{x}'_j crosses the $(i, 0)$ -th deformed part of $\bar{\nu}_{\mathcal{X}}^{\text{zig}}(\Gamma)^\sim$ for $i = r, r-1, \dots, 1$ in this order, and goes into the $(1, 0)$ -th irrelevant part. In any case, \tilde{x}'_j behaves in the same manner as $\tilde{x}_j(1)$ in this irrelevant part.

Then, \tilde{x}'_j goes into the $(r, -1)$ -th deformed part, in which case we consider the sub-zigzag path $x'_j(2)$ of Γ and the intersection between $\tilde{z}_r(-1)$ and $\tilde{x}'_j(2)$ on $\tilde{\Gamma}$. By the same arguments as above, we see that \tilde{x}'_j crosses the $(i, -1)$ -th deformed part of $\bar{\nu}_{\mathcal{X}}^{\text{zig}}(\Gamma)^\sim$ for $i = r, r-1, \dots, 1$ in this order. After that, it goes into $(1, -1)$ -th irrelevant part and behaves in the same manner as $\tilde{x}_j(2)$ in this irrelevant part.

Repeating these arguments, we finally see that \tilde{x}'_j crosses the $(i, -m_j + 1)$ -th deformed part of $\bar{\nu}_{\mathcal{X}}^{\text{zig}}(\Gamma)^\sim$ for $i = r, r-1, \dots, 1$ in this order, and behaves in the same manner as $\tilde{x}_j(m_j)$ in the $(1, -m_j + 1)$ -th irrelevant part. Then, \tilde{x}'_j goes into the $(r, -m_j)$ -th deformed part of $\bar{\nu}_{\mathcal{X}}^{\text{zig}}(\Gamma)^\sim$, in which case we denote the black node that is the entrance of this deformed part by B . Since $m_j = |x_j \cap z_i|$, the projection of $\tilde{x}_j \cap \tilde{z}_i(-m_j)$ on Γ coincides with $z_i[2m]$, which is the starting edge of our arguments. Thus, B coincides with $\tilde{b}_r[2m+1]$ if they are projected onto $\bar{\nu}_{\mathcal{X}}^{\text{zig}}(\Gamma)$, which means we can follow all edges of the zigzag path x'_j of $\bar{\nu}_{\mathcal{X}}^{\text{zig}}(\Gamma)$. By these arguments, we see that the slope of \tilde{x}'_j changes $[z]$ in each deformed part, and thus we have $[x'_j] = [x_j] + m_j[z]$.

Finally, we apply the operations (zig-5) and (join) to $\bar{\nu}_{\mathcal{X}}^{\text{zig}}(\Gamma)$. Then, we obtain the deformed dimer model $\nu_{\mathcal{X}}^{\text{zig}}(\Gamma)$ and the zigzag path on it having the same slope as \tilde{x}'_j . This zigzag path is determined uniquely by the construction, and we use the same notation for this zigzag path by abuse of the notation. Since (zig-5) and (join) do not change the slopes of zigzag paths, we have (7.3). ■

Since the slopes of zigzag paths $\nu_{\mathcal{X}}^{\text{zig}}(\Gamma)$ and $\nu_{\mathcal{Y}}^{\text{zag}}(\Gamma)$ do not depend on the choice of X_1, \dots, X_r (resp. Y_1, \dots, Y_r) by Propositions 7.5, 7.6 and 7.9, we obtain the proposition below. However, we remark that the deformed dimer model depends on the choice of zig-deformation parameters; thus $\nu_{\mathcal{X}}^{\text{zig}}(\Gamma, \{z_1, \dots, z_r\}) \not\cong \nu_{\mathcal{X}'}^{\text{zig}}(\Gamma, \{z_1, \dots, z_r\})$ in general (the zag version is similar).

Proposition 7.10. *For zig-deformation parameter $\mathcal{X}' := \{X'_1, \dots, X'_r\}$ and zag-deformation parameter $\mathcal{Y}' := \{Y'_1, \dots, Y'_r\}$ different from \mathcal{X} and \mathcal{Y} , we have*

$$\Delta_{\nu_{\mathcal{X}}^{\text{zig}}(\Gamma, \{z_1, \dots, z_r\})} = \Delta_{\nu_{\mathcal{X}'}^{\text{zig}}(\Gamma, \{z_1, \dots, z_r\})} \quad \text{and} \quad \Delta_{\nu_{\mathcal{Y}}^{\text{zag}}(\Gamma, \{z_1, \dots, z_r\})} = \Delta_{\nu_{\mathcal{Y}'}^{\text{zag}}(\Gamma, \{z_1, \dots, z_r\})}.$$

7.4 Remarks on the extended deformations of hexagonal and rectangular dimer models

As we mentioned in Remark 6.8, we can skip the operations (zig-4) and (zig-5) (resp. (zag-4) and (zag-5)) in the case of hexagonal and rectangular dimer models (see Definition 2.1), as we will see below. We note that hexagonal and rectangular dimer models are isoradial. These dimer models have been studied in several papers, with the following results being particularly noteworthy.

Proposition 7.11 (e.g., [21, 28, 31]). *Let Γ be a consistent dimer model. Then, we have the following.*

- (1) Γ is a hexagonal dimer model if and only if the PM polygon Δ_Γ is a triangle.
- (2) If Γ is a rectangular dimer model, then the PM polygon Δ_Γ is a parallelogram.

For these nice classes of dimer models, we may skip the operations (zig-4) and (zig-5) (or (zag-4) and (zag-5)) when we apply the extended deformation.

Proposition 7.12. *Let Γ be a hexagonal or rectangular dimer model. Then, the extended deformation $\nu_{\mathcal{X}}^{\text{zig}}(\Gamma, \{z_1, \dots, z_r\})$ is defined by the operations (zig-1)–(zig-3) and (join). Similarly, the extended deformation $\nu_{\mathcal{Y}}^{\text{zag}}(\Gamma, \{z_1, \dots, z_r\})$ is defined by the operations (zag-1)–(zag-3) and (join).*

In particular, the extended deformations coincide with the usual deformations:

$$\begin{aligned} \nu_{\mathcal{X}}^{\text{zig}}(\Gamma, \{z_1, \dots, z_r\}) &= \nu_{\mathbf{P}}^{\text{zig}}(\Gamma, \{z_1, \dots, z_r\}) \quad \text{and} \\ \nu_{\mathcal{Y}}^{\text{zag}}(\Gamma, \{z_1, \dots, z_r\}) &= \nu_{\mathbf{Q}}^{\text{zag}}(\Gamma, \{z_1, \dots, z_r\}). \end{aligned}$$

Proof. We will prove the case of the extended zig-deformation. The case of the extended zag-deformation is similar.

The zigzag paths z_1, \dots, z_r have the same slope, and this slope is the outer normal vector of an edge of the PM polygon Δ_Γ by Proposition 3.5.

- (1) Let Γ be a hexagonal dimer model. Then, Δ_Γ is a triangle by Proposition 7.11(1). Let e_1, e_2, e_3 be the edges of Δ_Γ ordered cyclically in the anti-clockwise direction. We may assume that the slopes of z_1, \dots, z_r are the outer normal vector of e_1 . We then consider the zigzag paths x_1, \dots, x_s (resp. y_1, \dots, y_t) intersecting with z_i at zags (resp. zigs) of z_i . Since Γ is isoradial, it is properly ordered. Thus, by Proposition 3.5 we see that $[x_1] = \dots = [x_s]$ (resp. $[y_1] = \dots = [y_t]$), and $[x_j]$ (resp. $[y_k]$) is the outer normal vector of e_2 (resp. of e_3).
- (2) Let Γ be a rectangular dimer model. Then, Δ_Γ is a parallelogram by Proposition 7.11(2). Let e_1, e_2, e_3, e_4 be the edges of Δ_Γ ordered cyclically in the anti-clockwise direction. In particular, $\{e_1, e_3\}$ and $\{e_2, e_4\}$ are pairs of edges that are parallel. We may assume that the slopes of z_1, \dots, z_r are the outer normal vector of e_1 , in which case the zigzag paths having the slope $-[z_i]$ correspond to e_3 . Then, in a similar way as above, we have the zigzag paths x_1, \dots, x_s (resp. y_1, \dots, y_t) such that $[x_j]$ (resp. $[y_k]$) is the outer normal vector of e_2 (resp. e_4).

In both cases, we see that any pair of zigzag paths in x_1, \dots, x_s (resp. y_1, \dots, y_t) does not have intersections on the universal cover by Lemma 3.15 because Γ is isoradial.

Next, we consider $\bar{\nu}_{\mathcal{X}}^{\text{zig}}(\Gamma, \{z_1, \dots, z_r\})$ for the case of $r \neq 1$ (see Remark 6.4 for the case of $r = 1$). By Lemma 7.7 and the fact that there is no intersection between x_1, \dots, x_s , we see that the edges removed by (zig-5) are bypasses added in (zig-4). Furthermore, by Observations 7.3 and 7.4 any zigzag path passing through a bypass takes the form \tilde{x}'_j . Since the slopes of x_1, \dots, x_s are all the same in our situation, those of x'_1, \dots, x'_s are all the same (see Proposition 7.9). Thus, any bypass on the universal cover of $\bar{\nu}_{\mathcal{X}}^{\text{zig}}(\Gamma, \{z_1, \dots, z_r\})$ is either

- (i) a self-intersection of a zigzag path \tilde{x}'_j , or
- (ii) the intersection of a pair of zigzag paths $\tilde{x}'_j, \tilde{x}'_{j'}$ with $[x'_j] = [x'_{j'}]$.

We also see that an edge which is either (i) or (ii) is certainly a bypass, because of Observation 7.4 and the fact that such an intersection can not appear in the irrelevant part. Moreover, if a bypass is the intersection of zigzag paths \tilde{x}'_j and $\tilde{x}'_{j'}$, then they have another intersection because $[x_j] = [x_{j'}]$, and such an intersection is also a bypass. Thus, if there exists a bypass that can not be removed by (zig-5), the consistency condition is prevented. Therefore, we can remove all bypasses added in (zig-4) by using (zig-5), and hence we may skip these operations. \blacksquare

8 Combinatorial mutations of the PM polygon are realized by extended deformations

Throughout this section, we still keep the notation of Sections 4 and 6 unless otherwise stated. In this section, we show that the combinatorial mutation of the PM polygon of a consistent dimer model coincides with the PM polygon of the deformed dimer model (see Theorem 8.3). First, we observe the relationship between the deformation data (see Definition 4.1) and the mutation data (see Definition 5.1).

Setting 8.1. Let Γ be a reduced consistent dimer model, and Δ_Γ be the PM polygon of Γ . We take a type I zigzag path z of Γ with $v := [z] \in \mathbb{Z}^2$. Then, by Proposition 3.5 there is an edge E of Δ_Γ whose outer normal vector is v . Since Δ_Γ is determined up to translation, there is ambiguity concerning the position of the origin. Thus, we fix the origin $\mathbf{0}$ for Δ_Γ so that $\mathbf{0} \in \Delta_\Gamma$. Let $w := -v$, and consider

$$\begin{aligned} h_{\max} &= h_{\max}(\Delta_\Gamma, w) := \max\{\langle w, u \rangle \mid u \in \Delta_\Gamma\}, \\ h_{\min} &= h_{\min}(\Delta_\Gamma, w) := \min\{\langle w, u \rangle \mid u \in \Delta_\Gamma\}. \end{aligned}$$

Now, we let $r := -h_{\min}$ and assume that $r \leq |\mathcal{Z}_v^I(\Gamma)|$. Since the length of the line segments of E is $|E \cap N| - 1$ and this is equal to $|\mathcal{Z}_v(\Gamma)|$ by Proposition 3.5, we have

$$-h_{\min} = r \leq |\mathcal{Z}_v^I(\Gamma)| \leq |\mathcal{Z}_v(\Gamma)| = |E \cap N| - 1.$$

Thus Δ_Γ admits the combinatorial mutation with respect to w (see Remark 5.3). Let $\ell(z) := 2n$. Then, by Lemma 3.9 we have

$$\begin{aligned} n &= \ell(z)/2 = |\mathbf{P} \cap z| + \langle h(\mathbf{P}, \mathbf{P}_i), w \rangle = |\mathbf{P} \cap z| + \langle h(\mathbf{P}, \mathbf{P}_0) - h(\mathbf{P}_i, \mathbf{P}_0), w \rangle \\ &= |\mathbf{P} \cap z| + \langle h(\mathbf{P}, \mathbf{P}_0), w \rangle - \langle h(\mathbf{P}_i, \mathbf{P}_0), w \rangle, \end{aligned}$$

where \mathbf{P} is a perfect matching on Γ , \mathbf{P}_0 is the reference perfect matching, and $\mathbf{P}_i \in \text{PM}_{\max}(z)$. Since $h(\mathbf{P}_i, \mathbf{P}_0)$ is a lattice point on E by Lemma 3.8, we have $\langle h(\mathbf{P}_i, \mathbf{P}_0), w \rangle = h_{\min}$. If $\mathbf{P} \in \text{PM}_{\min}(z)$, then $|\mathbf{P} \cap z| = 0$ by Lemma 3.12, and this means that $\langle h(\mathbf{P}, \mathbf{P}_0), w \rangle = h_{\max}$. Thus, we have $n = h_{\max} - h_{\min} = \text{width}(\Delta_\Gamma, w)$.

We show how the correspondence between mutation data and deformation data in Table 8.1.

Mutation data	Deformation data
w	$-v$
h_{\min}	$-r$
h_{\max}	h
$\text{width}(\Delta_\Gamma, w)$	n

Table 8.1. Relationships between the mutation data and the deformation data.

Using the integers r, h , we take type I zigzag paths z_1, \dots, z_r and the zig-deformation (resp. zag-deformation) parameter \mathcal{X} (resp. \mathcal{Y}) with respect to z_1, \dots, z_r as in Setting 6.1. We then have the deformed consistent dimer models $\nu_{\mathcal{X}}^{\text{zig}}(\Gamma) = \nu_{\mathcal{X}}^{\text{zig}}(\Gamma, \{z_1, \dots, z_r\})$ and $\nu_{\mathcal{Y}}^{\text{zag}}(\Gamma) = \nu_{\mathcal{Y}}^{\text{zag}}(\Gamma, \{z_1, \dots, z_r\})$.

We determine the origin of the PM polygons $\Delta_{\nu_{\mathcal{X}}^{\text{zig}}(\Gamma)}$ and $\Delta_{\nu_{\mathcal{Y}}^{\text{zag}}(\Gamma)}$ as follows. First, there are zigzag paths y'_1, \dots, y'_t on $\nu_{\mathcal{X}}^{\text{zig}}(\Gamma)$ whose slope respectively corresponds to the one of zigzag paths y_1, \dots, y_t on Γ by Proposition 7.6. Then, we put $\Delta_{\nu_{\mathcal{X}}^{\text{zig}}(\Gamma)}$ on Δ_Γ so that the edges corresponding to y'_1, \dots, y'_t respectively coincide with the edges of Δ_Γ corresponding to y_1, \dots, y_t . We determine

the origin for $\Delta_{\nu_x^{\text{zig}}(\Gamma)}$ so that it is in the same position as the origin for Δ_Γ . Considering the zigzag paths on $\nu_y^{\text{zag}}(\Gamma)$ obtained from the zigzag paths x_1, \dots, x_s on Γ , we can also determine the origin for $\Delta_{\nu_y^{\text{zag}}(\Gamma)}$.

Remark 8.2. In Setting 8.1, we assumed that $r \leq |\mathcal{Z}_v^1(\Gamma)|$ for defining the deformation data. As we mentioned in Remark 4.2, even if the number of type I zigzag paths is insufficient, we can sometimes change a type II zigzag path into a type I zigzag path without changing the PM polygon by using mutations of dimer models (see Appendix A). Moreover, it is known that for a given lattice polygon P there exists an isoradial dimer model giving P as the PM polygon by [14], in which case all zigzag paths are type I (see Definition 3.4), and hence $|\mathcal{Z}_v^1(\Gamma)| = |\mathcal{Z}_v(\Gamma)|$. Thus, if $-h_{\min} \leq |E \cap N| - 1$ we can find a certain isoradial dimer model Γ satisfying $-h_{\min} = r \leq |\mathcal{Z}_v^1(\Gamma)| = |E \cap N| - 1$.

For any edge E of Δ_Γ as in Setting 8.1, we take a primitive lattice element $u_E \in N$ such that $\langle w, u_E \rangle = 0$. Here, there are two choices of u_E and we fix u_E as follows. We recall the primitive lattice element $h(\mathbf{P}'_z, \mathbf{P}_z)$ given in Settings 7.8, which satisfies $\langle [z], h(\mathbf{P}'_z, \mathbf{P}_z) \rangle = 0$. We let $u_E := h(\mathbf{P}'_z, \mathbf{P}_z)$, and hence $\langle w, u_E \rangle = \langle -[z], u_E \rangle = 0$. We set the line segment F as $F := \text{conv}\{\mathbf{0}, u_E\}$. Using this with Setting 8.1 (and also Table 8.1), our main theorem can be stated as follows.

Theorem 8.3. *Let Γ be a reduced consistent dimer model with $\mathbf{0} \in \Delta_\Gamma$. Then, we have*

$$\begin{aligned} \text{mut}_w(\Delta_\Gamma, F) &= \Delta_{\nu_x^{\text{zig}}(\Gamma, \{z_1, \dots, z_r\})}, \\ \text{mut}_w(\Delta_\Gamma, -F) &= \Delta_{\nu_y^{\text{zag}}(\Gamma, \{z_1, \dots, z_r\})}. \end{aligned}$$

Proof. We will prove the first equation. The other one follows from a similar argument.

First, we show that

$$\varphi(\Delta_\Gamma^*) = \Delta_{\nu_x^{\text{zig}}(\Gamma, \{z_1, \dots, z_r\})}^*$$

where $\varphi = \varphi_{w, F}$ is the map given in (5.2).

Let $E_1 := E, E_2, \dots, E_m$ be the edges of Δ_Γ ordered cyclically in the anti-clockwise direction. As we mentioned in Setting 8.1, we suppose that $\mathbf{0} \in \Delta_\Gamma$. Let $w_1 := w, w_2, \dots, w_m$ be inner normal vectors corresponding to E_1, \dots, E_m , respectively (see Figure 8.1). Also, we let $v_i = -w_i$ for $i = 1, \dots, r$, which are the outer normal vectors corresponding to E_i . We then consider $u \in \Delta_\Gamma$ such that $\langle w_1, u \rangle = h_{\max}(\Delta_\Gamma, w_1) = h$; that is, we consider $w_{h_{\max}}(\Delta_\Gamma)$, which is either a vertex or an edge of Δ_Γ . If $w_{h_{\max}}(\Delta_\Gamma)$ is an edge, we easily see that it is parallel to E , in which case we may write $E_a := w_{h_{\max}}(\Delta_\Gamma)$ for some $1 < a < m$. If $w_{h_{\max}}(\Delta_\Gamma)$ is a vertex, we set the edges intersecting at $w_{h_{\max}}(\Delta_\Gamma)$ as E_{a-1}, E_{a+1} and set $E_a = \emptyset$ where $1 < a < m$. Recall that by Proposition 3.5, for each $E_i \neq \emptyset$ there exist zigzag paths on Γ such that the slopes coincide with v_i , and the set of such zigzag paths is denoted by $\mathcal{Z}_{v_i} = \mathcal{Z}_{v_i}(\Gamma)$.

First, we consider the edge E_1 and zigzag paths in $\mathcal{Z}_{v_1} = \mathcal{Z}_{(-w)}$. By definition, we have $\langle -v_1, u_E \rangle = 0$ and $\{z_1, \dots, z_r\} \subseteq \mathcal{Z}_{(-w)}^1 \subseteq \mathcal{Z}_{(-w)}$. If $|\mathcal{Z}_{(-w)}| > r$, then there exists a zigzag path in $\mathcal{Z}_{(-w)}$ that is not in $\{z_1, \dots, z_r\}$. If $E_a \neq \emptyset$, we have zigzag paths in \mathcal{Z}_{v_a} . Since E_1 and E_a are parallel, v_1 and v_a are linearly dependent, and hence $\langle v_a, u_E \rangle = 0$. Then, we see that zigzag paths in \mathcal{Z}_{v_a} do not intersect with any type I zigzag path z satisfying $[z] = v_1$ in the universal cover (see Lemma 3.15).

Next, we consider the edges E_2, \dots, E_{a-1} of Δ_Γ and zigzag paths in $\mathcal{Z}_1 := \mathcal{Z}_{v_2} \cup \dots \cup \mathcal{Z}_{v_{a-1}}$. We see that v_i with $i = 2, \dots, a-1$ satisfies $\langle -v_i, u_E \rangle < 0$ by a choice of the edges E_2, \dots, E_{a-1} . By the same argument as in the proof of Proposition 7.1, we see that the zigzag paths in \mathcal{Z}_1 intersect with a type I zigzag path z satisfying $[z] = v_1$ precisely once in the universal cover (see

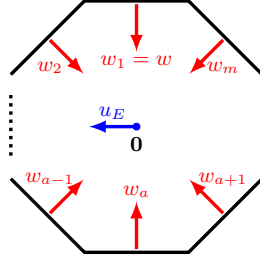


Figure 8.1. The PM polygon Δ_Γ and its inner normal vectors (the case where the origin is contained in the strict interior of Δ_Γ).

Lemma 3.15); specifically, they intersect with z in $\text{Zag}(z)$. Thus, we have $\mathcal{Z}_1 = \{x_1, \dots, x_s\}$, and for each $i = 2, \dots, a-1$ the vector v_i satisfies $v_i = [x_j]$ for some $j = 1, \dots, s$.

Next, we consider the edges E_{a+1}, \dots, E_m of Δ_Γ and zigzag paths in $\mathcal{Z}_2 := \mathcal{Z}_{v_{a+1}} \cup \dots \cup \mathcal{Z}_{v_m}$. We see that v_i with $i = a+1, \dots, m$ satisfies $\langle -v_i, u_E \rangle > 0$ by the choice of the edges E_{a+1}, \dots, E_m . By a similar argument as above, we see that the zigzag paths in \mathcal{Z}_2 intersect with a type I zigzag path z satisfying $[z] = v_1$ precisely once in the universal cover; specifically, they intersect with z in $\text{Zig}(z)$. Thus, we have $\mathcal{Z}_2 = \{y_1, \dots, y_t\}$, and for each $i = a+1, \dots, m$ the vector v_i satisfies $v_i = [y_k]$ for some $k = 1, \dots, t$.

Collectively, we see that any zigzag path of Γ takes one of the following forms:

- z_1, \dots, z_r ,
- $z'_1, \dots, z'_{r'}$ contained in $\mathcal{Z}_{(-w)} \setminus \{z_1, \dots, z_r\}$ for $w = -v_1$ with $\langle w, u_E \rangle = 0$ if $|\mathcal{Z}_{(-w)}| > r$,
- $z''_1, \dots, z''_{r''}$ contained in \mathcal{Z}_w for $w = -v_1$ with $\langle w, u_E \rangle = 0$ if $E_a \neq \emptyset$,
- x_j where $j = 1, \dots, s$, in which case it satisfies $\langle -[x_j], u_E \rangle < 0$,
- y_k where $k = 1, \dots, t$, in which case it satisfies $\langle -[y_k], u_E \rangle > 0$.

The slopes of these zigzag paths give the supporting hyperplanes of Δ_Γ by Proposition 3.5. More precisely, if Δ_Γ contains the origin $\mathbf{0}$ as an interior lattice point, then

$$H_{-[\zeta], \geq -k_\zeta} = \{u \in N_{\mathbb{R}} \mid \langle -[\zeta], u \rangle \geq -k_\zeta\}$$

is the supporting hyperplane of Δ_Γ for any zigzag path ζ of Γ and a certain positive integer k_ζ . If the origin $\mathbf{0}$ lies on the boundary of Δ_Γ , k_ζ is replaced by 0 for the zigzag paths corresponding to the edges that contain $\mathbf{0}$. By Proposition 5.6 and its proof, Δ_Γ^* can be written as $\Delta_\Gamma^* = Q + C$, where Q is a polygon and C is a polyhedral cone. Since the set of the slopes of zigzag paths of Γ coincides with $\{v_1, \dots, v_m\}$ if we identify the same slopes, we see that the set $\{u_1, \dots, u_p, u'_1, \dots, u'_q\}$, which generates Q and C in the proof of Proposition 5.6, is given by $\{w_1, \dots, w_m\}$ in our situation. In what follows, we assume that $\mathbf{0}$ is contained in the strict interior of Δ_Γ , in which case $\Delta_\Gamma^* = Q$ and $Q = \text{conv}(\{\frac{1}{k_1}w_1, \dots, \frac{1}{k_m}w_m\})$ for some positive integers k_i , giving the supporting hyperplanes $H_{w_i, \geq -k_i}$ of Δ_Γ for $i = 1, \dots, m$. We remark that $\frac{1}{k_a}w_a$ appears in the above generating set if $E_a \neq \emptyset$. Since $\langle w_i, u_E \rangle \geq 0$ for $i = 1, a, a+1, \dots, m$ and $\langle w_i, u_E \rangle < 0$ for $i = 2, \dots, a-1$, we see that

$$\varphi(\Delta_\Gamma^*) = \text{conv} \left(\left\{ \frac{1}{k_1}w_1, \frac{1}{k_2}w'_2, \dots, \frac{1}{k_{a-1}}w'_{a-1}, \frac{1}{k_a}w_a \text{ (if } E_a \neq \emptyset), \right. \right. \\ \left. \left. \frac{1}{k_{a+1}}w_{a+1}, \dots, \frac{1}{k_m}w_m \right\} \right), \quad (8.1)$$

where $w'_i := w_i - \langle w_i, u_E \rangle w$ for $i = 2, \dots, a-1$. We also note that when $E_a = \emptyset$, we can take the positive integer k_a so that the line $\{u \in N_{\mathbb{R}} \mid \langle v_1, u \rangle = -k_a\}$, which is parallel to E_1 , passes

through the vertex of Δ_Γ that is the intersection of E_{a-1} and E_{a+1} . By the choice of k_a , we have $\langle \frac{1}{k_a}v_1, u \rangle \geq -1$ for any $u \in \Delta_\Gamma$; thus $\frac{1}{k_a}v_1 = \frac{1}{k_a}(-w_1) \in \Delta_\Gamma^*$ and hence $\frac{1}{k_a}v_1 = \frac{1}{k_a}(-w_1) \in \varphi(\Delta_\Gamma^*)$.

We then consider the deformed dimer model $\nu_{\mathcal{X}}^{\text{zig}}(\Gamma) = \nu_{\mathcal{X}}^{\text{zig}}(\Gamma, \{z_1, \dots, z_r\})$. By Observation 7.2, the lift of any zigzag path of the form z'_i or z''_i on the universal cover is contained in some irrelevant part, and hence it does not change even if we apply the extended deformation. Also, by Proposition 7.9, we have the zigzag paths x'_1, \dots, x'_s on $\nu_{\mathcal{X}}^{\text{zig}}(\Gamma)$ satisfying

$$-[x'_j] = -[x_j] - \langle [x_j], h(\mathbf{P}'_z, \mathbf{P}_z) \rangle [z] = w_i - \langle w_i, u_E \rangle w$$

for $j = 1, \dots, s$ and some $i = 2, \dots, a-1$. Furthermore, by Proposition 7.6, we have the zigzag paths y'_1, \dots, y'_t on $\nu_{\mathcal{X}}^{\text{zig}}(\Gamma)$ satisfying

$$-[y'_k] = -[y_k] = w_i$$

for $k = 1, \dots, t$ and some $i = a+1, \dots, m$. Thus, we see that the zigzag paths x_j, y_k vary as they satisfy the condition (5.2) when we apply the extended deformation $\nu_{\mathcal{X}}^{\text{zig}}$ to Γ . In addition, we have the zigzag path of the form $z_{i,j}$ defined in (zig-3). Thus, the zigzag paths on the consistent dimer model $\nu_{\mathcal{X}}^{\text{zig}}(\Gamma)$ are

$$\begin{aligned} & \{z'_i\}_{1 \leq i \leq r'} \quad (\text{if } |\mathcal{Z}_{(-w)}| > r), \quad \{z''_i\}_{1 \leq i \leq r''} \quad (\text{if } E_a \neq \emptyset), \\ & \{x'_j\}_{1 \leq j \leq s}, \quad \{y'_k\}_{1 \leq k \leq t}, \quad \text{and} \quad \{z_{i,j}\}_{\substack{1 \leq i \leq r \\ 1 \leq j \leq p_i}}. \end{aligned}$$

By the description of their slopes and Proposition 3.5, we see that the inner normal vectors of $\Delta_{\nu_{\mathcal{X}}^{\text{zig}}(\Gamma)}$ are

$$\{w_1, w'_2, \dots, w'_{a-1}, w_a = -w_1, w_{a+1}, \dots, w_m\},$$

and these vectors give the supporting hyperplanes of $\Delta_{\nu_{\mathcal{X}}^{\text{zig}}(\Gamma)}$ just like for Δ_Γ . Here, w_1 appears in the above set if $|\mathcal{Z}_{(-w_1)}| = |\mathcal{Z}_{v_1}| > r$, but we always have $\frac{1}{k_1}w_1 \in \Delta_{\nu_{\mathcal{X}}^{\text{zig}}(\Gamma)}^*$ by the same argument as we used for showing $\frac{1}{k_a}(-w_1) \in \Delta_\Gamma^*$ above, whereas w_a certainly appears since $[z_{i,j}] = -[z_i] = -w_1 = w_a$ (see Lemma 7.5). Thus, we have

$$\Delta_{\nu_{\mathcal{X}}^{\text{zig}}(\Gamma)}^* = \text{conv} \left(\left\{ \frac{1}{k_1}w_1, \frac{1}{k_2}w'_2, \dots, \frac{1}{k_{a-1}}w'_{a-1}, \frac{1}{k_a}w_a, \frac{1}{k_{a+1}}w_{a+1}, \dots, \frac{1}{k_m}w_m \right\} \right).$$

By the description (8.1) and the fact that $\frac{1}{k_1}w_1$ and $\frac{1}{k_a}w_a = \frac{1}{k_a}(-w_1)$ are contained in both $\varphi(\Delta_\Gamma^*)$ and $\Delta_{\nu_{\mathcal{X}}^{\text{zig}}(\Gamma)}^*$, we see that $\varphi(\Delta_\Gamma^*) = \Delta_{\nu_{\mathcal{X}}^{\text{zig}}(\Gamma)}^*$.

The case where the origin $\mathbf{0}$ lies on the boundary of Δ_Γ can be proved by a similar argument if we consider the hyperplane $\{u \in N_{\mathbb{R}} \mid \langle -[\zeta], u \rangle \geq 0\}$ instead of $\{u \in N_{\mathbb{R}} \mid \langle -[\zeta], u \rangle \geq -k_\zeta\}$ for the zigzag paths corresponding to the edges that contain $\mathbf{0}$, in which case $-[\zeta]$ will be a generator of a polyhedral cone C .

By Propositions 5.6(ii) and 5.7, we conclude that $\text{mut}_w(\Delta_\Gamma, F) = \Delta_{\nu_{\mathcal{X}}^{\text{zig}}(\Gamma)}$. ■

Since $\text{mut}_w(\Delta_\Gamma, F) \cong \text{mut}_w(\Delta_\Gamma, -F)$ (see Remark 5.3), we immediately have the following.

Corollary 8.4. *We have*

$$\Delta_{\nu_{\mathcal{X}}^{\text{zig}}(\Gamma, \{z_1, \dots, z_r\})} \cong \Delta_{\nu_{\mathcal{Y}}^{\text{zag}}(\Gamma, \{z_1, \dots, z_r\})}.$$

That is, they are $\text{GL}(2, \mathbb{Z})$ -equivalent.

We next show that the extended zig-deformation and zag-deformation are mutually inverse operations on the level of the associated PM polygon as in Corollary 8.6 below. However, it is not true on the level of dimer models as we saw in Example 4.9.

Setting 8.5. Let $\nu_{\mathcal{X}}^{\text{zig}}(\Gamma, \{z_1, \dots, z_r\})$ be the reduced consistent dimer model. We consider the following deformation data for $\nu_{\mathcal{X}}^{\text{zig}}(\Gamma, \{z_1, \dots, z_r\})$. Let $z_{i,j}$ be a type I zigzag path which satisfies $[z_{i,j}] = -v =: w$ (see Proposition 7.5). Since $\{z_{i,j}\}_{\substack{1 \leq i \leq r \\ 1 \leq j \leq p_i}}$ is the subset of type I zigzag paths,

we have $|\mathcal{Z}_w^I(\nu_{\mathcal{X}}^{\text{zig}}(\Gamma))| \geq \sum_{i=1}^r p_i = h$. We take a subset $\{z'_1, \dots, z'_h\}$ of type I zigzag paths of $\nu_{\mathcal{X}}^{\text{zig}}(\Gamma)$, and perform the same procedure as in Setting 6.1. Then we have the zag-deformation parameter $\mathcal{Y}' = \{Y'_1, \dots, Y'_h\}$ of the weight $\mathbf{q}' = (q'_1, \dots, q'_h)$ with $\sum_{i=1}^h q'_i = r$. We can use the same arguments for the case of $\nu_{\mathcal{Y}}^{\text{zag}}(\Gamma, \{z_1, \dots, z_r\})$. Specifically, we take a subset $\{z''_1, \dots, z''_h\}$ of type I zigzag paths on $\nu_{\mathcal{Y}}^{\text{zag}}(\Gamma)$ and have the zig-deformation parameter $\mathcal{X}' = \{X'_1, \dots, X'_h\}$ of the weight $\mathbf{p}' = (p'_1, \dots, p'_h)$ with $\sum_{i=1}^h p'_i = r$.

Corollary 8.6. *Let the notation be the same as in Setting 8.5. Then, we have*

$$\Delta_{\nu_{\mathcal{Y}'}^{\text{zag}}(\nu_{\mathcal{X}}^{\text{zig}}(\Gamma, \{z_i\}_{i=1}^r), \{z'_\ell\}_{\ell=1}^h)} = \Delta_{\Gamma} \quad \text{and} \quad \Delta_{\nu_{\mathcal{X}'}^{\text{zig}}(\nu_{\mathcal{Y}}^{\text{zag}}(\Gamma, \{z_i\}_{i=1}^r), \{z''_\ell\}_{\ell=1}^h)} = \Delta_{\Gamma}.$$

Proof. This follows from Proposition 5.5(1) and Theorem 8.3. ■

As we mentioned in Section 1, the combinatorial mutation of Fano polygons is important from the viewpoint of mirror symmetry and the classification of Fano manifolds. To study the combinatorial mutation of Fano polygons using extended deformations of dimer models, we assume that the polygons Δ_{Γ} , $\Delta_{\nu_{\mathcal{X}}^{\text{zig}}(\Gamma, \{z_1, \dots, z_r\})}$ and $\Delta_{\nu_{\mathcal{Y}}^{\text{zag}}(\Gamma, \{z_1, \dots, z_r\})}$ contain the origin in their strict interiors. Then, we have the following corollary.

Corollary 8.7. *Let the notation be the same as above. Then, we see that Δ_{Γ} is Fano if and only if $\Delta_{\nu_{\mathcal{X}}^{\text{zig}}(\Gamma, \{z_1, \dots, z_r\})}$ (resp. $\Delta_{\nu_{\mathcal{Y}}^{\text{zag}}(\Gamma, \{z_1, \dots, z_r\})}$) is Fano.*

Proof. This follows from Proposition 5.5(2) and Theorem 8.3. ■

Note that since any lattice polygon can be obtained as the PM polygon of a reduced consistent dimer model by Theorem 2.6, we can discuss the combinatorial mutation of a polygon in terms of the extended zig-deformations and zag-deformation by the results shown in this section.

A Mutations of dimer models

In this section, we introduce another operation, called the *mutation of dimer models*. From the viewpoint of physics, dimer models and their mutations correspond to quiver gauge theories and Seiberg duality. The mutation of dimer models can be defined for each quadrangle face of a dimer model, and the operation called *spider move* (e.g., [6, 13]), which is the inverse operation shown in Figure A.1, is the main component used in defining this mutation.

We note that there are two types of the spider move (and hence the mutation) depending on the color of the two interior nodes.

Definition A.1 (mutation of dimer models). Let Γ be a dimer model. We pick a quadrangle face $f \in \Gamma_2$. Then, the *mutation* of Γ at f , denoted by $\mu_f(\Gamma)$, is the operation consisting of the following procedures:

- (I) If there exist black nodes on the boundary of f that are not 3-valent, we apply split moves to those nodes and make them 3-valent as shown in Figure A.2.

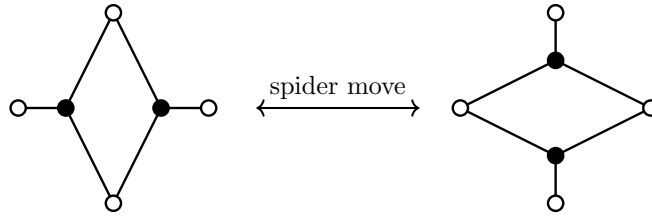


Figure A.1.

(II) We apply the spider move to f (see Figure A.1).

(III) If the resulting dimer model contains 2-valent nodes, we remove them by applying the join moves.

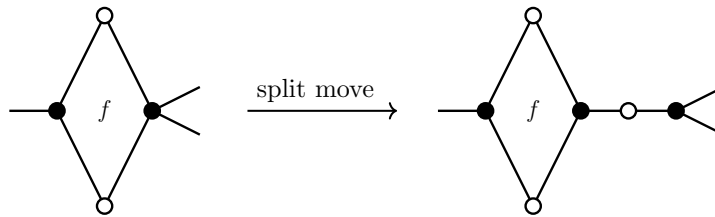


Figure A.2.

Applying a mutation at a quadrangle face, we obtain the new dimer model from a given one, although the mutation sometimes induces an isomorphic one. We also remark that the mutation is an involutive operation; that is, $\mu_f(\mu_f(\Gamma)) = \Gamma$ holds. We say that dimer models Γ and Γ' are *mutation-equivalent* if they are transformed into each other by repeating the mutation of dimer models. Moreover, we also see that the join, split and spider moves do not change the slopes of zigzag paths and preserve conditions in Definition 3.3. Thus we have the following.

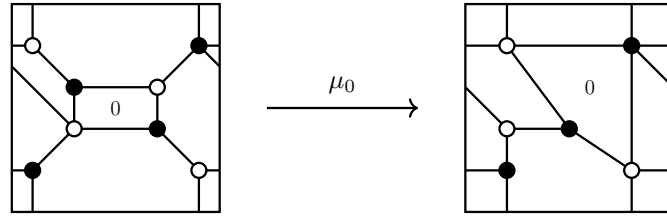
Proposition A.2. *A mutation of dimer models turns consistent dimer models into consistent dimer models associated with the same lattice polygon.*

Note that it has been conjectured that all consistent dimer models associated with the same lattice polygon are mutation-equivalent. This conjecture is still open in general (see [6, pp. 396–397]). We note that partial answers were given in several papers (e.g., [5, 13, 15, 27]).

Remark A.3. A mutation of a dimer model is also defined as the dual of the *mutation of a quiver with potential* ($= QP$) in the sense of [9] (see also [5, Section 7.2], [27, Section 4]). Although we can consider the mutation of a QP for any vertex of the quiver having no loops and 2-cycles, the resulting QP is not necessarily the dual of a dimer model. To make the resulting quiver the dual of a dimer model, we need to assume that the mutated vertex has two incoming (equivalently, two outgoing) arrows, which is equivalent to assuming that the face of a dimer model corresponding to such a vertex is a quadrangle.

In the theory of (extended) deformations of dimer models, type I zigzag paths are important. We can use mutations to change a type II zigzag path into type I as in the example below.

Example A.4. We consider the following dimer model Γ (the image on the left). Since the face 0 is a quadrangle, we can apply the mutation and obtain the dimer model $\mu_0(\Gamma)$ as follows.



We can see that the zigzag path on Γ whose slope is $(-1, 1)$ or $(1, -1)$ is type II. On the other hand, we see that $\mu_0(\Gamma)$ is isoradial, and hence all zigzag paths are type I.

B Large examples

As we mentioned in Remark 6.4 and Proposition 7.12, we sometimes skip the operations (zig-4) and (zig-5) (resp. (zag-4) and (zag-5)) when we define the extended deformation $\nu_{\mathcal{X}}^{\text{zig}}(\Gamma, \{z_1, \dots, z_r\})$ (resp. $\nu_{\mathcal{Y}}^{\text{zag}}(\Gamma, \{z_1, \dots, z_r\})$) of a consistent dimer model Γ . However, as the following example shows, (zig-4) and (zig-5) (resp. (zag-4) and (zag-5)) are indispensable to define extended deformations compatible with combinatorial mutations of polygons, as shown in Theorem 8.3. For example, we often encounter such a situation when we consider a consistent dimer model whose PM polygon is relatively large.

Example B.1. We consider the lattice polygon P shown on the left-hand side of Figure B.1. We assume that the double circle stands for the origin $\mathbf{0}$. We consider the edge E whose primitive inner normal vector is $w = (0, -1)$ with $h_{\min} = -3$ and $h_{\max} = 1$. We take $u_E = (-1, 0)$, which satisfies $\langle w, u_E \rangle = 0$, and consider the line segment $F = \text{conv}\{\mathbf{0}, u_E\}$. Then, the combinatorial mutation $\text{mut}_w(P, F)$ of the polygon P is as shown on the right-hand side of Figure B.1.

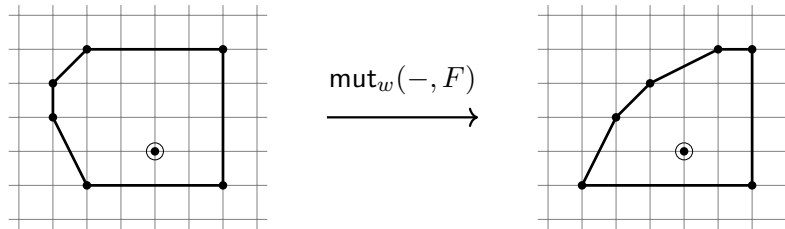


Figure B.1. The lattice polygons P and $\text{mut}_w(P, F)$ for $w = (0, -1)$ and $F = \text{conv}\{\mathbf{0}, (-1, 0)\}$.

Next, we consider the dimer model Γ shown in Figure B.2. The zigzag paths on this dimer model Γ are depicted in Figure B.3. One can check that Γ is consistent, and hence the PM polygon Δ_{Γ} coincides with P by Proposition 3.5.

We now consider the extended zig-deformation of Γ that realizes $\text{mut}_w(P, F)$ as the PM polygon (see Theorem 8.3). To do this, we first fix the deformation data (see Definition 4.1) as follows. First, the zigzag path z_i on Γ is type I with $\ell(z_i) = 8$, and its slope is $[z_i] = (0, 1) = -w$ for $i = 1, \dots, 4$. Let $r := -h_{\min} = 3$ and $h := h_{\max} = 1$ (see Table 8.1). These satisfy $r = 3 < |\mathcal{Z}_{(-w)}^{\text{I}}(\Gamma)| = 4$ and $r + h = \ell(z_i)/2 = 4$. We take the set of type I zigzag paths $\{z_1, z_2, z_3\}$, and consider the extended zig-deformation $\nu_{\mathcal{X}}^{\text{zig}}(\Gamma, \{z_1, z_2, z_3\})$ of Γ at $\{z_1, z_2, z_3\}$ with respect to \mathcal{X} , where \mathcal{X} is the zig-deformation parameter (see Setting 6.1) defined as follows. To define \mathcal{X} , we focus on x_1, x_2, x_3 shown in Figure B.3, which are the zigzag paths intersecting with z_i at some zags of z_i . They satisfy $m_1 := |x_1 \cap z_1| = 1$, $m_2 := |x_2 \cap z_2| = 1$, and $m_3 := |x_3 \cap z_3| = 2$ for any i ; thus we consider the set of sub-zigzag paths $\{x_1 = x_1^{(1)}, x_2 = x_2^{(1)}, x_3^{(1)}, x_3^{(2)}\}$. Here, we fix the intersection of z_3 and x_3 marked by \checkmark in Figure B.3 as the starting edge of $x_3^{(1)}$. We

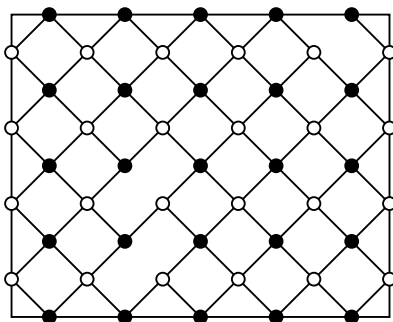


Figure B.2. A consistent dimer model Γ whose PM polygon coincides with P .

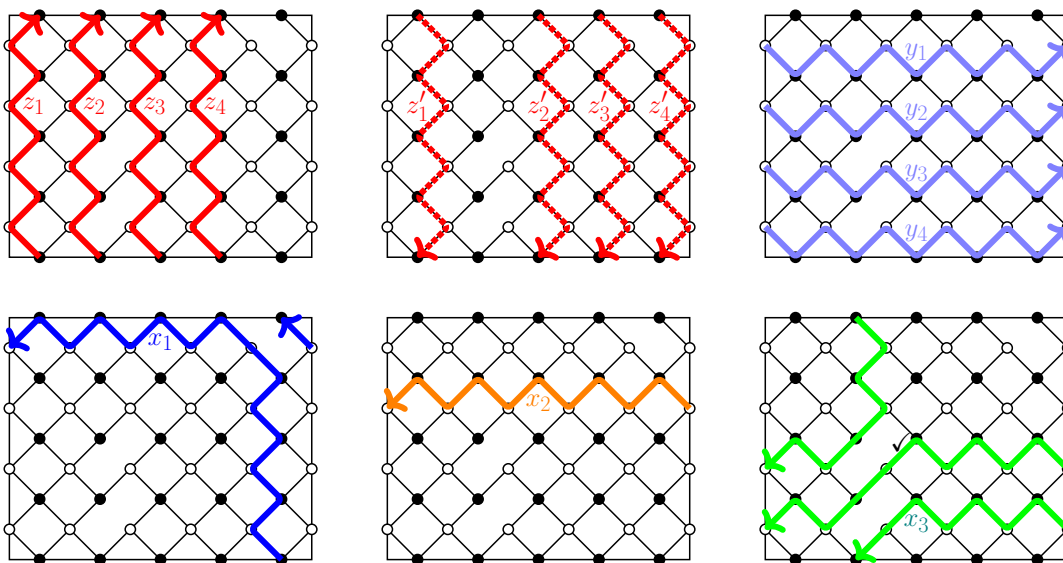


Figure B.3. The zigzag paths of Γ .

then set the zig-deformation parameter $\mathcal{X} := \{X_1, X_2, X_3\}$ with respect to $\{z_1, z_2, z_3\}$, where $X_1 = \{x_1 \cap z_1 = x_1^{(1)} \cap z_1\}$, $X_2 = \{x_2 \cap z_2 = x_2^{(1)} \cap z_2\}$ and $X_3 = \{x_3^{(1)} \cap z_3, x_3^{(2)} \cap z_3\}$, and hence the weight of \mathcal{X} is $\mathbf{p} = (0, 0, 1)$.

Using these deformation data, we apply the operations (zig-1)–(zig-3) to Γ . This gives us the dimer model shown in the left of Figure B.4. Here, we can easily see that the slopes of zigzag paths on this dimer model do not correspond bijectively to the primitive side segments of $\text{mut}_w(P, F)$, and thus we can not obtain Theorem 8.3 without the operations (zig-4) and (zig-5). We therefore apply (zig-4) – that is, we insert some bypasses. Then we have the dimer model $\bar{\nu}_{\mathcal{X}}^{\text{zig}}(\Gamma) = \bar{\nu}_{\mathcal{X}}^{\text{zig}}(\Gamma, \{z_1, z_2, z_3\})$, as shown in the right of Figure B.4. Some zigzag paths on $\bar{\nu}_{\mathcal{X}}^{\text{zig}}(\Gamma)$ are given in Figure B.5. For example, the zigzag path x_3 on Γ behaves as Figure 7.7 in $\{x_3^{(1)} \cap z_i, x_3^{(2)} \cap z_i \mid i = 1, 2\}$ and behaves as Figure 7.8 in $X_3 = \{x_3^{(1)} \cap z_3, x_3^{(2)} \cap z_3\}$ by our choice of \mathcal{X} , and hence we obtain the zigzag path x'_3 on $\bar{\nu}_{\mathcal{X}}^{\text{zig}}(\Gamma)$ as in Figure B.5. By Proposition 7.1, this dimer model is non-degenerate, but it is not consistent. Indeed, we can see that some nodes appearing on the zigzag path x'_3 shown in Figure B.5 are not properly ordered (see Definition 3.3(4)).

By Lemma 7.7, some edges constituting the zigzag paths x'_1, x'_2, x'_3 shown in Figure B.5 might be removed by the operation (zig-5). Thus, paying attention to these zigzag paths, we apply (zig-5) to $\bar{\nu}_{\mathcal{X}}^{\text{zig}}(\Gamma)$ and make it consistent. Namely, we remove pairs of edges (1)–(5) shown in the type A (left) of Figure B.6, which are the intersections of pairs of zigzag paths

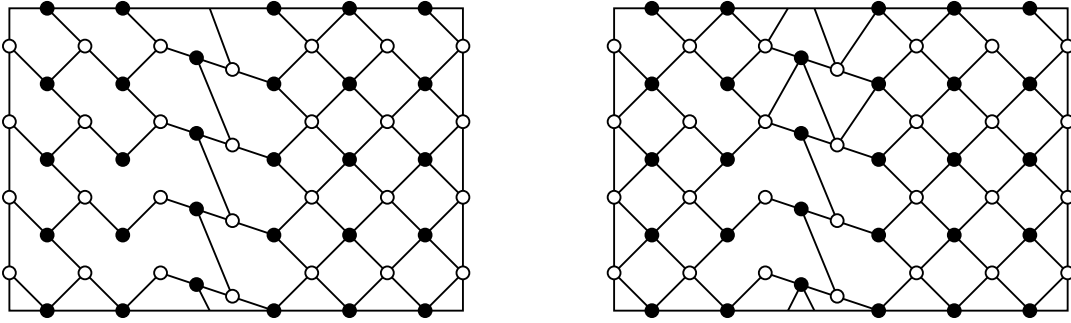


Figure B.4. The dimer model obtained by applying (zig-1)–(zig-3) to Γ (left), and the dimer model $\bar{\nu}_{\mathcal{X}}^{\text{zig}}(\Gamma, \{z_1, z_2, z_3\})$ obtained by applying (zig-1)–(zig-4) to Γ (right).

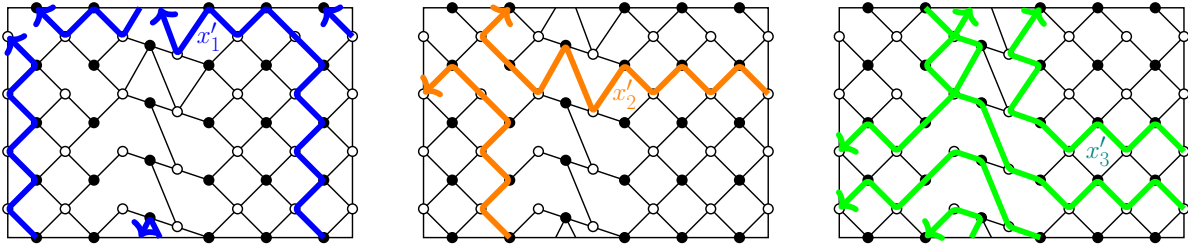


Figure B.5. The zigzag paths x'_1, x'_2, x'_3 of $\bar{\nu}_{\mathcal{X}}^{\text{zig}}(\Gamma, \{z_1, z_2, z_3\})$.

on the universal cover that intersect with each other in the same direction more than once, from $\bar{\nu}_{\mathcal{X}}^{\text{zig}}(\Gamma)$ with this order. Then we have the dimer model shown in the left of Figure B.7. Applying (join), we finally have the dimer model $\nu_{\mathcal{X}}^{\text{zig}}(\Gamma, \{z_1, z_2, z_3\})$ shown in the right of Figure B.7.

There are also other ways to remove edges. For example, if we remove pairs of edges (1)–(5) shown in the type B (right) of Figure B.6, then we have the dimer model shown in the left of Figure B.8, and applying (join) we have the dimer model $\nu_{\mathcal{X}}^{\text{zig}}(\Gamma, \{z_1, z_2, z_3\})$ shown in the right of Figure B.8.

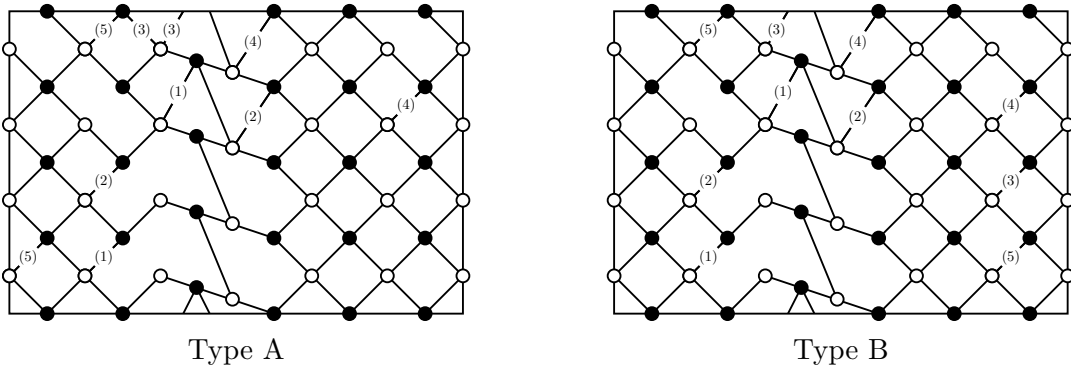


Figure B.6. The two ways to remove edges from $\bar{\nu}_{\mathcal{X}}^{\text{zig}}(\Gamma, \{z_1, z_2, z_3\})$ by (zig-5).

Let Γ_A (resp. Γ_B) be the deformed dimer model shown in the right of Figure B.7 (resp. Figure B.8). We can check that Γ_A and Γ_B are not isomorphic, but they are mutation-equivalent. Indeed, by applying the mutations of Γ_B at the faces $1, \dots, 10$ in this order (see Figure B.9), we recover Γ_A . Here, we recall that a mutation of a dimer model can be defined at any quadrangle

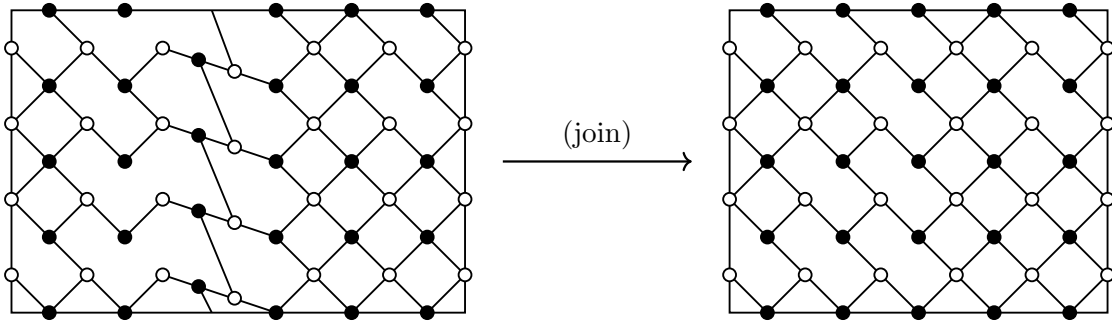


Figure B.7. The dimer model $\nu_{\chi}^{\text{zig}}(\Gamma, \{z_1, z_2, z_3\})$ obtained from the type A of Figure B.6.

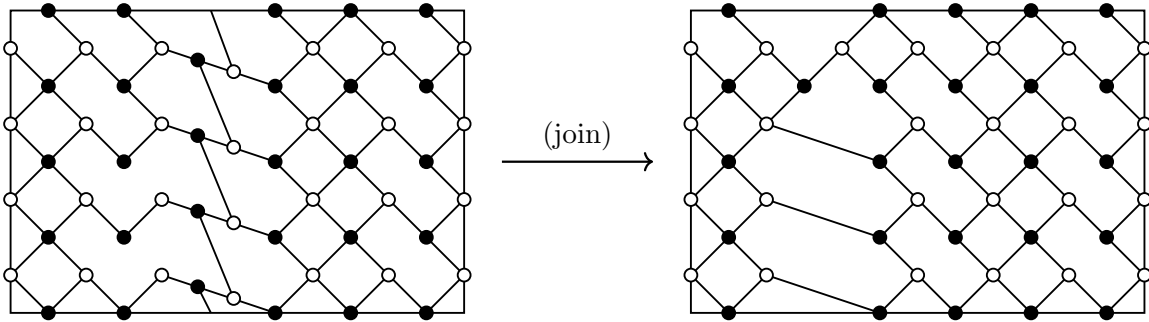


Figure B.8. The dimer model $\nu_{\chi}^{\text{zig}}(\Gamma, \{z_1, z_2, z_3\})$ obtained from the type B of Figure B.6.

face. Although some faces indexed by $\{1, \dots, 10\}$ are not quadrangle, such faces will become quadrangles during the process of this series of mutations.

The PM polygons of the dimer models Γ_A and Γ_B are the same (see Proposition A.2), and it coincides with the lattice polygon shown on the right-hand side of Figure B.1 by Theorem 8.3.

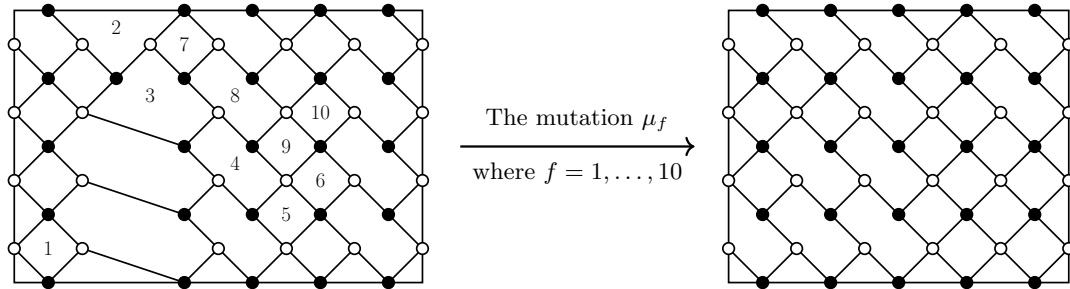


Figure B.9. The mutations of Γ_B (left) at the faces $1, \dots, 10$ induce Γ_A (right).

Acknowledgements

The authors would like to thank Alexander Kasprzyk for valuable lectures and discussions on the combinatorial mutation of Fano polygons. The authors would also like to thank the anonymous referees for their numerous valuable comments and suggestions. The first author is supported by JSPS Grant-in-Aid for Scientific Research (C) 20K03513. The second author was supported by World Premier International Research Center Initiative (WPI initiative), MEXT, Japan, and is supported by JSPS Grant-in-Aid for Early-Career Scientists 20K14279.

References

- [1] Akhtar M., Coates T., Corti A., Heuberger L., Kasprzyk A., Oneto A., Petracci A., Prince T., Tveiten K., Mirror symmetry and the classification of orbifold del Pezzo surfaces, *Proc. Amer. Math. Soc.* **144** (2016), 513–527, [arXiv:1501.05334](#).
- [2] Akhtar M., Coates T., Galkin S., Kasprzyk A.M., Minkowski polynomials and mutations, *SIGMA* **8** (2012), 094, 707 pages, [arXiv:1212.1785](#).
- [3] Beil C., Ishii A., Ueda K., Cancellativization of dimer models, [arXiv:1301.5410](#).
- [4] Bocklandt R., Consistency conditions for dimer models, *Glasg. Math. J.* **54** (2012), 429–447, [arXiv:1104.1592](#).
- [5] Bocklandt R., Generating toric noncommutative crepant resolutions, *J. Algebra* **364** (2012), 119–147, [arXiv:1104.1597](#).
- [6] Bocklandt R., A dimer ABC, *Bull. Lond. Math. Soc.* **48** (2016), 387–451, [arXiv:1510.04242](#).
- [7] Broomhead N., Dimer models and Calabi–Yau algebras, *Mem. Amer. Math. Soc.* **215** (2012), viii+86 pages, [arXiv:0901.4662](#).
- [8] Coates T., Corti A., Galkin S., Golyshev V., Kasprzyk A., Mirror Symmetry and Fano Manifolds, in European Congress of Mathematics, *Eur. Math. Soc.*, Zürich, 2013, 285–300, [arXiv:1212.1722](#).
- [9] Derksen H., Weyman J., Zelevinsky A., Quivers with potentials and their representations. I. Mutations, *Selecta Math. (N.S.)* **14** (2008), 59–119, [arXiv:0704.0649](#).
- [10] Duffin R.J., Potential theory on a rhombic lattice, *J. Combinatorial Theory* **5** (1968), 258–272.
- [11] Franco S., Hanany A., Vegh D., Wecht B., Kennaway K.D., Brane dimers and quiver gauge theories, *J. High Energy Phys.* **2006** (2006), no. 1, 096, 48 pages, [arXiv:hep-th/0504110](#).
- [12] Galkin S., Usnich A., Mutations of potentials, Preprint IPMU 10–0100, 2010.
- [13] Goncharov A.B., Kenyon R., Dimers and cluster integrable systems, *Ann. Sci. Éc. Norm. Supér. (4)* **46** (2013), 747–813, [arXiv:1107.5588](#).
- [14] Gulotta D.R., Properly ordered dimers, R -charges, and an efficient inverse algorithm, *J. High Energy Phys.* **2008** (2008), no. 10, 014, 31 pages, [arXiv:0807.3012](#).
- [15] Hanany A., Seong R.K., Brane tilings and reflexive polygons, *Fortschr. Phys.* **60** (2012), 695–803, [arXiv:1201.2614](#).
- [16] Hanany A., Vegh D., Quivers, tilings, branes and rhombi, *J. High Energy Phys.* **2007** (2007), no. 10, 029, 35 pages, [arXiv:hep-th/0511063](#).
- [17] Higashitani A., Nakajima Y., Combinatorial mutations of Newton–Okounkov polytopes arising from plabic graphs, *Adv. Stud. Pure Math.*, to appear, [arXiv:2107.04264](#).
- [18] Ilten N.O., Mutations of Laurent polynomials and flat families with toric fibers, *SIGMA* **8** (2012), 047, 7 pages, [arXiv:1205.4664](#).
- [19] Ishii A., Ueda K., A note on consistency conditions on dimer models, in Higher Dimensional Algebraic Geometry, *RIMS Kôkyûroku Bessatsu*, Vol. B24, Res. Inst. Math. Sci. (RIMS), Kyoto, 2011, 143–164, [arXiv:1012.5449](#).
- [20] Ishii A., Ueda K., Dimer models and the special McKay correspondence, *Geom. Topol.* **19** (2015), 3405–3466, [arXiv:0905.0059](#).
- [21] Iyama O., Nakajima Y., On steady non-commutative crepant resolutions, *J. Noncommut. Geom.* **12** (2018), 457–471, [arXiv:1509.09031](#).
- [22] Kasprzyk A., Nill B., Prince T., Minimality and mutation-equivalence of polygons, *Forum Math. Sigma* **5** (2017), e18, 48 pages, [arXiv:1501.05335](#).
- [23] Kennaway K.D., Brane tilings, *Internat. J. Modern Phys. A* **22** (2007), 2977–3038, [arXiv:0706.1660](#).
- [24] Kenyon R., An introduction to the dimer model, in School and Conference on Probability Theory, *ICTP Lect. Notes*, Vol. 17, Abdus Salam Int. Cent. Theoret. Phys., Trieste, 2004, 267–304, [arXiv:math.CO/0310326](#).
- [25] Kenyon R., Schlenker J.M., Rhombic embeddings of planar quad-graphs, *Trans. Amer. Math. Soc.* **357** (2005), 3443–3458, [arXiv:math-ph/0305057](#).
- [26] Mercat C., Discrete Riemann surfaces and the Ising model, *Comm. Math. Phys.* **218** (2001), 177–216, [arXiv:0909.3600](#).

-
- [27] Nakajima Y., Mutations of splitting maximal modifying modules: the case of reflexive polygons, *Int. Math. Res. Not.* **2019** (2019), 470–550, [arXiv:1601.05203](#).
 - [28] Nakajima Y., Semi-steady non-commutative crepant resolutions via regular dimer models, *Algebr. Comb.* **2** (2019), 173–195, [arXiv:1608.05162](#).
 - [29] Rietsch K., Williams L., Newton–Okounkov bodies, cluster duality, and mirror symmetry for Grassmannians, *Duke Math. J.* **168** (2019), 3437–3527, [arXiv:1712.00447](#).
 - [30] Schrijver A., Theory of linear and integer programming, *Wiley-Interscience Series in Discrete Mathematics*, John Wiley & Sons, Ltd., Chichester, 1986.
 - [31] Ueda K., Yamazaki M., A note on dimer models and McKay quivers, *Comm. Math. Phys.* **301** (2011), 723–747, [arXiv:math.AG/0605780](#).